DEVELOPMENT OF A POLYVINYL ALCOHOL CRYOGEL COVERED STENT

A Dissertation
Presented to
The Academic Faculty

By

Jason David Weaver

In Partial Fulfillment
Of the Requirements for the Degree
Doctor of Philosophy in
Biomedical Engineering

Georgia Institute of Technology

August 2010

DEVELOPMENT OF A POLYVINYL ALCOHOL CRYOGEL COVERED STENT

Approved by:

Dr. David N. Ku, Advisor
Department of Mechanical Engineering
Georgia Institute of Technology

Dr. Aloke V. Finn
Department of Cardiology
Emory University

Dr. W. Robert Taylor, Advisor
Department of Biomedical Engineering
Georgia Institute of Technology

Dr. Rudolph L. Gleason
Department of Biomedical Engineering
Georgia Institute of Technology

Dr. Elliot L. Chaikof
Department of Biomedical Engineering
Georgia Institute of Technology

Dr. Larry V. McIntire
Department of Biomedical Engineering
Georgia Institute of Technology

Date Approved: May 10, 2010

To my brother Marc.

You are missed.

ACKNOWLEDGEMENTS

First and foremost I would like to thank my advisor, Dr. Ku, for all his help and support. I have learned so much during my time in graduate school and I am grateful for the opportunity he gave me to work in his laboratory. Second, I would like to thank the rest of my committee (Dr. Taylor, Dr. Chaikof, Dr. Finn, Dr. Gleason, and Dr. McIntire) for their thoughtful input which helped shape this dissertation from the beginning of the project to its completion.

Another group of people that deserve special recognition are my labmates (past and present): Jason Bach, Dave Bark, Jinwu Fan, Laura-Lee Farrell, Prem Midha, Andrea Para, Beth Pavlik, Tamera Scholz, Sarah Shieh, and Peter Wellings. Each of you brought something unique to lab and I am grateful for all the advice, help with experiments, and willingness to listen that made this lab environment a fun place to work. Additionally, I would like to thank Dr. Alexander Rachev, Angela Lin, Matt Henry, Xi Liu, Sathya Raghavan, Casey Holliday, Alyssa Ngangan, Song Seto, Diane Sutcliffe, Dr. Naren Gupta, Emory Animal Care, Aqua Asberry, and Jack Horner, Jr. for their help with various portions of this work.

On a personal level, I would like to thank my parents, brother Greg, sister-in-law Jenni, nieces Lauren and Katelyn, Gramps, and my cousin Stacie and her family for all their love and support during my time in graduate school. Of course, I couldn't have made it through graduate school without my friends (in Atlanta and elsewhere) who were always willing to provide a welcome distraction whenever I needed one so thank you. Lastly, I'd like to thank Priya for her support and companionship since my first year in Atlanta. I couldn't have done it without you.

TABLE OF CONTENTS

LIST OF TABLES

LIST OF FIGURES

LIST OF ABBREVIATIONS

ANCOVA ..... analysis of covariance

ANOVA ..... analysis of variance

BMS ..... bare metal stent

BSA ..... bovine serum albumin

CAD ..... computer-aided design

CVI ..... chronic venous insufficiency

DES ..... drug-eluting stent

DMEM ..... dulbecco's modified eagle medium

DPBS ..... dulbecco's phosphate buffered saline

ePTFE ..... expanded poly[tetrafluoroethylene]

ESEM ..... environmental scanning electron microscope

FBS ..... fetal bovine serum

FEA ..... finite element analysis

HEPES ..... 4-(2-hydroxyethyl)-1-piperazineethanesulfonic acid

PDGF ..... platelet derived growth factor

PEO ..... poly[ethylene oxide]

PET ..... poly[ethylene terephthalate]

PTCA ..... percutaneous transluminal coronary angioplasty

PTFE ..... poly[tetrafluoroethylene]

PVA ..... poly[vinyl alcohol]

SFA ..... superficial femoral artery

SMC ..... smooth muscle cells

SUMMARY

Atherosclerosis is the number one cause of death in the United States and one of the most common treatments is the implantation of a stent – a small expandable metal scaffold which serves to hold the artery open and maintain proper blood flow. The two most common complications after stenting are restenosis and thrombosis. In order to eliminate these complications, a novel covered stent is investigated. Covered stents could reduce occlusions from restenosis by reducing artery wall prolapse and preventing cellular ingrowth without cytotoxic drugs. Covered stents could reduce thrombosis complications by employing a relatively non-thrombogenic material. Clinical results with covered stents to date have been mixed – in part because of material issues. A covered stent membrane should be able to undergo large stretch, prevent restenosis caused by smooth muscle cell (SMC) migration, and be relatively non-thrombogenic. This dissertation aims to evaluate polyvinyl alcohol (PVA) cryogels for covered stents in terms of their mechanics, ability to prevent restenosis, and thrombogenicity.

Mechanical testing included uniaxial tensile testing, puncture testing, and the fabrication and expansion of PVA cryogel covered stents. Uniaxial testing results showed PVA cryogels to have sufficient ultimate stretch which was similar to bare metal stents during deployment. Puncture testing revealed that PVA cryogels are highly resistant to this failure mechanism and not likely to puncture *in vivo*. PVA cryogel covered stents were examined visually and by environmental scanning electron microscope after expansion. No tears were seen in the membrane which was much thinner than the stent struts and therefore not likely to increase crimped profile greatly.

Finite element analysis of PVA cryogel covered stents was used to determine the membrane's effect on artery wall stress. PVA cryogel covered stents were able to reduce both artery wall stress and tissue prolapse when compared to equivalent uncovered stents. Migration assays were used to determine if PVA cryogels are able to block the SMC migration seen during restenosis. PVA cryogels significantly reduced SMC migration in modified Boyden chambers – suggesting that they would be able to prevent restenosis *in vivo*.

Thrombogenicity was tested *in vitro* with a gravity-fed flow loop using porcine blood and *in vivo* with a sheep model. PVA cryogels were found to be less thrombogenic than polyester controls in terms of flow rate and amount of thrombus deposited with the flow loop system. The sheep study demonstrated the feasibility of implanting PVA cryogel covered stents. After explantation of the covered stents, no gross inflammation or fibrotic response was observed. Additionally, the PVA cryogel membranes were intact – providing *in vivo* evidence for the durability of PVA cryogel covered stents.

Overall, this work provides evidence that covered stents made with PVA cryogels are a feasible device in terms of their mechanics, ability to prevent restenosis, and low thrombogenicity. PVA cryogel covered stents may be able to prevent both restenosis and thrombosis. This work represents a major advancement in the development of PVA cryogel covered stents and provides necessary safety and feasibility data for future clinical trials.

CHAPTER 1:

Introduction

1.1 Atherosclerosis & Current Treatments

Cardiovascular disease has been the number one cause of death in the United States since 1919 with coronary heart disease and stroke, caused by underlying atherosclerosis, accounting for over two thirds of those deaths [1]. Commonly known as 'hardening of the arteries,' atherosclerosis is characterized by fatty buildups, atheromata, along the artery wall that lead to plaque formation and loss of elasticity. It is a slow, progressive disease that begins in childhood and leads to the formation of atheromata in the aorta, medium, and large sized arteries. Atherosclerotic lesions are classified by the American Heart Association from a Type I initial lesion to a Type VI complicated lesion [2]. Stenoses in the arteries leading to the heart and brain limit blood flow and can cause death.

Treatments for atherosclerosis depend on the location of the lesion, its classification, and other patient dependent factors including family history, smoking, etc. These treatments may include lifestyle changes, medication, percutaneous transluminal angioplasty, stent implantation, other catheter-based treatments, or vascular surgery. Two separate studies in 1994 showed that the placement of stents, expandable metal scaffolds delivered via catheter, in the coronary arteries improved vessel patency over angioplasty alone (32% vs. 22% at seven months and 42.1% vs. 31.6% at six months) and since then, stenting has become one of the most common treatments for

atherosclerosis [3-5]. The two most problematic complications associated with stenting are restenosis and thrombosis [6].

1.2 Restenosis & Thrombosis

Restenosis is the process by which a treated vessel's luminal diameter decreases in size over a period of time, usually six months to a year, and occurs in approximately 20 – 45% of bare metal stents depending on risk factors such as diabetes, number of stents, and stent length among others [7-9]. Restenosis is typically defined as a 50% or greater reduction in diameter by angiogram [10]. While restenosis can be caused by elastic recoil or negative remodeling, in-stent restenosis is usually caused by neointimal hyperplasia [11]. During neointimal hyperplasia, vascular smooth muscle cells migrate from the media to the intima where they begin to proliferate and produce large amounts of extracellular material [12]. As the neointimal layer grows, it reduces the lumen size and blood flow through the affected area. Restenosis is a significant clinical problem which leads to a large number of repeat procedures and hospitalizations [13].

Thrombosis is the process of blood clot formation and in-stent thrombosis can be a very serious problem as occlusive clots can form rapidly [14, 15]. For bare metal stents, the risk of stent thrombosis is now less than 2% (at one month) mostly due to the practices of high balloon inflation pressure to ensure proper stent apposition and dual anti-platelet therapy, i.e. aspirin and ticlopidine [16-18]. Although drug-eluting stents have decreased restenosis rates by a relative 50% to 80% [11], concerns are now being raised about an increased risk of late (greater than one year after implantation) stent thrombosis [19, 20]. Given the high associated mortality rate, 45% at 9-month follow-up in a recent study of paclitaxel- and sirolimus-eluting stents [21], significant research efforts are being made

to understand the causes of late stent thrombosis and create less thrombogenic stent materials [14, 22, 23].

1.3 Developments in Stent Technology

Drug-eluting stents are made by coating a bare metal stent with a polymer which contains an anti-proliferative drug, e.g. sirolimus or paclitaxel, intended to disrupt smooth muscle cell proliferation [24]. While drug-eluting stents have been successful in the coronary arteries [24], that success has not been duplicated in the periphery where the need for innovative new treatments is great [25]. As already mentioned, drug-eluting stents have been drawing criticism lately because they may have an increased risk of late-stent thrombosis when compared to bare metal stents [19]. Late-stent thrombosis in drug-eluting stents could be caused by a delayed endothelialization process [22]. One recent study showed that while bare metal stents were completely endothelialized in 6 to 7 months, drug-eluting stents had not completely endothelialized by 40 months [22]. The cessation of anti-platelet therapy has been shown to be a significant risk factor for late stent thrombosis [22], but there is still no consensus on the appropriate duration of anti-platelet therapy after drug-eluting stent implantation [20].

Bioabsorbable stents are another active area of research. Bioabsorbable stents may help reduce chronic inflammation, eliminate the need for prolonged anti-platelet therapy, and lower the risk of thrombosis complications by eroding away once the acute phase after stent implantation (when mechanical support is required to maintain patency) has passed [26, 27]. The two materials which have been investigated most for bioabsorbable stents are magnesium alloy and poly-L-lactic acid [26]. Bioabsorbable stents hold promise as a future treatment, but the problems of low radial force and

variable degradation rates must still be solved before this treatment can become a reality [27, 28].

Biomechanical factors affecting artery wall stress are of great importance. Kastrati et al. has shown that stent design can have a profound effect on clinical restenosis rates [29]. Finite element analysis can be a powerful tool for investigating stent and artery interactions. Artery wall stress, which is affected by stent design, is also related to tissue prolapse – an inward draping of tissue which can reduce lumen diameter by up to 20% [30]. Several studies have used finite element analysis to compare different stent designs and their effect on vessel stresses and tissue prolapse [31, 32]. One recent investigation has demonstrated a link between high artery wall stress and high clinical restenosis rates [33], highlighting the need for biomechanical analyses when new stents are being designed.

1.4 Covered Stents as a New Treatment Modality

Covered stents are made by combining a bare metal stent with a membrane material, e.g. poly[tetrafluoroethylene] (PTFE), poly[ethylene terephthalate] (polyester or trade name Dacron^{TM}), silicone, or salmon collagen, which covers the gaps (cells) between stent struts [34-37]. While covered stents have typically been used in vessel repair situations or aneurysm repair, they are now being considered as a treatment for atherosclerosis [28]. Covered stents have the potential to block the vascular smooth muscle cell migration seen during neointimal hyperplasia with a physical barrier and without cytotoxic drugs, thereby reducing in-stent restenosis complication rates [37-39]. If the membrane were made of a non-thrombogenic material, complications from thrombosis could be minimized as well. Materials which have been used for covered

stent membranes implanted in humans include PTFE and polyester [28]. Initial results with polyester covered stents, however, were disappointing due to low patency, high thrombosis rates, and significant inflammatory response [40-42]. Most industry effort since then has focused on expanded PTFE (ePTFE) covered stents [28]. Covered stents with ePTFE have had success in longer superficial femoral artery lesions in patients with decent inflow and runoff status [43], although they generally are not used in smaller diameter vessels because of thrombosis concerns [44].

In addition to preventing complications from restenosis and thrombosis, covered stent membranes must also be mechanically suitable. During deployment, stents deform such that their diameters increase to between 2.7 and 4.6 times their crimped size [45]. Covered stent membranes should also be able to expand similarly in order to maintain a reduced device profile and avoid membrane tearing problems. Additionally, covered stent membranes should be able to resist puncture because this failure mode could lead to membrane embolization and the blockage of a downstream vessel. To the author's knowledge, there are currently no materials available that meet all these mechanical requirements and are able to prevent restenosis and thrombosis.

1.5 Polyvinyl Alcohol Cryogels

Polyvinyl alcohol (PVA) is a polymer with a hydrophilic hydroxyl side group and has been used safely in medical applications, e.g. contact lenses, for many years. PVA cryogels are a new class of biomaterial which offer more strength than a typical hydrogel and have water content similar to human soft tissue [46]. By varying the percent weight PVA, molecular weight of the PVA, number of freeze/thaw cycles, or the cycle duration, one can control the mechanical properties of the material making it stronger, stiffer, or

more porous as required [47]. In general, the material has similar strength to native soft tissue [46, 48]. This material, developed at Georgia Tech and protected under US patents 5,981,826 and 6,231,605 [46, 48], is now sold under the trade name Salubria™ and has been used by SaluMedica, LLC, Carticept, Inc., Mimedx, Inc., and Arthrex, Inc. in medical devices implanted in humans for nine years without any medical device reports. PVA cryogels have been shown to be approximately 50 times more compliant than polyester or PTFE [49] and may therefore be mechanically suitable for covered stent membranes. Additionally, one study has shown that important cell adhesion proteins do not readily adsorb onto PVA hydrogels [50]. This prevented cells from attaching to the material –suggesting that PVA cryogels may be able to prevent both restenosis and thrombosis.

1.6 Specific Aims

A stent covered with a non-thrombogenic membrane could prevent restenosis from neointimal hyperplasia and thrombosis. However, the membrane material must also be able to expand reliably on a stent. PVA cryogels are a promising class of biomaterials which could provide these functions. By demonstrating that these design objectives can be met, this dissertation will provide important pre-clinical feasibility and safety information for future animal and clinical trials through the following three specific aims.

I. **Evaluate PVA cryogels mechanically for covered stent applications in terms of their ultimate stretch, puncture resistance, and ability to handle the crimping and expansion processes.**

Ultimate stretch is evaluated through uniaxial tensile testing of ring segments while puncture testing is done with a modified ASTM method. PVA cryogel covered stents are fabricated by hand, crimped down, expanded on a balloon catheter, and then inspected for defects.

II. Characterize the capacity of biomaterial membranes to reduce restenosis with computational and biological models.

Finite element analysis is employed to evaluate the capacity of covered stent membranes to reduce tissue prolapse and artery wall stress. Modified Boyden chambers are used to evaluate the ability of PVA cryogel membranes to reduce vascular smooth muscle cell migration.

III. Evaluate biomaterial thrombogenicity through *in vitro* and *in vivo* testing.

For *in vitro* testing, gravity fed flow loops with porcine blood are used. *In vivo* testing is done with a sheep model as part of a study on prosthetic vein valves for chronic venous insufficiency.

1.7 References

1. Rosamond, W., et al., *Heart disease and stroke statistics--2008 update: a report from the American Heart Association Statistics Committee and Stroke Statistics Subcommittee.* Circulation, 2008. **117**(4): p. e25-146.

2. Stary, H.C., et al., *A definition of advanced types of atherosclerotic lesions and a histological classification of atherosclerosis. A report from the Committee on Vascular Lesions of the Council on Arteriosclerosis, American Heart Association.* Circulation, 1995. **92**(5): p. 1355-74.

3. Burt, H.M. and W.L. Hunter, *Drug-eluting stents: a multidisciplinary success story.* Adv Drug Deliv Rev, 2006. **58**(3): p. 350-7.

4. Serruys, P.W., et al., *A comparison of balloon-expandable-stent implantation with balloon angioplasty in patients with coronary artery disease. Benestent Study Group.* N Engl J Med, 1994. **331**(8): p. 489-95.

5. Fischman, D.L., et al., *A randomized comparison of coronary-stent placement and balloon angioplasty in the treatment of coronary artery disease. Stent Restenosis Study Investigators.* N Engl J Med, 1994. **331**(8): p. 496-501.

6. Schwartz, R.S. and D.R. Holmes, *Pigs, Dogs, Baboons, and Man - Lessons for Stenting from Animal Studies.* J Interv Cardiol, 1994. **7**(4): p. 355-368.

7. Kasaoka, S., et al., *Angiographic and intravascular ultrasound predictors of in-stent restenosis.* J Am Coll Cardiol, 1998. **32**(6): p. 1630-5.

8. Kastrati, A., et al., *Predictive factors of restenosis after coronary stent placement.* J Am Coll Cardiol, 1997. **30**(6): p. 1428-36.

9. Schofer, J., et al., *Sirolimus-eluting stents for treatment of patients with long atherosclerotic lesions in small coronary arteries: double-blind, randomised controlled trial (E-SIRIUS).* Lancet, 2003. **362**(9390): p. 1093-9.

10. Roubin, G.S., S.B. King, 3rd, and J.S. Douglas, Jr., *Restenosis after percutaneous transluminal coronary angioplasty: the Emory University Hospital experience.* Am J Cardiol, 1987. **60**(3): p. 39B-43B.

11. Topol, E.J., *Textbook of Interventional Cardiology*. 5th ed. 2008, Philadelphia: Saunders/Elsevier. xxi, 1286 p.

12. Lowe, H.C., S.N. Oesterle, and L.M. Khachigian, *Coronary in-stent restenosis: current status and future strategies.* J Am Coll Cardiol, 2002. **39**(2): p. 183-93.

13. Chen, M.S., et al., *Bare metal stent restenosis is not a benign clinical entity.* Am Heart J, 2006. **151**(6): p. 1260-4.

14. Finn, A.V., et al., *Pathological correlates of late drug-eluting stent thrombosis: strut coverage as a marker of endothelialization.* Circulation, 2007. **115**(18): p. 2435-41.

15. Ku, D.N. and C.J. Flannery, *Development of a flow-through system to create occluding thrombus.* Biorheology, 2007. **44**(4): p. 273-284.

16. Topol, E.J. and P.W. Serruys, *Frontiers in interventional cardiology.* Circulation, 1998. **98**(17): p. 1802-20.

17. Hall, P., et al., *A randomized comparison of combined ticlopidine and aspirin therapy versus aspirin therapy alone after successful intravascular ultrasound-guided stent implantation.* Circulation, 1996. **93**(2): p. 215-22.

18. Schomig, A., et al., *A randomized comparison of antiplatelet and anticoagulant therapy after the placement of coronary-artery stents.* N Engl J Med, 1996. **334**(17): p. 1084-9.

19. Bavry, A.A., et al., *Late thrombosis of drug-eluting stents: a meta-analysis of randomized clinical trials.* Am J Med, 2006. **119**(12): p. 1056-61.

20. Laskey, W.K., C.W. Yancy, and W.H. Maisel, *Thrombosis in coronary drug-eluting stents: report from the meeting of the Circulatory System Medical Devices Advisory Panel of the Food and Drug Administration Center for Devices and Radiologic Health, December 7-8, 2006.* Circulation, 2007. **115**(17): p. 2352-7.

21. Iakovou, I., et al., *Incidence, predictors, and outcome of thrombosis after successful implantation of drug-eluting stents.* JAMA, 2005. **293**(17): p. 2126-30.

22. Joner, M., et al., *Pathology of drug-eluting stents in humans: delayed healing and late thrombotic risk.* J Am Coll Cardiol, 2006. **48**(1): p. 193-202.

23. Schmehl, J.M., et al., *Silicon carbide coating of nitinol stents to increase antithrombogenic properties and reduce nickel release.* Cardiovasc Revasc Med, 2008. **9**(4): p. 255-62.

24. Slavin, L., A. Chhabra, and J.M. Tobis, *Drug-eluting stents: preventing restenosis.* Cardiol Rev, 2007. **15**(1): p. 1-12.

25. Schwarzwalder, U. and T. Zeller, *Below-the-knee revascularization. Advanced techniques.* J Cardiovasc Surg (Torino), 2009. **50**(5): p. 627-34.

26. Lobodzinski, S.S., *Bioabsorbable coronary stents.* Cardiol J, 2008. **15**(6): p. 569-71.

27. Waksman, R., *Promise and challenges of bioabsorbable stents.* Catheter Cardiovasc Interv, 2007. **70**(3): p. 407-14.

28. Ansel, G.M. and A.B. Lumsden, *Evolving modalities for femoropopliteal interventions.* J Endovasc Ther, 2009. **16**(2 Suppl 2): p. II82-97.

29. Kastrati, A., et al., *Restenosis after coronary placement of various stent types.* Am J Cardiol, 2001. **87**(1): p. 34-9.

30. Kim, S.W., et al., *Frequency and severity of plaque prolapse within Cypher and Taxus stents as determined by sequential intravascular ultrasound analysis.* American Journal of Cardiology, 2006. **98**(9): p. 1206-1211.

31. Capelli, C., et al., *Assessment of tissue prolapse after balloon-expandable stenting: influence of stent cell geometry.* Med Eng Phys, 2009. **31**(4): p. 441-7.

32. Prendergast, P.J., et al., *Analysis of prolapse in cardiovascular stents: a constitutive equation for vascular tissue and finite-element modelling.* J Biomech Eng, 2003. **125**(5): p. 692-9.

33. Lally, C., F. Dolan, and P.J. Prendergast, *Cardiovascular stent design and vessel stresses: a finite element analysis.* J Biomech, 2005. **38**(8): p. 1574-81.

34. Gu, L.X., et al., *Finite element analysis of covered microstents.* Journal of Biomechanics, 2005. **38**(6): p. 1221-1227.

35. Nagai, N., et al., *Development of novel covered stents using salmon collagen.* J Artif Organs, 2009. **12**(1): p. 61-6.

36. Deutschmann, H.A., et al., *Placement of Hemobahn stent-grafts in femoropopliteal arteries: early experience and midterm results in 18 patients.* J Vasc Interv Radiol, 2001. **12**(8): p. 943-50.

37. Dutra, C.F. and A.H. Pereira, *Digital morphometric analysis of the aortic wall in pigs following implantation of dacron-covered stents versus non-covered stents.* Acta Cir Bras, 2004. **19**(3).

38. Henry, M., et al., *Initial experience with the Cragg Endopro System 1 for intraluminal treatment of peripheral vascular disease.* J Endovasc Surg, 1994. **1**: p. 31-43.

39. Elsner, M., et al., *Coronary stent grafts covered by a polytetrafluoroethylene membrane.* Am J Cardiol, 1999. **84**(3): p. 335-8, A8.

40. Ahmadi, R., et al., *Femoropopliteal arteries: immediate and long-term results with a Dacron-covered stent-graft.* Radiology, 2002. **223**(2): p. 345-50.

41. Henry, M., et al., *Occlusive and aneurysmal peripheral arterial disease: assessment of a stent-graft system.* Radiology, 1996. **201**(3): p. 717-24.

42. Maynar, M., et al., *Cragg Endopro System I: early experience. I. Femoral arteries.* J Vasc Interv Radiol, 1997. **8**(2): p. 203-7.

43. Mewissen, M.W., *Primary nitinol stenting for femoropopliteal disease.* J Endovasc Ther, 2009. **16**(2 Suppl 2): p. II63-81.

44. Saxon, R.R., et al., *Long-term patency and clinical outcome of the Viabahn stent-graft for femoropopliteal artery obstructions.* J Vasc Interv Radiol, 2007. **18**(11): p. 1341-9; quiz 1350.

45. Serruys, P.W. and M.J.B. Kutryk, *Handbook of Coronary Stents*. 3rd ed. 2000, London, Malden, Mass., USA: Martin Dunitz; Distributed in the USA by Blackwell Science. xii,424 p.

46. Ku, D.N., L.G. Braddon, and D.M. Wootton, *Poly(vinyl alcohol) cryogel*. 1999, Georgia Tech Research Corporation, US Patent 5981826.

47. McRae-Depp, M., *PVA cryogel optimization and diffusion studies*, in *Bioengineering*. 1998, Georgia Institute of Technology: Atlanta, GA.

48. Ku, D.N., *Poly(vinyl alcohol) hydrogel*. 2001, Restore Therapeutics, US Patent 6231605.

49. Fan, J., *Dynamic strength of porcine arteries*. 2007, Georgia Institute of Technology: Atlanta, Ga.

50. Nuttelman, C.R., et al., *Attachment of fibronectin to poly(vinyl alcohol) hydrogels promotes NIH3T3 cell adhesion, proliferation, and migration.* J Biomed Mater Res, 2001. **57**(2): p. 217-23.

PART 1:

Mechanical Testing of Polyvinyl Alcohol Cryogels

CHAPTER 2:

Uniaxial Tensile Testing of Polyvinyl Alcohol Cryogels

2.1 Background

2.1.1 Bare Metal Stents

Treatment for atherosclerosis was revolutionized in the late 1970s with the invention of percutaneous transluminal coronary angioplasty (PTCA) by Andreas Grüntzig, which allowed for non-surgical management of atherosclerotic plaques. The next major change in treatment came in the 1990s when bare metal stents (BMS) were introduced and shown to be superior to PTCA alone in two clinical trials [1, 2]. BMS are small metal scaffolds that are delivered to the lesion site via catheter and deployed by either a balloon or a self-expansion mechanism. Typical BMS expand to 2.7 to 4.6 times their crimped diameter during deployment [3]. Although new types of stents have been introduced, complications from restenosis and thrombosis persist [4, 5]. Research on new stent designs and materials continues to be very active [6, 7].

2.1.2 Polyvinyl Alcohol Cryogels

Polyvinyl alcohol (PVA) is a polymer with a hydrophilic hydroxyl side group that has been used safely in medical applications, e.g. contact lenses, for many years. PVA cryogels are a new class of biomaterial which offer more strength than a typical hydrogel and have water content similar to human soft tissue [8]. By varying the percent weight PVA, molecular weight of the PVA, number of freeze-thaw cycles, or the cycle duration, one

can control the mechanical properties of the material making it stronger, stiffer, or more porous as required [9]. Greater control over the final mechanical properties makes PVA cryogels an ideal choice for covered stents because it gives the design engineer the ability to meet multiple design constraints at the same time by adjusting manufacturing parameters. In general, the material has similar strength to native soft tissue [8, 10]. This material, developed at Georgia Tech and protected under US patents 5,981,826 and 6,231,605 [8, 10], is now sold under the trade name Salubria™.

2.1.3 Uniaxial Tensile Testing

Uniaxial tensile testing of ring segments provides important information on mechanical properties such as ultimate stress, ultimate stretch, and modulus of elasticity. This method has been used to study both arteries and synthetic materials [11, 12]. Testing of ring segments is preferred over dumbbell sections to avoid problems with slipping or tearing near the grips of a dumbbell test [11, 13]. Biaxial testing can also provide useful information of mechanical properties, but was deemed unnecessary since complete constitutive models for PVA cryogels can be generated with uniaxial test data [14, 15].

2.2 Methods

2.2.1 PVA Cryogel Ring Segment Preparation

PVA (Air Products and Chemicals, Inc.) was dissolved in deionized water until it was completely solubilized by employing a combination of heat and pressure as described by Ku et al. [8]. Two different percent weight, *wt%*, formulations were prepared at 10% and

20% according to Equation 2.1 where m_{PVA} is the mass of PVA in grams and V_{H2O} is the volume of water in milliliters.

$$wt\% = \frac{m_{PVA}(g)}{V_{H_2O}(mL) + m_{PVA}(g)} \tag{2.1}$$

These formulations were chosen as practical low and high percent weights; formulations outside of this range can be used, but were deemed unlikely to have the desired mechanical characteristics *a priori*. Once prepared, the solutions were mixed to ensure uniformity and injected into tubular molds. The mold and solution were then placed in a sealed container to prevent water evaporation and subjected to four freeze-thaw cycles in order to solidify the cryogel. After thermal cycling, the newly formed cryogel tubes were removed from the mold and cut into ring segments of appropriate length for each test. Each ring segment was individually imaged alongside a reference object of known size as in Figure 2.1. Each ring segment's dimensions were determined by comparing the number of pixels of the desired dimension to the reference object using either GNU Image Manipulation Program (GNU Project) or ImageJ (National Institutes of Health) software. Each dimension was measured three times and the average is reported. Ring segments were stored in deionized water at room temperature until testing.

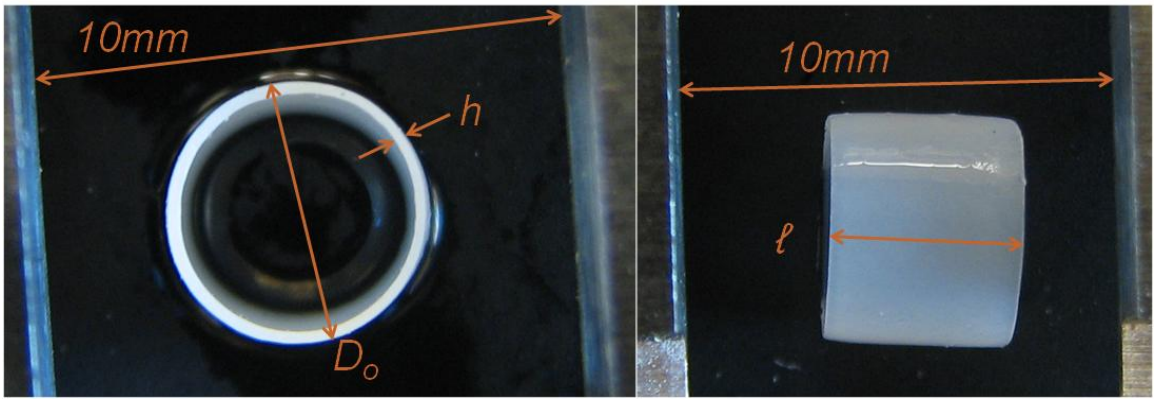

Figure 2.1: Sample measurement photos of a PVA cryogel ring segment from front (left) and side (right).

2.2.2 Calculating Stress

Stress in the ring segment is calculated as previously described [11]. To begin, the volume of the stretched ring segment is calculated by

$$V_f = \frac{\pi \ell}{4}\left(d_o^2 - \left(d_o - 2h\right)^2\right) = \pi d_o h \ell - \pi h^2 \ell \tag{2.2}$$

where V_f is final (or current) volume, ℓ is length, d_o is final outer diameter, and h is thickness. Cross-sectional area is defined as

$$A = 2h\ell \,. \tag{2.3}$$

Stretch ratio, λ, is defined as

$$\lambda = \frac{C_f}{C_i} = \frac{\pi a_0 + 2b}{\pi D_o - 2h} \tag{2.4}$$

where C_i and C_f are the initial and final circumference, D_o is the initial (unexpanded) outer diameter, and a_0 (hook diameter) and b (separation distance) are as shown as in Figure 2.2.

Assuming material incompressibility [14, 15], the initial volume can be set equal to the final volume. By eliminating small terms (less than 5% of the total numerical value), the final cross-sectional area, A_f, can be given in terms of the initial cross-sectional area, A_i, with

$$A_f = \frac{A_i}{\lambda} . \tag{2.5}$$

Cauchy stress can then be calculated by dividing the measured force, f, by the final cross-sectional area and is given by

$$\sigma = \frac{f\lambda}{2h\ell} . \tag{2.6}$$

2.2.3 Uniaxial Tensile Testing

A total of 36 ring segments were prepared, 18 of 10% PVA and 18 of 20% PVA. Dimensions for the segments were as follows: outer diameter ranged from 3.47 mm to 4.84 mm; thickness ranged from 100 μm to 280 μm; and length was between 2.73 mm

and 4.73 mm. Specialized hook fixtures were created to stretch the samples in an ElectroForce 3200 mechanical tester (Bose Corporation) with a 5 lb load cell as shown in Figure 2.3. The ring segments were placed onto the hook fixtures which were moved to a position that corresponded to a stretch ratio of 1.0. The test began by holding one hook stationary while the other advanced at a rate of either 0.1 mm/s or 1.0 mm/s until the ring segment broke. The two test speeds were chosen as reasonable lower and upper limits of expansion rates to which a membrane could be exposed during stent expansion. Nine samples of each formulation were tested at each speed and kept hydrated by a drip of deionized water. Force and displacement were continuously measured with Wintest software and exported to a data file after every test. All statistical analyses (ANOVA and ANCOVA with significance set at 0.05) were completed with SPSS Statistics 17.0 (SPSS Inc.).

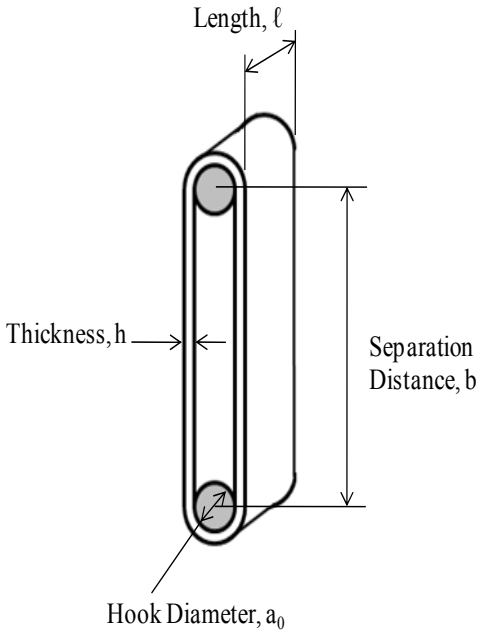

Figure 2.2: Diagram of stretched ring segment with dimensions labeled.

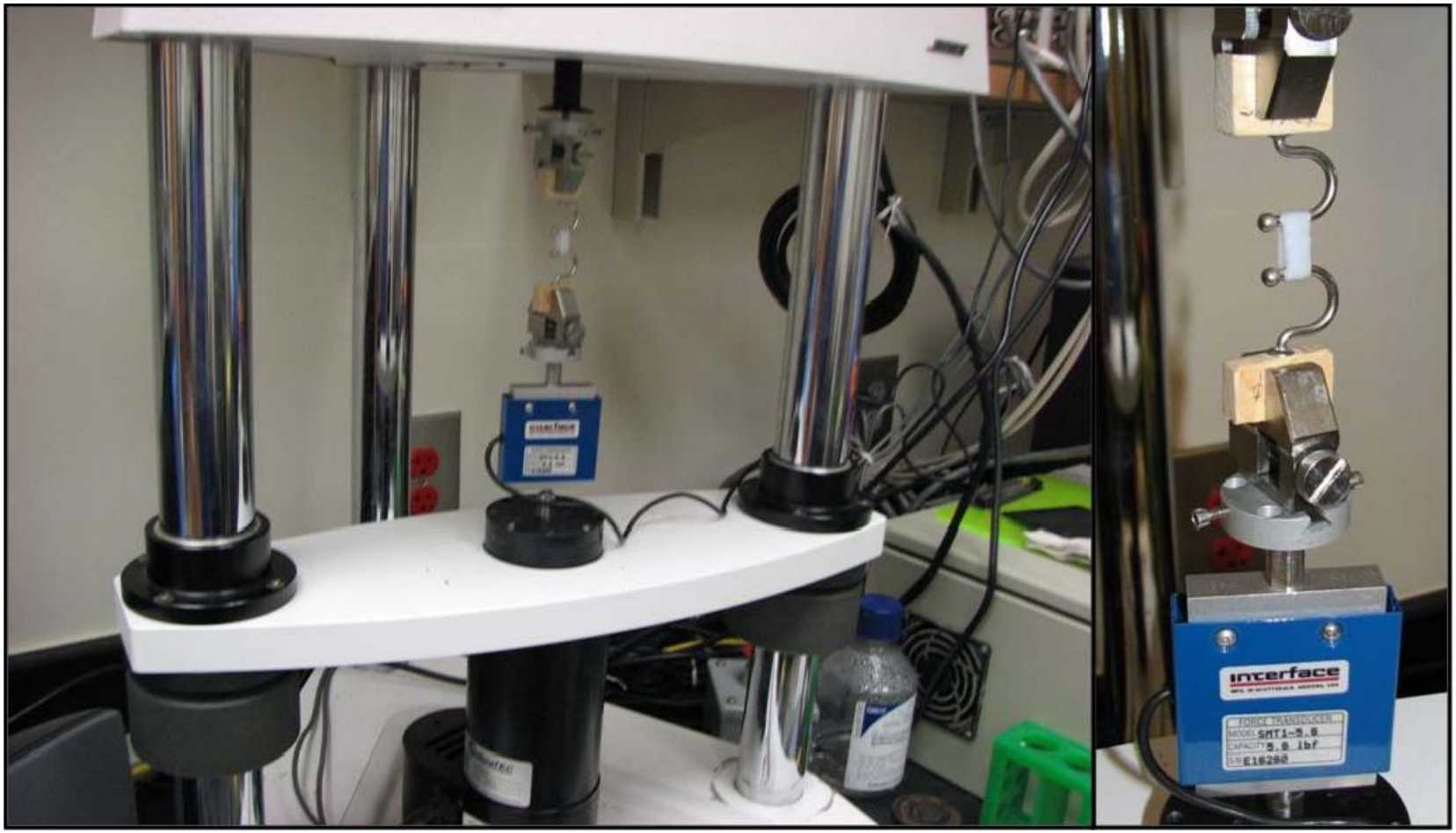

Figure 2.3: Uniaxial tensile test setup (left) and close-up view of ring segment (right).

2.3 Results

Stress-strain behavior of the PVA cryogel ring segments was non-linearly elastic with strain hardening similar to arterial tissue. Figure 2.4 shows typical loading scenarios for both a 10% and 20% PVA cryogel at the test speed of 0.1 mm/s and their relation to typical BMS expansion. The average PVA cryogel ring segment ultimate stretch ratio fell within the lower range of typical BMS stretch ratios. The ultimate strength of all samples ranged from 500 kPa to 6700 kPa depending on the percent weight formulation. The ultimate stress of the 20% PVA cryogel was significantly higher than the 10% PVA cryogel regardless of test speed ($p<0.05$). There was no statistically significant difference in ultimate stress between test speeds for either PVA formulation. Ultimate stretch ratios were similar across all variables tested. The 10% and 20% formulations both had ultimate stretch ratios of approximately 3.0. The only statistically significant difference was that the 20% PVA cryogel had a lower ultimate stretch ratio of 2.74 at the faster speed of 1.0 mm/s when compared to the slower test speed of 0.1 mm/s ($p<0.05$). Secant elastic moduli, E_{sec}, were calculated from stretch ratios of 1.0 to 1.5. Overall, the membranes increased in stiffness with increasing percent weight PVA and increasing test speed ($p<0.05$). The samples were not randomly distributed between sample groups based on the dimensions. In order to account for this, dimensions were included in the statistical analysis as covariates. See Table 2.1 for a complete breakdown of ultimate stress, ultimate stretch, and secant modulus by test speed and percent weight PVA.

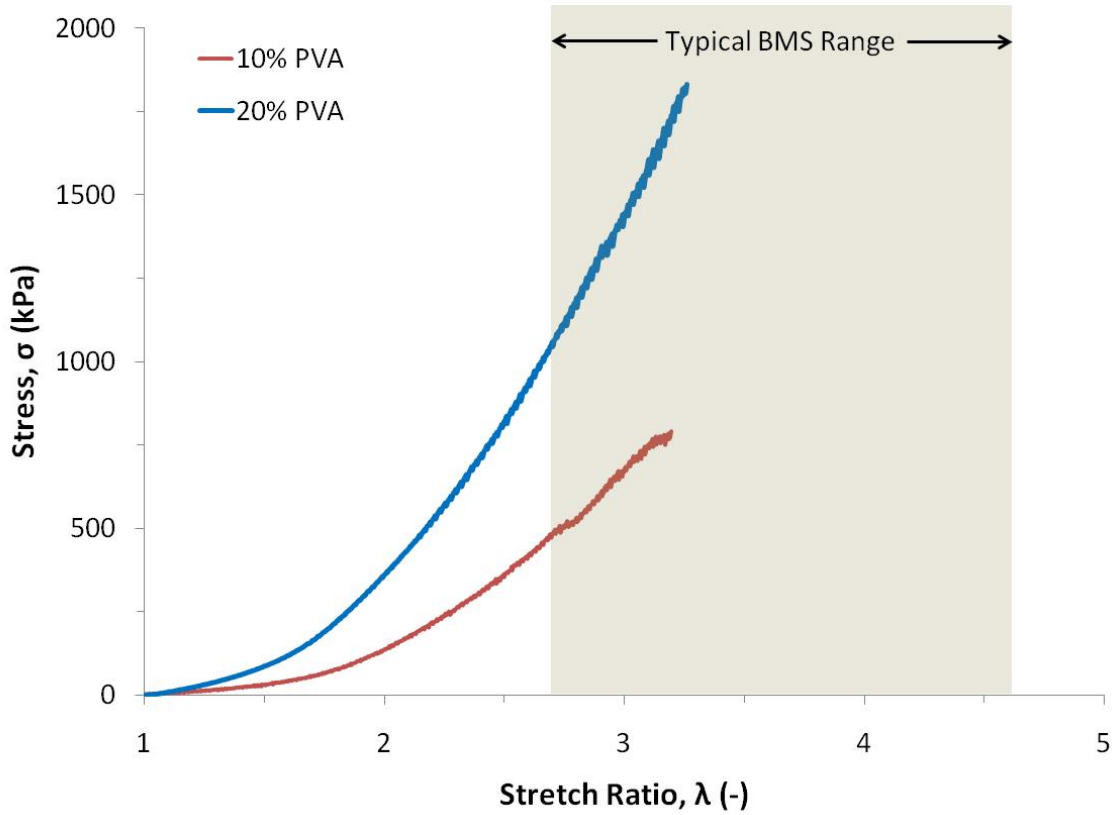

Figure 2.4: Typical stress-stretch ratio curves during uniaxial tensile testing of a 10% and 20% PVA cryogel ring segment (both at 0.1 mm/s). The ultimate stretch ratios fall within the lower half of typical BMS expansion range.

Table 2.1: Uniaxial tensile test results by percent weight PVA and test speed.

	Test Speed (mm/s)	10% PVA	20% PVA
σ_{ult} (kPa)	0.1	1200 ± 500	3500 ± 1500*
	1.0	1700 ± 810	2800 ± 1100*
λ_{ult} (-)	0.1	3.03 ± 0.28	3.08 ± 0.28
	1.0	3.08 ± 0.44	2.74 ± 0.18†
E_{sec} (kPa)	0.1	110 ± 65	360 ± 130*
	1.0	140 ± 58	490 ± 130*†

Mean ± one standard deviation. * is statistically different from 10% PVA at same test speed, $p<0.05$. † is statistically different from 0.1 mm/s at same percent weight PVA, $p<0.05$.

2.4 Discussion

Thin PVA cryogel ring segments had relatively high ultimate stretch ratios of approximately 300%. Since typical BMS stretch ratios are of the same magnitude, it is expected that PVA cryogels could serve as covered stent membranes, capable of stretching with a BMS during deployment. While one group of PVA cryogel ring segments tested (20% PVA at 1.0 mm/s) did have a slightly lower ultimate stretch ratio (274%), they still fell within the typical values for BMS and are thus deemed acceptable. The secant elastic modulus calculated over a potential working range is similar to measurements of elastic moduli of human arteries [16, 17]. The matching of elasticity could reduce restenosis caused by compliance mismatch as the mechanical properties of the membrane are similar to those of the surrounding tissue – a problem seen in vascular grafts [18].

Thick PVA cryogels have been shown previously to have ultimate stretch ratios greater than 300% [11] and thin PVA cryogels are shown here to have similar ultimate stretch ratios. The two materials currently used as synthetic vascular grafts – poly[tetrafluoroethylene] (PTFE) and poly[ethylene terephthalate] (polyester or trade name Dacron^{TM}) – are generally known to be stiff and noncompliant [13], although some expanded PTFE (ePTFE) materials are now being made with higher ultimate stretch values [19]. For covered stent applications, a compliant membrane that is able to stretch with the metal of a BMS has the potential to reduce the crimped device profile. This property has enormous potential as it improves deliverability – an extremely important parameter for surgeons when implanting stents in tortuous vessels. The PVA cryogel membranes tested here were of approximately the same thickness as a stent strut [6]

and are thus not expected to increase device profile greatly when compared to uncovered BMS.

One limitation of the present study is that while the PVA cryogel ring segments did expand to approximately the same amount as typical BMS, they fell within the lower half of that range. Given the current manufacturing techniques, these PVA cryogels would likely fail mechanically in a stent that required larger stretch. Several factors are known to affect the final mechanical properties of this material, including molecular weight and number of thermal cycles, and these parameters could be adjusted in order to achieve higher ultimate stretch [8, 20]. Alternatively, a PVA cryogel covered stent could be designed such that the membrane was not required to stretch large amounts. By covering a BMS in an expanded or partially-expanded state, and then crimping it onto a catheter, the PVA cryogel material would not be required to stretch as much as the metal during deployment. Several PVA cryogel covered stents have been made using this technique and a full description is given in Chapter 4.

In conclusion, the PVA cryogel ring segments tested had high ultimate stretch ratios and appear to be mechanically capable of expanding with a stent during deployment. The ring segments tested were approximately as thick as a stent strut and are therefore not expected to increase the crimped device profile. Furthermore, given the material's compliant nature, PVA cryogel covered stents may be able have smaller crimped profiles when compared to other non-compliant covered stent membrane materials.

2.5 References

1. Fischman, D.L., et al., *A randomized comparison of coronary-stent placement and balloon angioplasty in the treatment of coronary artery disease. Stent Restenosis Study Investigators.* N Engl J Med, 1994. **331**(8): p. 496-501.

2. Serruys, P.W., et al., *A comparison of balloon-expandable-stent implantation with balloon angioplasty in patients with coronary artery disease. Benestent Study Group.* N Engl J Med, 1994. **331**(8): p. 489-95.

3. Serruys, P.W. and M.J.B. Kutryk, *Handbook of Coronary Stents*. 3rd ed. 2000, London, Malden, Mass., USA: Martin Dunitz; Distributed in the USA by Blackwell Science. xii,424 p.

4. Bavry, A.A., et al., *Late thrombosis of drug-eluting stents: a meta-analysis of randomized clinical trials.* Am J Med, 2006. **119**(12): p. 1056-61.

5. Scott, N.A., *Restenosis following implantation of bare metal coronary stents: pathophysiology and pathways involved in the vascular response to injury.* Adv Drug Deliv Rev, 2006. **58**(3): p. 358-76.

6. Hara, H., et al., *Role of stent design and coatings on restenosis and thrombosis.* Adv Drug Deliv Rev, 2006. **58**(3): p. 377-86.

7. Serruys, P.W., M.J. Kutryk, and A.T. Ong, *Coronary-artery stents.* N Engl J Med, 2006. **354**(5): p. 483-95.

8. Ku, D.N., L.G. Braddon, and D.M. Wootton, *Poly(vinyl alcohol) cryogel*. 1999, Georgia Tech Research Corporation, US Patent 5981826.

9. McRae-Depp, M., *PVA cryogel optimization and diffusion studies*, in *Bioengineering*. 1998, Georgia Institute of Technology: Atlanta, GA.

10. Ku, D.N., *Poly(vinyl alcohol) hydrogel*. 2001, Restore Therapeutics, US Patent 6231605.

11. Fan, J., *Dynamic strength of porcine arteries*. 2007, Georgia Institute of Technology: Atlanta, Ga.

12. Lillie, M.A. and J.M. Gosline, *Mechanical properties of elastin along the thoracic aorta in the pig.* J Biomech, 2007. **40**(10): p. 2214-21.

13. Sawyer, P.N., *Modern vascular grafts*. 1987, New York: McGraw-Hill. x, 326 p.

14. Rachev, A., T. ElShazly, and D.N. Ku. *Constitutive Formulation of the Mechanical Properties of Synthetic Hydrogels*. in *ASME International Mechanical Engineering Congress*. 2004. Anaheim, CA USA.

15. Swieszkowski, W., et al., *An elastic material for cartilage replacement in an arthritic shoulder joint.* Biomaterials, 2006. **27**(8): p. 1534-41.

16. Hansen, F., et al., *Diameter and compliance in the human common carotid artery--variations with age and sex.* Ultrasound Med Biol, 1995. **21**(1): p. 1-9.

17. Riley, W.A., et al., *Ultrasonic measurement of the elastic modulus of the common carotid artery. The Atherosclerosis Risk in Communities (ARIC) Study.* Stroke, 1992. **23**(7): p. 952-6.

18. Salacinski, H.J., et al., *The mechanical behavior of vascular grafts: a review.* J Biomater Appl, 2001. **15**(3): p. 241-78.

19. *Jostent Stent Graft Peripheral (Abbott Laboratories)*. [4/2/2010]; Available from: http://www.abbottvascular.com/av_dotcom/url/content/en_US/10.10.145.10:10/general_content/Abtdiv_General_Content_0000147.htm.

20. Depp, M.M., *PVA cryogel optimization and diffusion studies*. 1998, School of Chemical Engineering, Georgia Institute of Technology, 1999. Directed by David N. Ku. p. x, 232 leaves.

CHAPTER 3:

Puncture Testing of Polyvinyl Alcohol Cryogels

3.1 Background

3.1.1 Puncture Risk

The inclusion of membranes which could detach from the metal portion of covered stents introduces a risk of membrane embolization not present with regular bare metal stents. In order to mitigate this risk, which could lead to the blockage of downstream vessels, a membrane material must be strong enough to withstand various mechanical insults without failing. One potential mechanical insult is puncture by either a stent strut or an atherosclerotic plaque. Membrane puncture would cause a tear that could lead to portions of the membrane separating from the stent, traveling downstream, and becoming lodged in smaller vessels.

3.1.2 Puncture Testing

Puncture testing is a common mechanical test that is performed in several industries including food and textile [1-3]. Puncture testing has also previously been used on vascular prostheses as a measure of “suturability” [4]. While test methods vary slightly based on application, all puncture tests consist of a membrane which is held in place while a probe of known size is advanced towards the membrane. Force and displacement are measured continuously while the probe is in contact with the membrane, which may or may not rupture depending on the parameters of the test.

During deployment, a covered stent membrane would displace from the vessel center to its edge. Thus, the deployed covered stent radius should represent a maximum value for displacement and is chosen as a minimum safety requirement against this failure mode. In the present study, the safety requirement for puncture resistance was set as a push-through displacement equal to the radius of the test mandrel on which the PVA cryogel ring segment specimens were held in place.

3.2 Methods

3.2.1 PVA Cryogel Ring Segment Preparation

PVA cryogel ring segments for puncture testing were prepared and measured by the same method as those used in the uniaxial tensile testing (Section 2.2.1). The only difference between the ring segments used in the puncture testing versus those used in the uniaxial tensile testing was that length was not measured in this study. For puncture testing, the samples only had to be long enough to cover the transverse hole and fit into the test apparatus (approximately 10 mm). Sample outer diameters ranged from 4.05 mm to 5.37 mm while the thickness ranged from 110 μm to 350 μm.

3.2.2 Puncture Testing

The puncture test method employed here was modified for covered stent membranes from an ASTM standard on the puncture testing of geotextiles [1]. PVA cryogel ring segments were placed onto a cylindrical mandrel which had a transverse hole drilled through the center; the area of the transverse hole (7.16 mm^2 or 8.04 mm^2) is typical of the area between adjacent expanded stent struts [5]. The diameter of the mandrel, 7.80

mm, was chosen in order to give the ring segments a circumferential stretch ratio between 1.5 and 2.0 – values that are expected to be within design constraints for a PVA cryogel covered stent. The sample was held stationary with vice grips while a cylindrical probe advanced towards the sample at a rate of 1 mm/s on an ElectroForce 3200 mechanical tester (Bose Corporation) with a 5 lb load cell as shown in Figure 3.1.

Every test began with the probe slightly above the test sample; the point of zero displacement was determined *post hoc* by noting the location where the load first started to increase. Each test was run until the ring segment was punctured. Six 10% and six 20% PVA cryogel ring segments were tested twice each (the two puncture sites were located 180° apart around the circumference) for a total of 24 tests. Two different diameter probes (0.84 mm and 1.37 mm) were used to represent two different sized objects which could puncture the membrane. These probe diameters were chosen in order to maintain an approximate ratio of 1:3 between the probe diameter and the transverse hole diameter (3.02 mm or 3.20 mm) to be consistent with ASTM guidelines and previous investigations on puncture strength [1, 6]. Force and displacement measurements were recorded during each test with Wintest software and exported to a data file for processing.

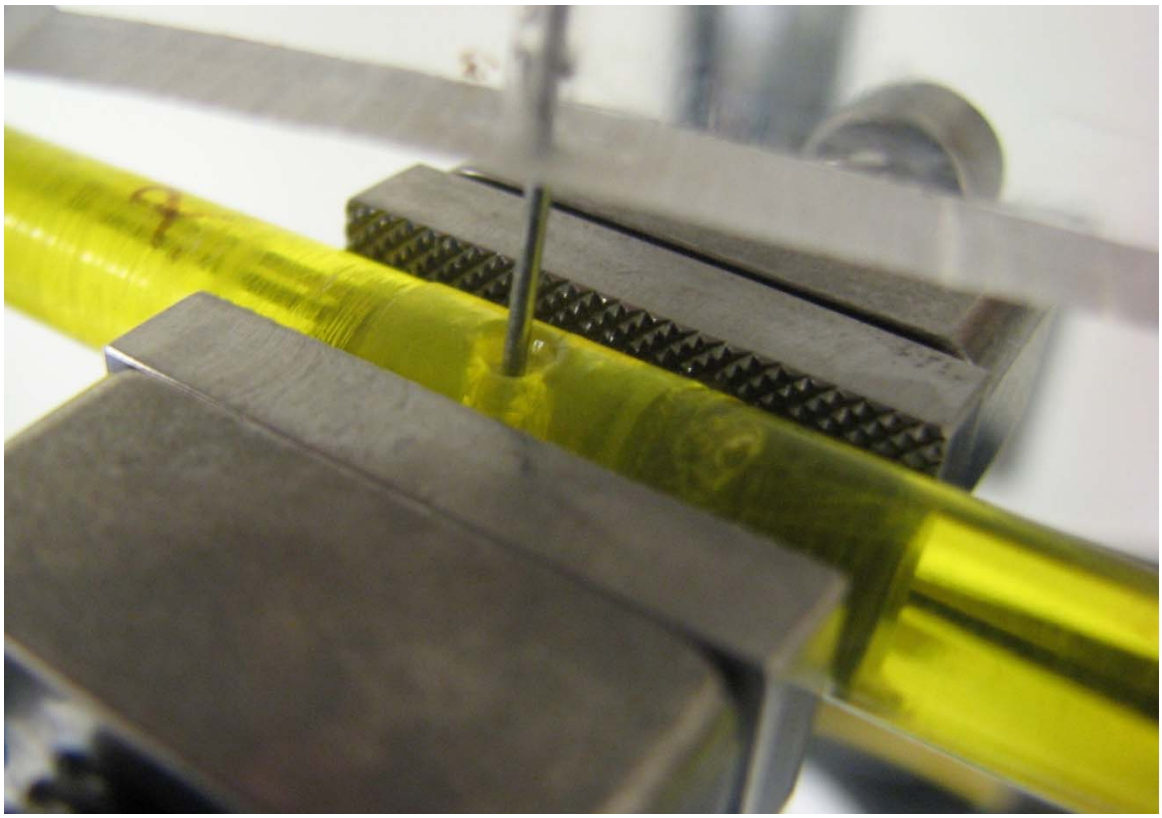

Figure 3.1: Close-up view of puncture test apparatus.

Puncture pressure was calculated by dividing the load by the cross-sectional area of the transverse hole. It is reported in mmHg and is expected to be a worst case means of comparison for extraluminal pressure. The puncture pressure represents the worst case loading scenario as it is a point load from the probe and not distributed across the entire transverse hole area. Fractional displacement is calculated by dividing the actual displacement by the test mandrel radius (3.90 mm) such that a value of 1.00 represents the pre-determined safety requirement. Membrane stiffness is reported in terms of the push-through load over thickness and as the push-through displacement over thickness. All statistical analyses were completed with SPSS Statistics 17.0 (SPSS Inc.).

3.3 Results

PVA cryogel ring segments met the pre-determined safety requirement of a push-through displacement greater than the radius of the test mandrel as seen in Figure 3.2. The 95% confidence interval of the push-through displacement was from 4.55 mm to 5.00 mm and exceeded the safety requirement of 3.9 mm. The average fractional push-through displacement was 1.22 ± 0.14 for all PVA cryogel membranes tested. Figure 3.3 shows the general shape of the load-displacement curve for two sample PVA cryogel ring segments. The only variable found to have a statistically significant effect on push-through displacement was probe diameter. The larger probe diameter had a larger push-through displacement which was significant at the $p<0.05$ level (4.56 mm vs. 4.99 mm). Fractional push-through displacement was the only other variable for which probe diameter achieved statistical significance, see Table 3.1 for a complete breakdown of all relevant variables by probe diameter.

Table 3.1: Puncture test results by probe diameter.

	0.84 mm	**1.37 mm**
Push-Through Displacement (mm)	4.56 ± 0.35	4.99 ± 0.61*
Fractional Push-Through Displacement (-)	1.17 ± 0.09	1.28 ± 0.16*
Push-Through Displacement / Thickness (-)	25.26 ± 4.04	27.02 ± 10.49
Push-Through Load (N)	0.39 ± 0.12	0.47 ± 0.25
Push-Through Load / Thickness (N/mm)	2.18 ± 0.77	2.19 ± 0.58
Push-Through Puncture Pressure (mmHg)	387.4 ± 119.3	463.7 ± 234.5

Mean ± one standard deviation. * is statistically different from 0.84 mm, $p<0.05$.

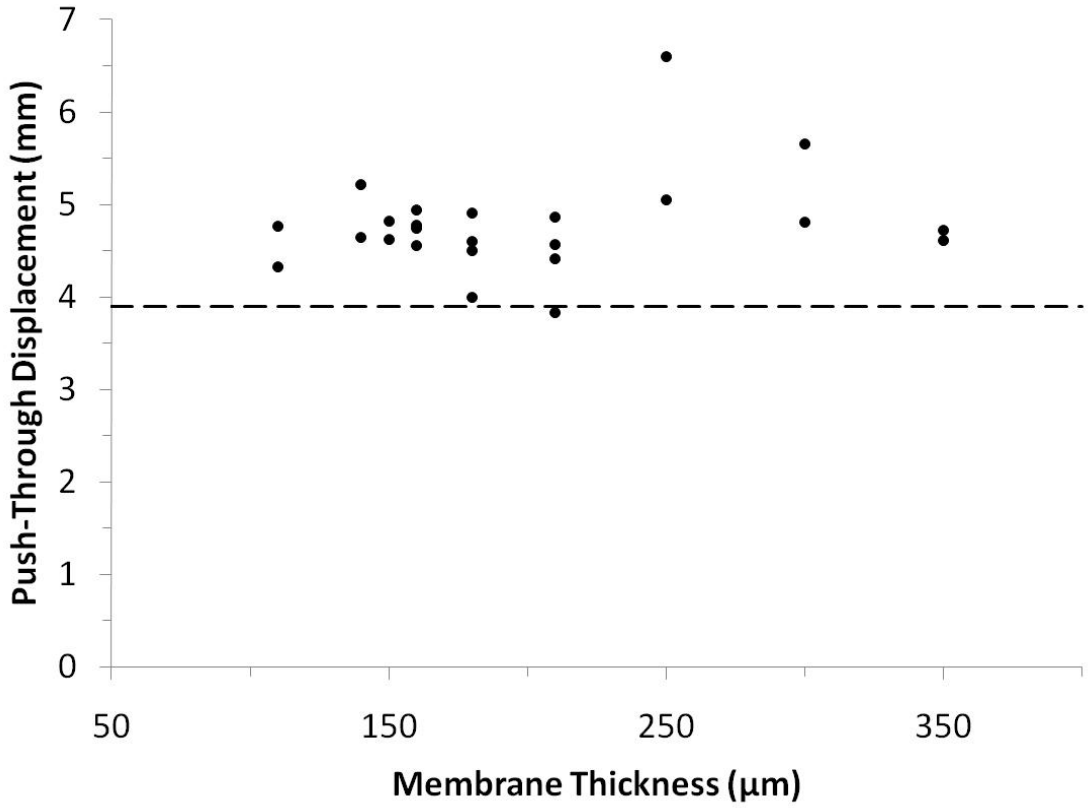

Figure 3.2: Push-through displacement versus membrane thickness for all puncture tests. The dashed line represents the pre-determined safety requirement.

Although there was no statistically significant difference in push-through displacement for percent weight PVA, 20% PVA did trend towards a larger push-through displacement value. Push-through displacement did not correlate with membrane thickness within the range tested as can be seen in Figure 3.2 ($r=0.243$, $p=0.252$). The 20% PVA formulation was stronger and stiffer than the 10% PVA formulation in that it had significantly larger push-through load, push-through puncture pressure, and push-through load over thickness ($p<0.05$). A complete breakdown of the relevant variables by percent weight PVA is given in Table 3.2. Test samples were not distributed randomly based on their stretch ratio or membrane thickness. To account for this,

stretch ratio was included as a covariate in the statistical analyses for those variables that it correlated with: puncture pressure ($r=0.570$, $p=0.004$), push-through displacement over thickness ($r=0.708$, $p<0.001$), and push-through load ($r=-0.558$, $p=0.005$). Membrane thickness was included as a covariate for both puncture pressure ($r=0.624$, $p=0.001$) and push-through load ($r=0.990$, $p<0.001$).

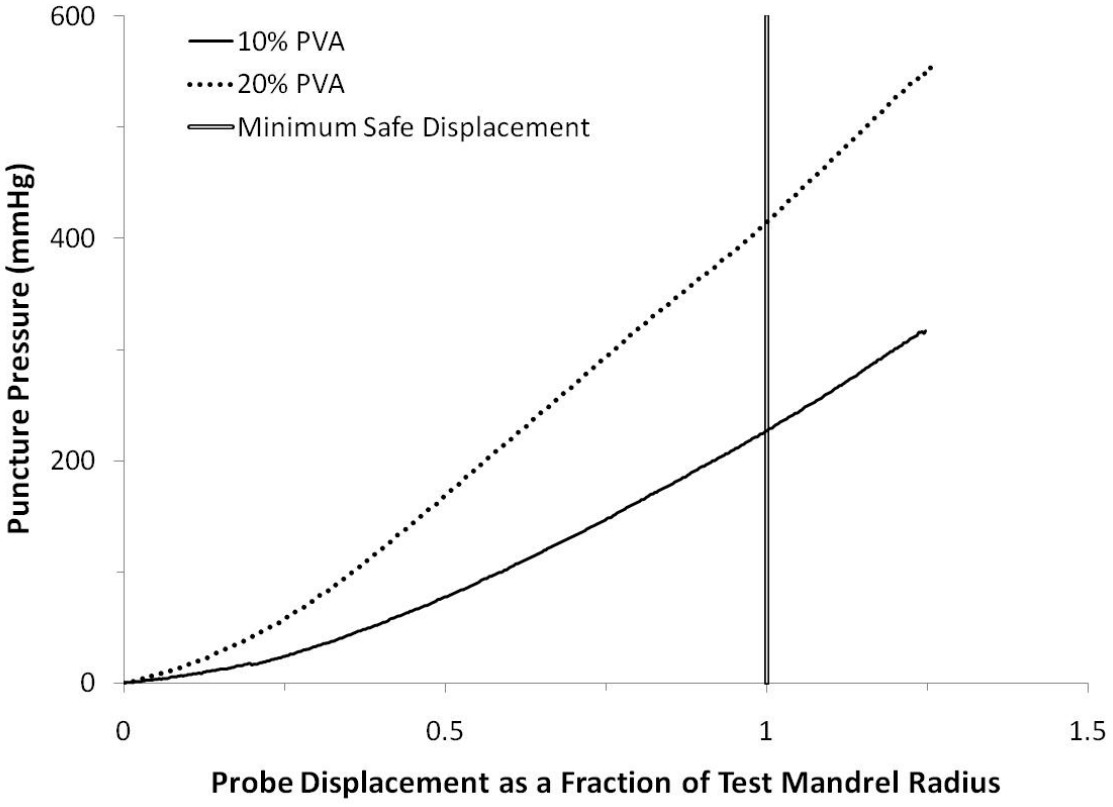

Figure 3.3: Puncture pressure (force over cross-sectional hole area) versus probe displacement for two typical PVA cryogels. A fractional displacement of 1.0 is set as the safety requirement against puncture failure.

Table 3.2: Puncture test results by percent weight PVA.

	10% PVA	20% PVA
Push-Through Displacement (mm)	4.65 ± 0.35	4.90 ± 0.66
Fractional Push-Through Displacement (-)	1.19 ± 0.09	1.26 ± 0.17
Push-Through Displacement / Thickness (-)	30.08 ± 7.79	22.20 ± 5.78
Push-Through Load (N)	0.28 ± 0.04	0.58 ± 0.17*
Push-Through Load / Thickness (N/mm)	1.81 ± 0.41	2.56 ± 0.67*
Push-Through Puncture Pressure (mmHg)	282.2 ± 47.4	425.6 ± 18.6*

Mean ± one standard deviation. * is statistically different from 10% PVA, $p<0.05$.

3.4 Discussion

Puncture testing has been used previously in many industries. Since covered stent membranes could puncture, embolize, and become lodged downstream, it is necessary to test PVA cryogels for puncture resistance before using them as covered stent membranes. The results of the present study show that PVA cryogel membranes are able to resist puncture to a pre-determined safety requirement, i.e. a push-through displacement greater than the radius of the test mandrel. For example, if the same ring segments had been placed onto a stent on a 9 Fr catheter and expanded to a diameter of 7.8 mm (the same as the test mandrel), on average they would have a factor of safety of approximately 2.0 against puncture failure. As expected, 20% PVA cryogels were stiffer and had a larger push-through load, push-through load over membrane thickness, and push-through puncture pressure than 10% PVA cryogels [7, 8]. No statistically significant difference was seen for push-through displacement between PVA formulations, although the 20% PVA cryogels did trend towards a higher value. Within the range tested, push-through displacement did not depend on membrane thickness.

Therefore, membranes as thin as 110 μm may be used without loss of puncture resistance.

The general shape of the puncture pressure-probe displacement curve (Figure 3.3) agrees well with the sample curve from the ASTM puncture testing standard [1] which gives the test method employed here validity. One limitation of the present study is that PVA cryogel ring segments were used and PVA cryogel covered stents were not. While the use of covered stents instead of ring segments is not expected to change the results significantly, it would provide a more realistic approximation of the *in vivo* case. Once a PVA cryogel covered stent design has been fixed, a second round of puncture testing is recommended to ensure that PVA cryogel covered stents have the same puncture resistance as PVA cryogel ring segments.

In conclusion, the results presented here show that PVA cryogel ring segments possess sufficient puncture strength to not tear and embolize based on the pre-determined safety requirement. Based on these findings, either PVA formulation would be acceptable although 20% PVA cryogels may be preferred in order to provide a stiffer membrane towards puncture insults and because they trended towards a higher push-through displacement. Lastly, push-through displacement did not depend on membrane thickness within the range tested (110 μm to 350 μm), allowing for a reduced crimped profile and increased deliverability with no loss of puncture resistance.

3.5 References

1. *Standard Test Method for the Static Puncture Strength of Geotextiles and Geotextile-Related Products Using a 50-mm Probe*. 2004, ASTM International D6241-04.

2. Sabato, S.F., et al., *Mechanical and barrier properties of cross-linked soy and whey protein based films.* Journal of Agricultural and Food Chemistry, 2001. **49**(3): p. 1397-1403.

3. Gontard, N., S. Guilbert, and J.L. Cuq, *Edible Wheat Gluten Films - Influence of the Main Process Variables on Film Properties Using Response-Surface Methodology.* Journal of Food Science, 1992. **57**(1): p. 190-&.

4. Larena-Avellaneda, A., et al., *Silicone-based vascular prosthesis: assessment of the mechanical properties.* Ann Vasc Surg, 2008. **22**(1): p. 106-14.

5. Bosiers, M., et al., *Does free cell area influence the outcome in carotid artery stenting?* Eur J Vasc Endovasc Surg, 2007. **33**(2): p. 135-41; discussion 142-3.

6. Park, S.K., et al., *Mechanical properties and water-vapor permeability of soy-protein films affected by calcium salts and glucono-delta-lactone.* Journal of Agricultural and Food Chemistry, 2001. **49**(5): p. 2308-2312.

7. Ku, D.N., *Poly(vinyl alcohol) hydrogel*. 2001, Restore Therapeutics, US Patent 6231605.

8. Ku, D.N., L.G. Braddon, and D.M. Wootton, *Poly(vinyl alcohol) cryogel*. 1999, Georgia Tech Research Corporation, US Patent 5981826.

CHAPTER 4:

PVA Cryogel Covered Stent Fabrication & Expansion

4.1 Background

4.1.1 Covered Stent Uses

Covered stents are typically made by combining a bare metal stent (BMS) with a membrane that spans the open areas between stent struts. Until recently, stent grafts and covered stents had been used mainly in vessel repair situations such as aneurysm or traumatic injury [1]. Today, covered stents are being investigated as a treatment for occlusive atherosclerosis [2-5]. Covered stents have the potential to prevent the vascular smooth muscle cell migration seen during in-stent restenosis with a physical barrier [6-8]. Poly[tetrafluoroethylene] (PTFE) and poly[ethylene terephthalate] (polyester or trade name Dacron^{TM}) are two potential choices for covered stent membranes given their success as synthetic vascular grafts [9]. Initial results with polyester covered stents, however, were disappointing due to high complication rates and low patency [10-12]. Since then, most industry effort has focused on PTFE or expanded PTFE (ePTFE) covered stents [1]. While progress has been made in ePTFE stents, they have not been as widely accepted as drug-eluting stents and can suffer from thrombosis problems at small diameters [13], similar to how small diameter PTFE vascular grafts have lower patency than large diameter grafts [14].

4.1.2 Covered Stent Clinical Trials

Covered stents have undergone several clinical trials in various regions including the coronary arteries, superficial femoral artery (SFA), and femoropopliteal arteries. Some of these results are summarized briefly here. The Jostent is a balloon-expandable covered stent made by sandwiching a PTFE membrane between two BMS [8] resulting in a device which is thicker than an equivalent uncovered stent. The RECOVERS trial compared the Jostent and BMS in the treatment of saphenous vein grafts of the coronary arteries. After 6 months, there was no statistically significant difference between the two groups in terms of restenosis rates and major adverse cardiac event rates, but the Jostent group did have a higher incidence of non-Q-wave myocardial infarction (12.8% versus 4.1%, p=0.013) [5]. The authors believe this difference may have been caused by a delayed endothelialization process which predisposed the PTFE covered stents to thrombotic occlusion.

The Viabahn endoprosthesis, formerly known as the Hemobahn endoprosthesis, was given FDA approval in 2005 for implantation in the SFA [1]. The Viabahn endoprosthesis is a self-expanding device which consists of an ePTFE lining with a nitinol stent externally mounted along its entire length [1]. Kedora et al. recently compared the use of the Viabahn endoprosthesis with synthetic (Dacron™ or ePTFE) femoral-popliteal bypass in the treatment of SFA occlusive disease in 100 limbs in 86 patients [3]. The study found no significant differences in primary or secondary patency between the two groups. Primary patency was 84%, 82%, 75.6%, and 73.5% for the stent graft group and 90%, 81.8%, 79.7%, and 74.2% for the bypass group at 3, 6, 9 and 12 months of follow-up. They conclude that the two treatment modes are comparable and recommend longer follow-up to determine ongoing efficacy. While this study

showed favorable results for the Viabahn endoprosthesis, other studies have shown highly variable results with six month primary patency ranging from 49% (18 patients) to 90% (80 limbs) at six months [2, 4]. The VIBRANT (Viabahn veRsus bAre Nitinol stenT) trial seeks to understand the differences between placement of an ePTFE covered stent versus an equivalent BMS in long femoropopliteal lesions. Enrollment in this study was completed at the end of 2007 and three year follow-up data should help clarify the differences between these two treatment options [1].

4.1.3 Polyvinyl Alcohol Cryogels for Covered Stents

Polyvinyl alcohol (PVA) cryogels represent a new material option for covered stents and a potential way to reduce complications from both restenosis and thrombosis. Their ability to prevent restenosis is investigated in Part 2 and their ability to prevent thrombosis in Part 3 of this dissertation. In Chapter 2, it was demonstrated that PVA cryogels have high ultimate stretch and may therefore be mechanically suitable for covered stents. Since the membranes tested were no thicker than a stent strut, they should not add much bulk to the device – resulting in a low crimped profile and high deliverability. Additionally, PVA cryogels can be used as a drug-delivery agent [15] to target drugs specifically to the lesion site if necessary. Altogether, PVA cryogels may be able to resolve current covered stent problems – making this treatment option viable for a larger number of patients and reducing the associated complication rates at the same time.

4.2 Methods

4.2.1 PVA Solution Preparation & Covering of Stents

Two PVA formulations were prepared at 15% and 20% by weight as described in Section 2.2.1; 10% PVA was not used as it was found to not fully coat stents. Concurrently, six balloon-expandable BMS made of 316L stainless steel (2 Express Biliary LD and 4 Palmaz Genesis on Opta Pro) were expanded to near their fully expanded diameter and removed from their catheter. These two stent types were selected because they were easily obtained through a vascular surgeon collaborator. Stents were dip-coated with either the 15% or 20% PVA solution to make three covered stents of each PVA formulation. Gravity caused excess PVA solution to flow out of the stent as seen in Figure 4.1. Any excess PVA solution that did not flow out of the stent was removed manually with a guide wire in order to ensure that an even coat of PVA solution covered the entire stent and was no thicker than the stent struts which were approximately 100 μm thick. Covered stents were then quickly placed into a cycling freezer for a total of eight freeze/thaw cycles in order to solidify the cryogel. Upon completion of thermal cycling, the covered stents were placed into vials of deionized water in order to maintain the material hydrated until testing could begin.

4.2.2 Crimping & Expanding of PVA Cryogel Covered Stents

To begin, each covered stent was placed back onto its original balloon catheter and crimped down by hand. The covered stent was then expanded by inflating the balloon to the manufacturer recommended value – between 8 and 10 atm. Covered stent diameter was measured with a caliper before crimping, after crimping, and after expansion. Once

expanded, each covered stent was visually inspected for tears in the PVA cryogel and separation of the PVA cryogel from the metal.

Figure 4.1: Removing excess PVA solution from stent after dip-coating. Gravity causes PVA solution to flow out of the stent – leaving behind a thin covering.

4.2.3 Environmental Scanning Electron Microscope Imaging

Images of two expanded covered stents were taken with an environmental scanning electron microscope (ESEM). The Quanta 200 (FEI Corporation) was used with a 15 kV

accelerating voltage, beam spot size of 3, and a chamber pressure of 1 Torr. In order to fit the covered stents into the ESEM chamber, a section of approximately 1 cm^2 was cut with a small scissor and laid out nearly flat. The interior of one Express stent and the exterior of one Palmaz Genesis stent (both covered with 20% PVA cryogel) were imaged at varying magnifications.

4.3 Results

Generally, coverage of stents with the PVA solution was good although on some stents there were a few cells on one or both ends that the PVA solution did not completely cover. All membranes tolerated the crimping and expansion procedure well and Table 4.1 shows the measured diameters after coating (coated diameter), after crimping (crimped diameter), and after expansion (expanded diameter) as well as the stretch ratios (crimped over coated, expanded over crimped, and expanded over coated) between the various states. The Express Biliary LD covered stents had more metal and thus were more difficult to hand-crimp than the Palmaz Genesis covered stents; as a result, their crimped diameter is slightly larger. Figure 4.2 shows a Palmaz Genesis covered stent crimped onto its balloon catheter before expansion. The average stretch ratio from the crimped to expanded state was 1.32 for the Express and 1.78 for the Palmaz Genesis covered stents. The average stretch ratio from the coated to the expanded state was 1.11 for the Express and 1.14 for the Palmaz Genesis covered stents.

Table 4.1: Covered Stent Diameter Data

Stent #	Type	Size (Mfg. Diameter x Length)	Percent Weight PVA	Coated Diameter	Crimped Diameter	Expanded Diameter	Crimped Over Coated	Expanded Over Crimped	Expanded Over Coated
1	Express Biliary LD	6 x 27	15	6.09	4.95	6.67	0.81	1.35	1.10
2	Express Biliary LD	6 x 27	20	5.86	5.1	6.59	0.87	1.29	1.12
3	Palmaz Genesis on Opta Pro	6.4 x 27	15	5.11	3.14	5.8	0.61	1.85	1.14
4	Palmaz Genesis on Opta Pro	6.4 x 27	20	5.17	3.73	6.05	0.72	1.62	1.17
5	Palmaz Genesis on Opta Pro	7.4 x 26	15	6.01	3.39	6.65	0.56	1.96	1.11
6	Palmaz Genesis on Opta Pro	7.4 x 26	20	6.19	4.14	7.03	0.67	1.7	1.14

All dimensions in mm.

Figure 4.2: Crimped PVA cryogel covered stent on balloon catheter prior to expansion.

None of the membranes had visible tears after expansion, although there was some slight separation of the PVA cryogel membrane from the metal at the s-joints on two of the Palmaz Genesis covered stents. No separation of the membrane from the metal was seen on the Express stents which did not have s-joints. Additionally, there was no tearing or loss of coverage during expansion of the cells that were not completely covered during the coating process. Photographs of an expanded Express and Palmaz Genesis stent are shown in Figure 4.3.

ESEM images of expanded PVA cryogel covered stents can be seen in Figures 4.4 to 4.8. Excellent coverage of stent struts with the PVA cryogel material was found on all covered stents that were imaged. When examining the interior (luminal) surface of the covered stents, it was difficult to locate stent struts beneath the PVA cryogel layer – indicating a smooth luminal surface which was completely covered with the PVA cryogel. On the exterior surface, stent struts were easily located and found to be entirely covered with the PVA cryogel. Slight folding of the PVA cryogel layer was found adjacent to

some stent struts as shown in Figure 4.5. No tears were found on the PVA cryogel material except at the sample edge where the covered stent had been purposely cut.

The PVA cryogel formed an extremely thin coating of all metal struts which spanned the cells between struts. In Figure 4.8, the PVA cryogel layer can be seen to be much thinner than the stent strut. By measuring the thickness in pixels and comparing to the scale bar, the PVA cryogel layer is found to be approximately 10 μm thick. Since the PVA cryogel membrane is thinner than the stent struts, it did not fill the entire volume created by neighboring struts. The PVA cryogel formed a thin layer close to the luminal side as shown in the diagram in Figure 4.9.

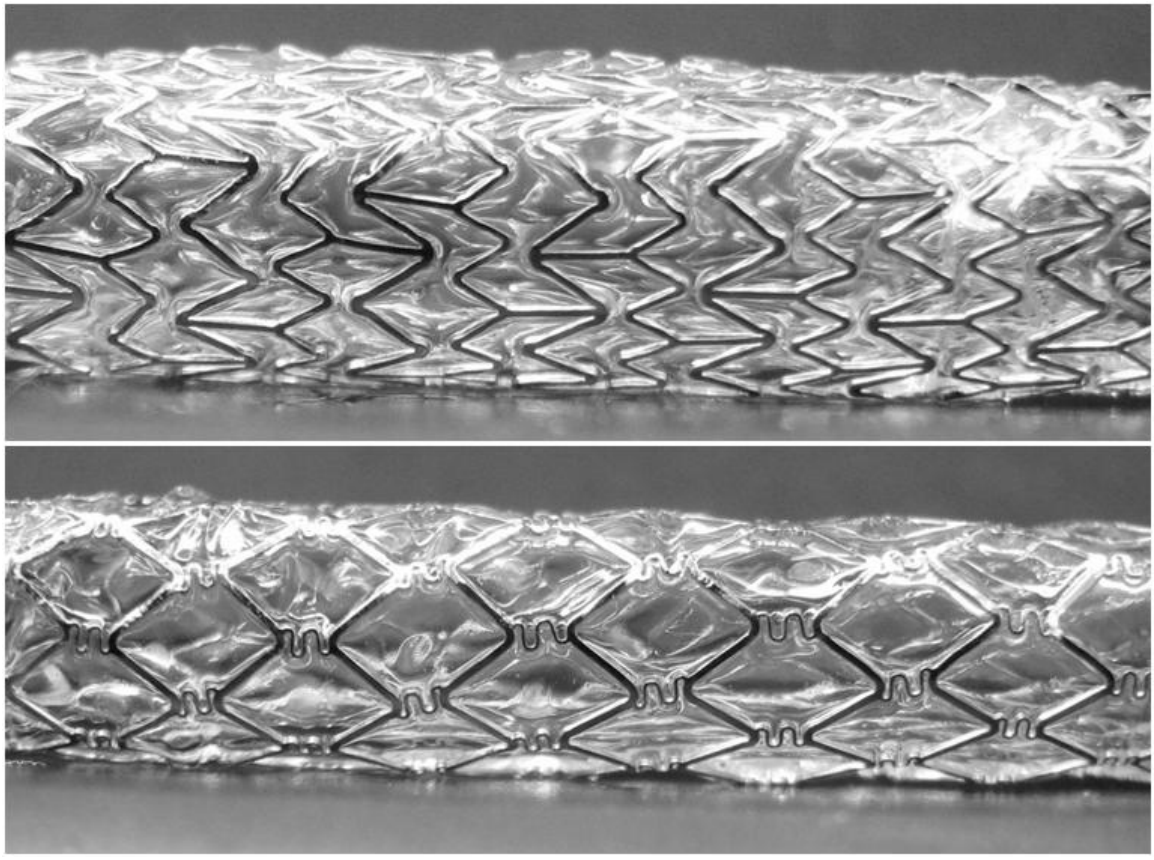

Figure 4.3: Close-up view of an expanded PVA cryogel covered Express (top) and Palmaz Genesis stent (bottom).

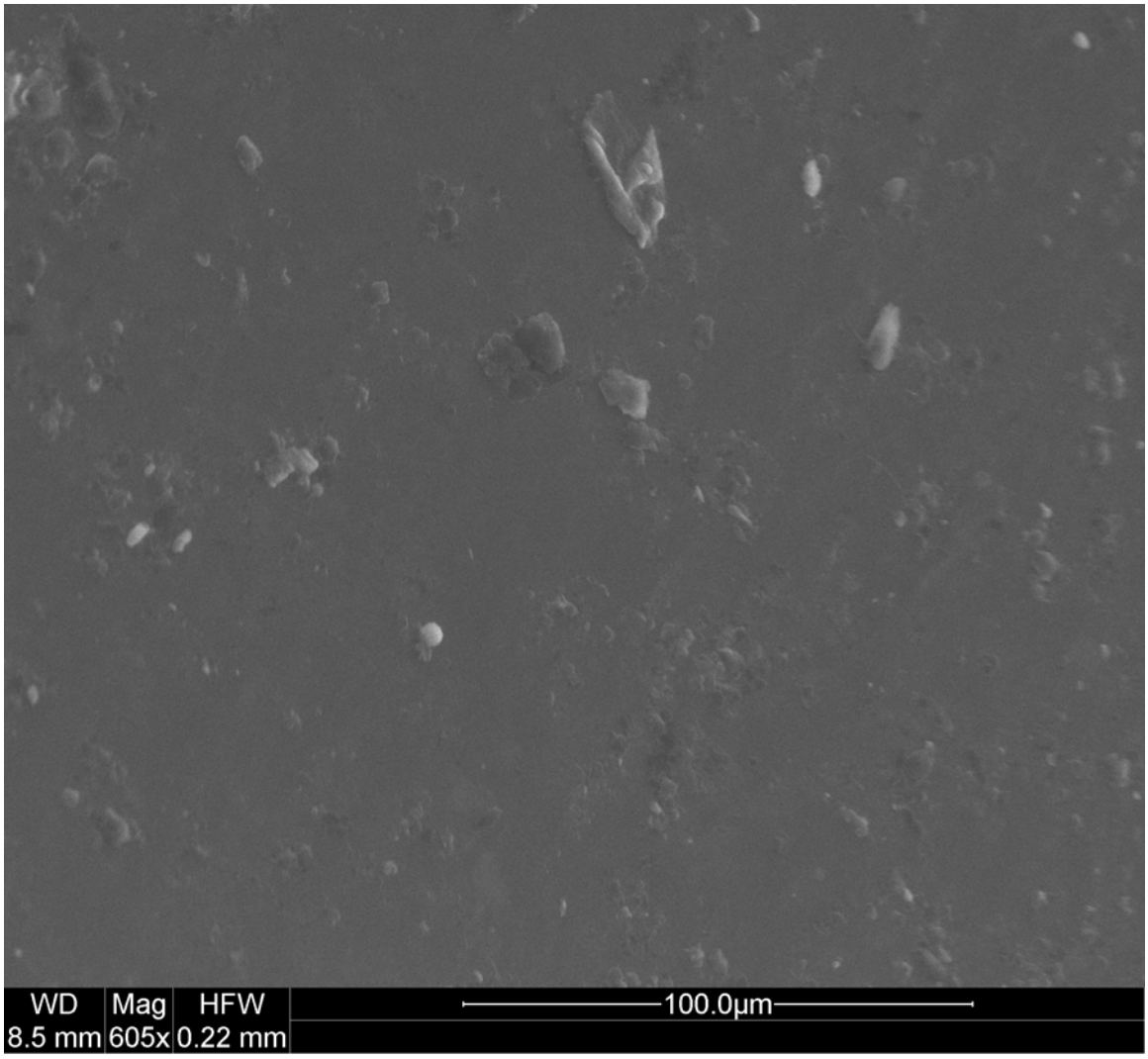

Figure 4.4: ESEM image of the interior of an expanded PVA cryogel covered Express stent. The PVA cryogel surface shown here does not appear to be porous and some small dust particles can be seen attached to the surface.

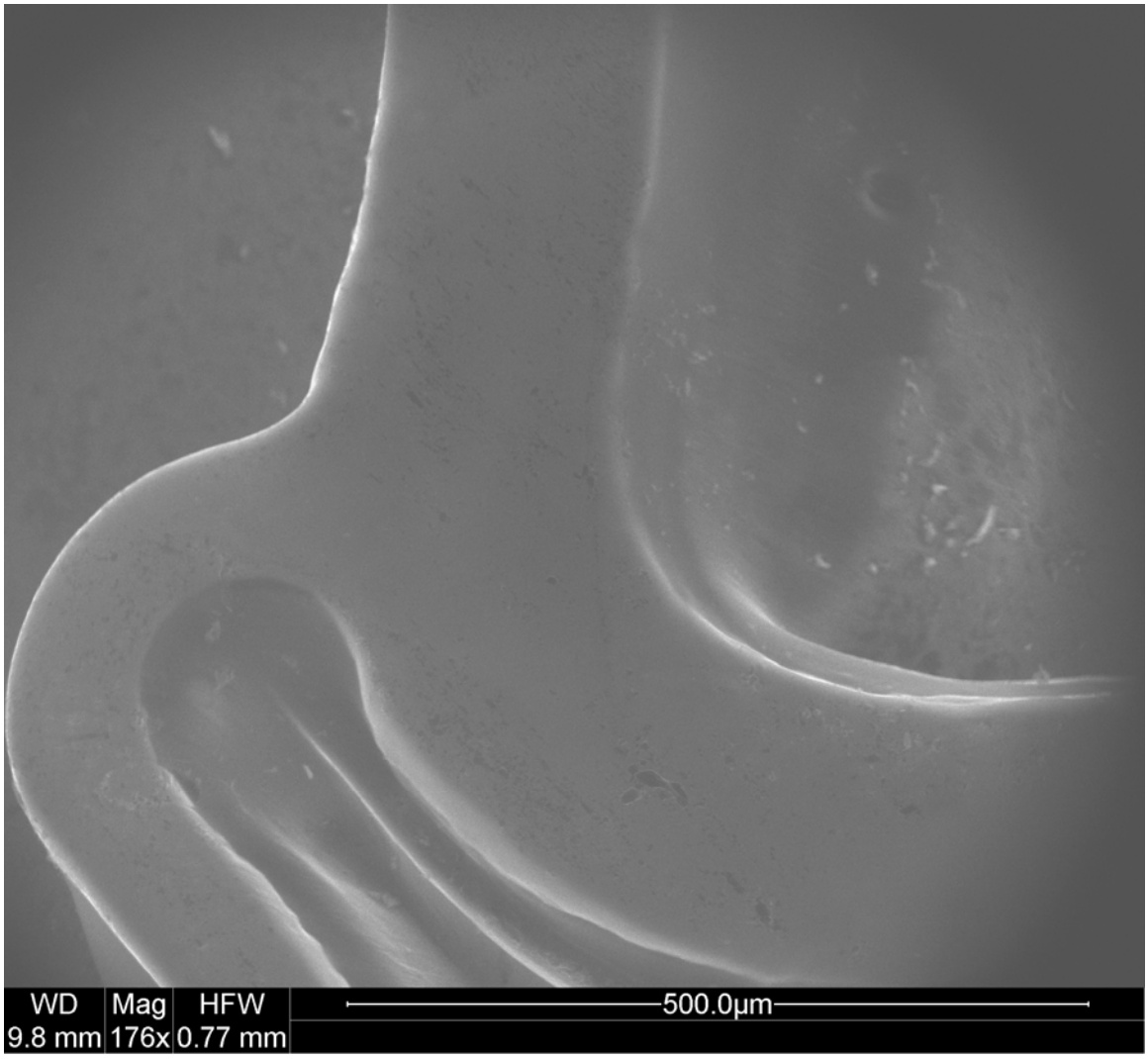

Figure 4.5: ESEM image of the exterior of an expanded PVA cryogel covered Palmaz Genesis stent. The PVA cryogel is seen here to cover the entire stent strut. Slight folding of the PVA cryogel can be seen in the region immediately adjacent to the strut.

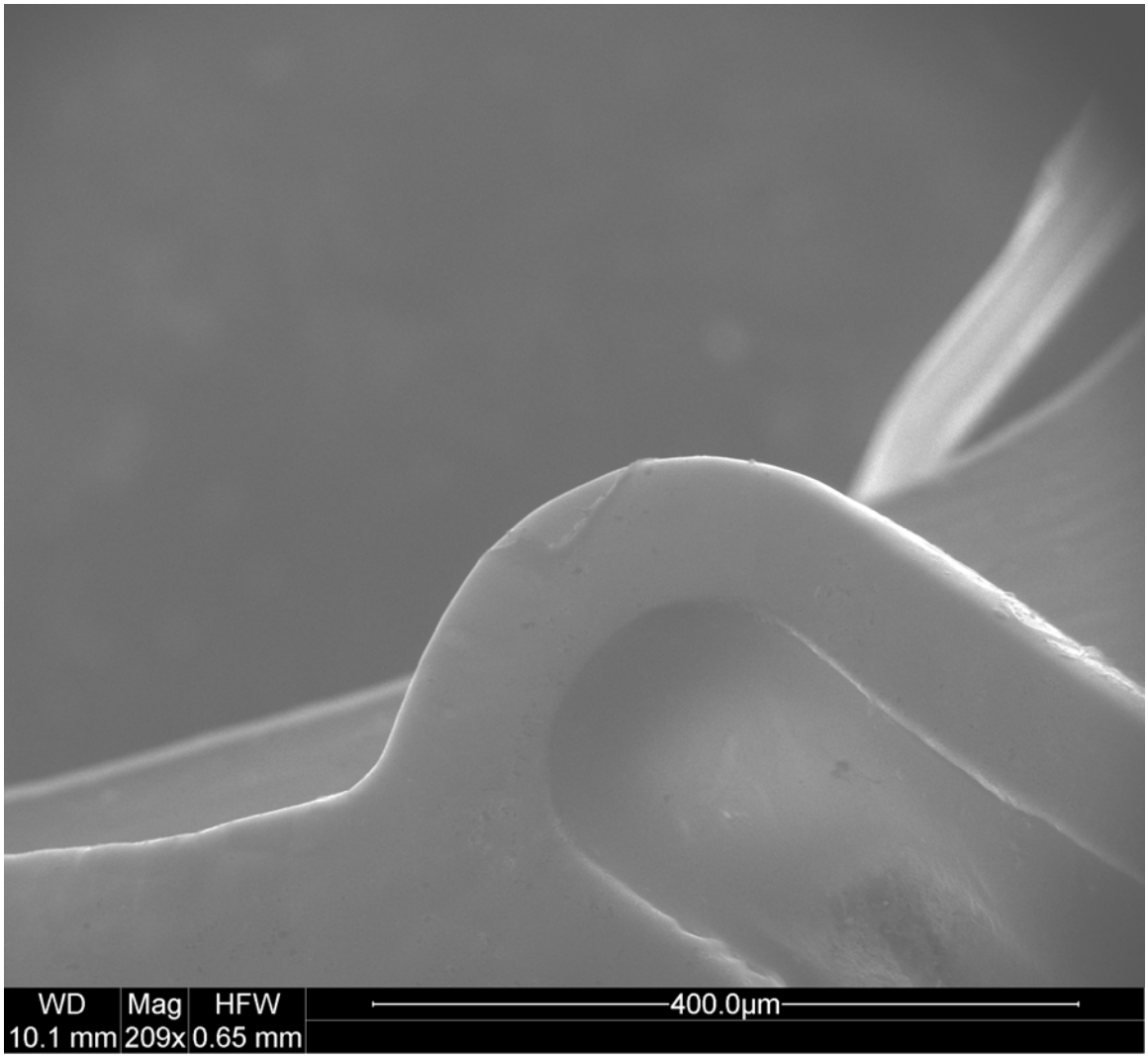

Figure 4.6: ESEM image of the exterior of an expanded PVA cryogel covered Palmaz Genesis stent at the edge where the sample was cut to fit into the ESEM. The cut edge of the PVA cryogel can be seen in the background while the foreground shows a covered stent strut with a slight tear – likely caused when the covered stent was cut.

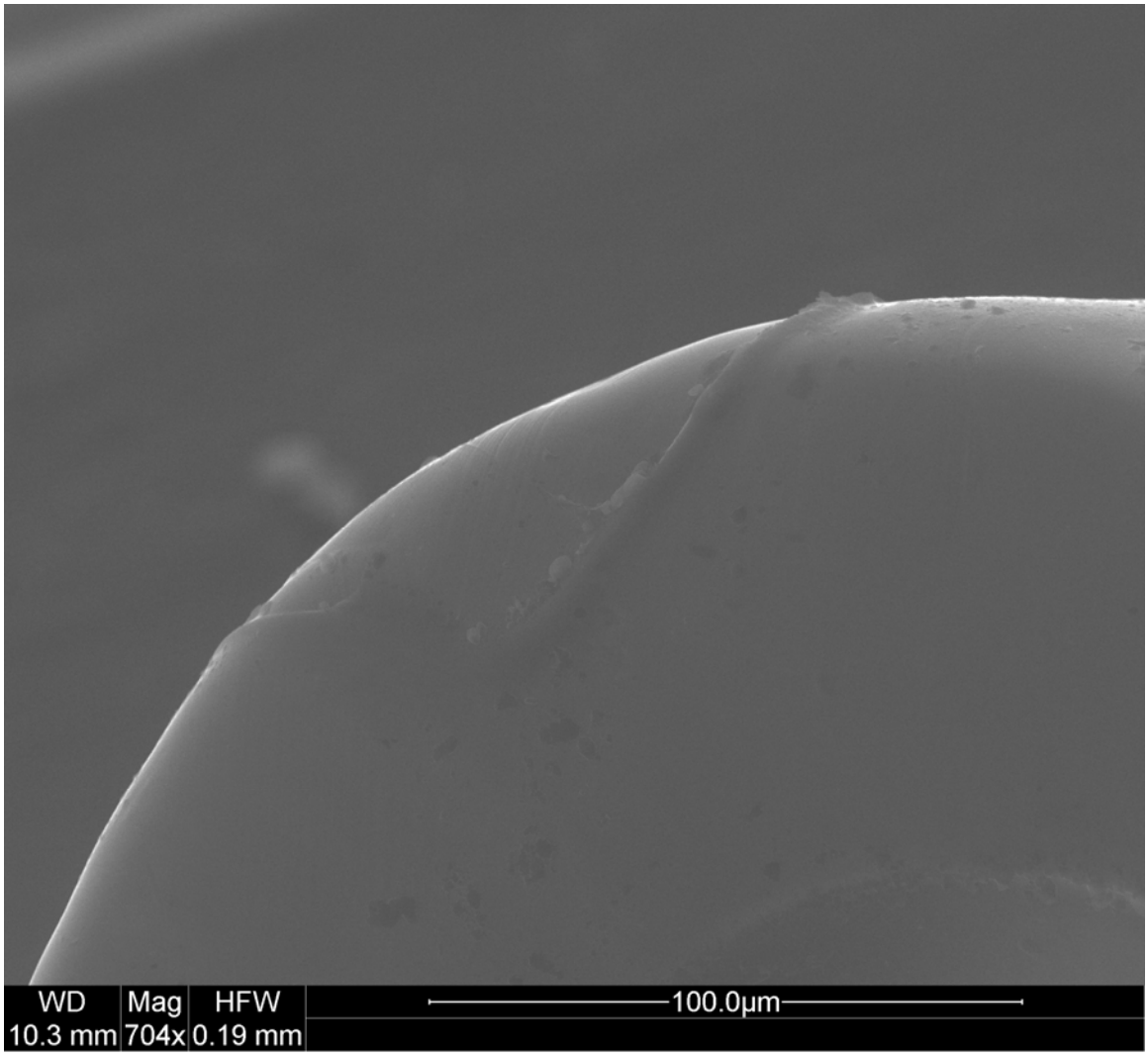

Figure 4.7: A second view of the tear in Figure 4.6 shown at higher magnification.

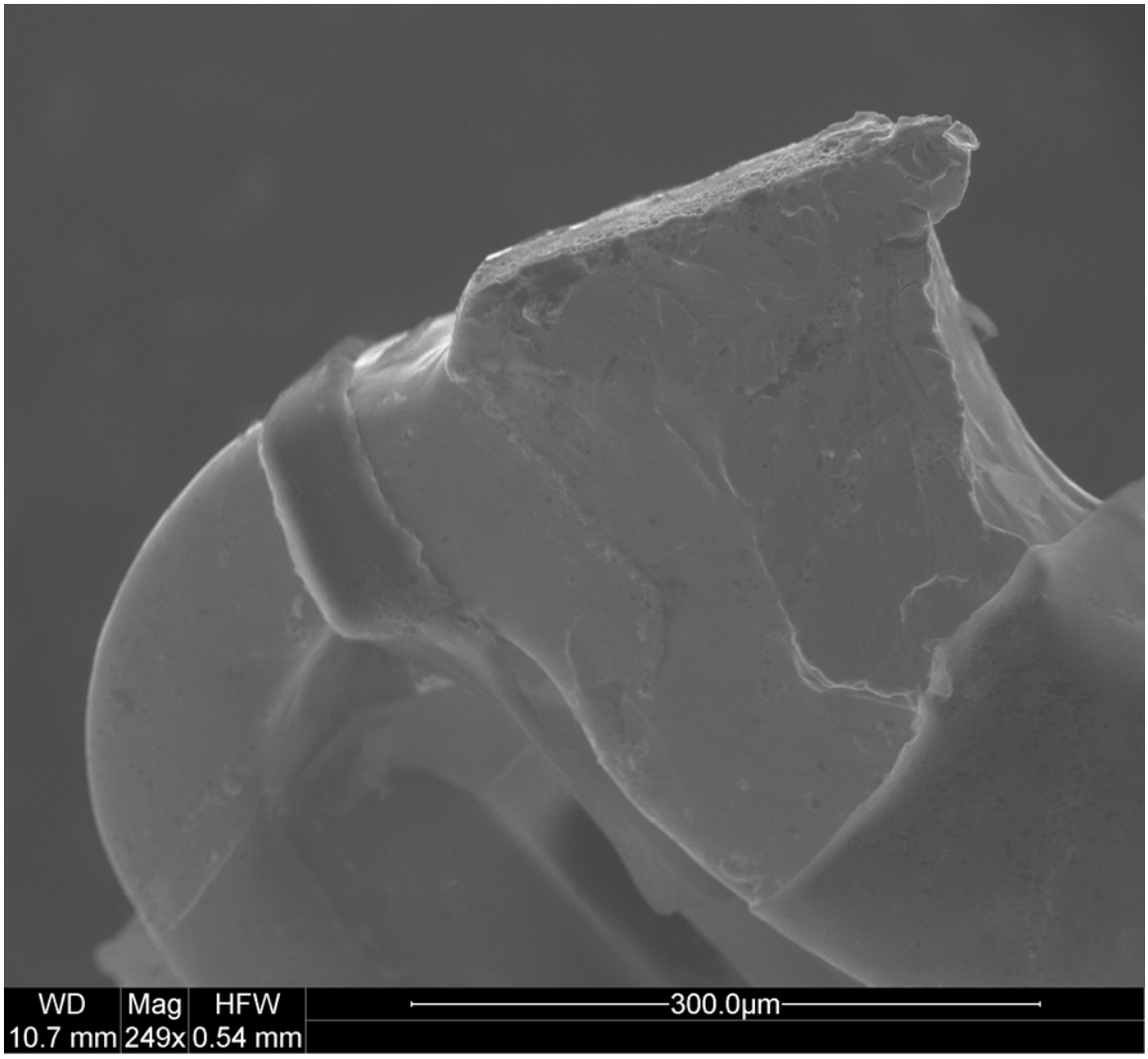

Figure 4.8: ESEM image of a Palmaz Genesis covered stent at the edge where it was cut. The PVA cryogel covering can be seen pushed back – exposing the stent metal beneath. The PVA cryogel covering is much thinner than the stent strut.

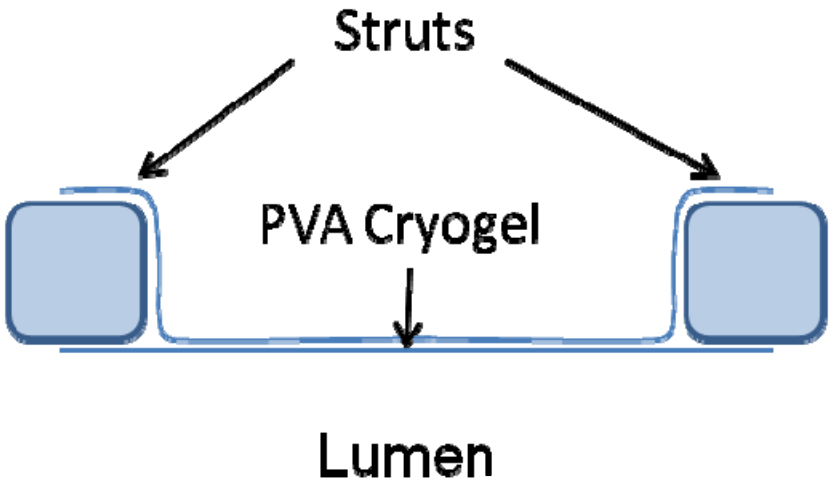

Figure 4.9: Diagram of PVA cryogel coverage of stent struts and cells.

4.4 Discussion

Vascular surgeons have begun using covered stents in a limited capacity recently as a treatment for atherosclerosis that could reduce restenosis rates when compared to BMS. Given the variability of clinical results, a greater diversity in available devices – especially materials – could lead to innovative new covered stents. Since currently available covered stents typically have high thrombosis rates in small vessels [13], exploring new materials, such as PVA cryogels, could result in the development of a covered stent with reduced thrombotic complications. Furthermore, if the material were mechanically suitable and able to form thin membranes, it could lead to a device with improved deliverability over existing covered stents.

These results demonstrate the feasibility of creating PVA cryogel covered stents, crimping them onto a balloon catheter for delivery, and expanding them to physiologically relevant diameters. No major differences were noted between the 15% and 20% PVA cryogel covered stents during the coating, hand-crimping, and expansion processes. By expanding the stents prior to coating with the PVA solution, the uniaxial tension curves in Figure 2.4 are essentially shifted to the right and a larger expanded diameter becomes possible. While only balloon-expandable stents were tested here, PVA cryogels can be used to cover self-expanding stents as well. In fact, self-expanding stents may be preferred because the multiple plastic deformations used in the covered stent fabrication process described here may induce unacceptable micro-fractures in the 316L stainless steel. This could reduce fatigue life, although no fracture issues were noticed in this study. Since self-expanding stents are designed to flex, they could be coated with PVA solution at the expanded diameter and then crimped down for delivery. Another option for making balloon-expandable PVA cryogel covered stents is to coat the stents at the unexpanded diameter. Although this fabrication method proved difficult with the hand-manufacturing techniques employed here, it should be possible with machinery. Stents covered in this manner would require further testing to ensure that the PVA cryogel membrane is able to expand without tearing. Future work should include refinements to the fabrication process of both self-expandable and balloon-expandable stents. These incremental improvements, e.g. machinery for the crimping procedure, will reduce the crimped profile beyond what was achieved here and improve device deliverability.

Differences between the two stents investigated point towards several design issues that could improve reliability and deliverability. The Express stents, which have no s-joints, had no separation of the PVA cryogel from the metal. Because of this, it is suggested

that future PVA cryogel covered stents eliminate this type of feature. Additionally, the Palmaz Genesis stents, which had fewer struts than the Express stents, could be crimped to a smaller diameter. Therefore, a covered stent with fewer struts could have a decreased crimped profile and improved deliverability. Further investigation of different stent designs will help elucidate other features to incorporate or eliminate in PVA cryogel covered stents. It is likely that both self-expandable and balloon-expandable covered stents would be useful in different areas of the vasculature, as is the case with existing stents. Since covered stents can block flow to vessels that branch off the stented segment, they would be best suited to vessels with minimal branching like the superficial femoral, femoropopliteal, and internal carotid arteries. Additionally, PVA cryogel covered stents may be useful in the treatment of abdominal aortic aneurysms as a means of excluding the aneurysm and reinforcing the vessel wall.

When examining the expanded stents visually and with ESEM, no major damage was found to the PVA cryogel membrane except for some separation at the s-joints. ESEM images clearly showed an intact PVA cryogel membrane which completely covered stent struts. The PVA cryogel layer, which was thinner than the stent strut, spanned stent cells closer to the luminal side – leaving a relatively smooth luminal surface where stent struts were difficult to locate with ESEM. The coating of stent struts and resulting smooth luminal surface will likely help to reduce platelet adhesion as the presence of stent struts has been shown to increase platelet adhesion through alterations in blood flow [16].

In conclusion, these results demonstrate the feasibility of creating PVA cryogel covered stents which are capable of withstanding crimping and expansion processes without failing mechanically. This represents a major step forward towards the creation of a new

class of covered stents which could reduce both restenosis and thrombosis rates when compared to other treatment options. Since general feasibility of PVA cryogel covered stent fabrication has been demonstrated here, future work should focus on incremental changes to stent design which can further improve reliability and deliverability.

4.5 References

1. Ansel, G.M. and A.B. Lumsden, *Evolving modalities for femoropopliteal interventions.* J Endovasc Ther, 2009. **16**(2 Suppl 2): p. II82-97.

2. Deutschmann, H.A., et al., *Placement of Hemobahn stent-grafts in femoropopliteal arteries: early experience and midterm results in 18 patients.* J Vasc Interv Radiol, 2001. **12**(8): p. 943-50.

3. Kedora, J., et al., *Randomized comparison of percutaneous Viabahn stent grafts vs prosthetic femoral-popliteal bypass in the treatment of superficial femoral arterial occlusive disease.* J Vasc Surg, 2007. **45**(1): p. 10-6; discussion 16.

4. Lammer, J., et al., *Peripheral arterial obstruction: prospective study of treatment with a transluminally placed self-expanding stent-graft. International Trial Study Group.* Radiology, 2000. **217**(1): p. 95-104.

5. Stankovic, G., et al., *Randomized evaluation of polytetrafluoroethylene-covered stent in saphenous vein grafts: the Randomized Evaluation of polytetrafluoroethylene COVERed stent in Saphenous vein grafts (RECOVERS) Trial.* Circulation, 2003. **108**(1): p. 37-42.

6. Dutra, C.F. and A.H. Pereira, *Digital morphometric analysis of the aortic wall in pigs following implantation of dacron-covered stents versus non-covered stents.* Acta Cir Bras, 2004. **19**(3).

7. Henry, M., et al., *Initial experience with the Cragg Endopro System 1 for intraluminal treatment of peripheral vascular disease.* J Endovasc Surg, 1994. **1**: p. 31-43.

8. Elsner, M., et al., *Coronary stent grafts covered by a polytetrafluoroethylene membrane.* Am J Cardiol, 1999. **84**(3): p. 335-8, A8.

9. Prager, M., et al., *Collagen versus gelatin-coated Dacron versus stretch polytetrafluoroethylene in abdominal aortic bifurcation graft surgery: results of a seven-year prospective, randomized multicenter trial.* Surgery, 2001. **130**(3): p. 408-14.

10. Ahmadi, R., et al., *Femoropopliteal arteries: immediate and long-term results with a Dacron-covered stent-graft.* Radiology, 2002. **223**(2): p. 345-50.

11. Henry, M., et al., *Occlusive and aneurysmal peripheral arterial disease: assessment of a stent-graft system.* Radiology, 1996. **201**(3): p. 717-24.

12. Maynar, M., et al., *Cragg Endopro System I: early experience. I. Femoral arteries.* J Vasc Interv Radiol, 1997. **8**(2): p. 203-7.

13. Saxon, R.R., et al., *Long-term patency and clinical outcome of the Viabahn stent-graft for femoropopliteal artery obstructions.* J Vasc Interv Radiol, 2007. **18**(11): p. 1341-9; quiz 1350.

14. Kannan, R.Y., et al., *Current status of prosthetic bypass grafts: a review.* J Biomed Mater Res B Appl Biomater, 2005. **74**(1): p. 570-81.

15. Depp, M.M., *PVA cryogel optimization and diffusion studies*. 1998, School of Chemical Engineering, Georgia Institute of Technology, 1999. Directed by David N. Ku. p. x, 232 leaves.

16. Robaina, S., et al., *Platelet adhesion to simulated stented surfaces.* J Endovasc Ther, 2003. **10**(5): p. 978-86.

CHAPTER 5:

Part 1: Conclusions, Significance, and Future Directions

The uniaxial tensile testing described in Chapter 2 demonstrated that polyvinyl alcohol (PVA) cryogel ring segments are capable of stretching to 300% of their original size – similar to how much a typical bare metal stent expands during deployment. Ultimate stretch ratios of this magnitude are a necessary characteristic of a covered stent membrane in order to avoid mechanical failure during deployment. While the ultimate stretch ratio of PVA cryogels was within the lower half of that of typical bare metal stents, PVA cryogels may not have to stretch that much if the stent is covered while in an already expanded state – a concept which was demonstrated in Chapter 4. The ring segments tested were as thin as a stent strut and thus should not increase device profile greatly. Additionally, because of the compliant nature of PVA cryogels, they may be able to reduce covered stent profile when compared to the relatively noncompliant materials polyester and polytetrafluoroethylene.

Puncture testing results indicated a high push-through displacement for all PVA cryogel membranes which was not dependent on thickness within the range tested, but was higher for the larger probe diameter. The high push-through displacement (larger than test mandrel radius) of PVA cryogel membranes is significant because it mitigates the safety concern of membrane puncture and potential embolization. Since push-through displacement did not depend on membrane thickness within the range tested, thin membranes (110 μm) could be used to make covered stents with high deliverability and no loss of puncture resistance.

The ability to make PVA cryogel covered stents by hand, crimp them onto balloon catheters, and expand them represents a major milestone in the development of these devices. While there was some minor variability between covered stents due to the hand manufacturing, visual inspection and environmental scanning electron microscope imaging showed smooth PVA cryogel surfaces and complete coverage of stent metal without tears. While the stent metal did not fracture here, multiple plastic deformations of stainless steel stents could induce micro-fractures and reduce fatigue life. In order to avoid this potential issue, balloon-expandable stents could be coated with PVA solution at the unexpanded diameter. Alternatively, self-expanding stents could be covered with PVA solution at the expanded diameter and crimped down for delivery – similar to how they are currently produced. Future PVA cryogel covered stents should be designed similar to the Viabahn Endoprosthesis to minimize the number of struts and geometry like s-joints where the PVA cryogel tended to separate from the metal. Future work should include refinements to the fabrication process including control of the PVA cryogel membrane thickness, quality control to ensure complete coverage of all stent cells, and improvement of the crimping procedure to achieve the smallest crimped profile possible.

Altogether, PVA cryogels performed well in the various mechanical tests – meeting the design requirements of high ultimate stretch and puncture resistance – and appear to be suitable for covered stents. Manufacturing feasibility was demonstrated by making, crimping down, and expanding PVA cryogel covered stents successfully without damaging the membrane. PVA cryogels represent a new material choice for covered stents and could be the key to reducing complications from both restenosis and thrombosis in the future, especially in vessels without extensive branching like the superficial femoral, femoropopliteal, and carotid arteries.

PART 2:

Polyvinyl Alcohol Cryogels for the Prevention of Restenosis

CHAPTER 6:

Finite Element Analysis of Tissue Prolapse in Stent Cells

6.1 Background

6.1.1 Finite Element Analysis of Stents & Arteries

Finite element analysis (FEA) is a powerful computational tool which can be used to analyze a number of biomechanical problems and has been employed extensively in the study of stents and arteries. One important study has shown a link between elevated arterial wall stress (calculated by FEA) and clinical restenosis rates [1]. In the study, two different stents (Medtronic's S7 and Boston Scientific's NIR) were analyzed to determine the stress that they induce on the vessel wall. The investigators found that the NIR stent induced stresses above 4 MPa in a larger volume of tissue than the S7. Clinically, the NIR stent has a six-month restenosis rate of 19% while the S7 stent had a six-month restenosis rate of 10.1% [2, 3]. While this FEA study does not provide conclusive evidence that higher artery stresses cause higher restenosis rates, it does provide some evidence and illustrates the utility of FEA in evaluating stent designs. Other investigations have focused on the stent alone and studied the effect of stent geometry on various mechanical parameters like stent recoil, longitudinal shortening, and balloon deployment pressure [4, 5]. These kinds of studies can be helpful for stent manufacturers as they create new stent designs. More complicated models have been developed which include contact between the stent, artery, and plaque [6]. One recent study combined FEA with an optimization algorithm to determine how geometrical parameters affect the competing mechanical concerns of wall stress, lumen gain, and

cyclic deflection [7]. While not directly clinically relevant, studies like this one could eventually lead to lesion-specific or patient-specific stenting by understanding the competing mechanical factors involved in these procedures.

6.1.2 Tissue Prolapse & Covered Stents

Tissue prolapse is a common event during stenting wherein the tissue between stent struts deflects inward towards the lumen. Prolapse is detectable by intravascular ultrasound, and occurs from 20% to 40% of the time, reducing lumen diameter by up to 20% [8, 9]. Two separate studies have recently used FEA to study the effects of stent cell geometry on tissue prolapse and arterial stress [10, 11]. Both studies found tissue prolapse and arterial wall stress to depend on stent cell geometry and recommended FEA as a tool to investigate future stent designs.

Covered stents have not been modeled with FEA as extensively as bare stents, although one recent study has used FEA to examine the expansion of silicone covered microstents [12]. The authors found that expansion pressure, elastic recoil, and longitudinal shortening all increased for the covered microstents when compared to bare microstents. Since covered stents span the area between stent struts with a membrane material, they will likely influence both tissue prolapse and arterial wall stress. To the author's knowledge, no study has been carried out which aims to quantify tissue prolapse and stress changes caused by covered stents when compared to bare stents.

6.2 Methods

6.2.1 Stent Cell Geometry

Two common stent cell geometries were chosen for this analysis: the “diamond” and the “w” shapes which are present in the Palmaz Genesis and Express stents shown in Chapter 4. To create the geometries, each shape was drawn on a flat plane and projected onto a cylinder that was either 3.5 mm or 7.4 mm in diameter using SolidWorks 2009 (Dassault Systèmes) in order to represent either a coronary or an iliac artery [11, 13]. The wall thicknesses were set at 0.5 mm for the coronary artery [11] and 1.3 mm for the iliac artery [13]. Each part file was exported to ProEngineer Wildfire 4.0 (Parametric Technology Corporation) where it was then converted to the IGES file format. Direct conversion to the IGES file format within SolidWorks was not done because of a compatibility issue that arose with the FEA software.

6.2.2 Material Models

Arterial tissue is assumed to be incompressible, isotropic, homogeneous, and elastic [11]. It was modeled with a reduced form of the generalized Mooney-Rivlin model given by

$$W_{artery} = a_{10}(I_1 - 3) + a_{01}(I_2 - 3) + a_{20}(I_1 - 3)^2 + a_{11}(I_1 - 3)(I_2 - 3) + a_{30}(I_1 - 3)^3 \quad (6.1)$$

I_1 and I_2 are the first and second strain invariants given by Equation 6.2 and Equation 6.3 in terms of the principal stretch ratios λ_1, λ_2, and λ_3.

$$I_1 = \lambda_1^2 + \lambda_2^2 + \lambda_3^2 \tag{6.2}$$

$$I_2 = \lambda_1^{-2} + \lambda_2^{-2} + \lambda_3^{-2} \tag{6.3}$$

Values for the model coefficients a_{10} to a_{30} are taken from a previous study of uniaxial and biaxial testing of human femoral arterial tissue and are shown in Table 6.1 [11].

Polyvinyl alcohol (PVA) cryogels are assumed to be incompressible, isotropic, homogeneous, and elastic [14]. A 20% PVA formulation was chosen as it was determined to be a likely formulation for a covered stent in Chapter 4. This material was also modeled with the Mooney-Rivlin model (Equation 6.1). Values for the model coefficients, see Table 6.1, for a 20% PVA cryogel model were calculated in ANSYS 12.0 (ANSYS, Inc.) with a linear regression algorithm based on the uniaxial test data of PVA cryogel ring segments at 0.1 mm/s in Chapter 2. Figure 6.1 shows the generated 20% PVA cryogel model with the corresponding experimental data.

Table 6.1: Mooney-Rivlin model coefficients (kPa).

	Artery [11]	**20% PVA Cryogel**
$\mathbf{a_{10}}$	18.90	-101.28
$\mathbf{a_{01}}$	2.75	107.15
$\mathbf{a_{20}}$	590.42	46.183
$\mathbf{a_{11}}$	857.18	-205.15
$\mathbf{a_{30}}$	0	330.72

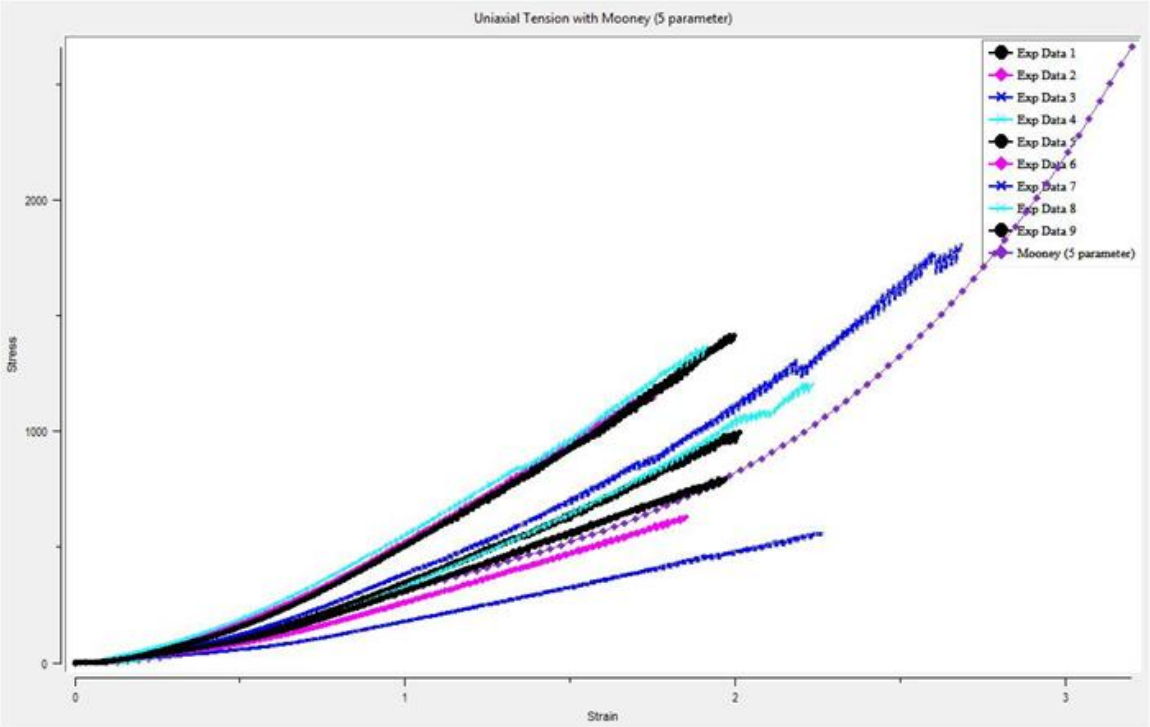

Figure 6.1: Stress-strain plot of 20% PVA cryogel material model shown with test data from Chapter 2.

6.2.3 Finite Element Analysis Parameters

Tissue prolapse is analyzed by modeling the vascular tissue contained within the stent repeating unit using ANSYS 12.0. Following the method developed by Prendergast et al. [11], an external pressure of 450 mmHg, the maximum *in vivo* pressure a stent is expected to experience, is applied to the arterial tissue. The sides of the tissue are rigidly constrained where the stent struts would be in contact with the artery wall and the luminal surface is left unconstrained. Tetrahedral SOLID285 elements (4 node, mixed u-P) were chosen for the analysis because they work well with geometries produced by CAD packages and are capable of handling the Mooney-Rivlin material model. Meshed

volumes of both the diamond- and w-shape can be seen in Figure 6.2. The diamond-shape has been reduced to a quarter model and the w-shape has been cut in half because of symmetry.

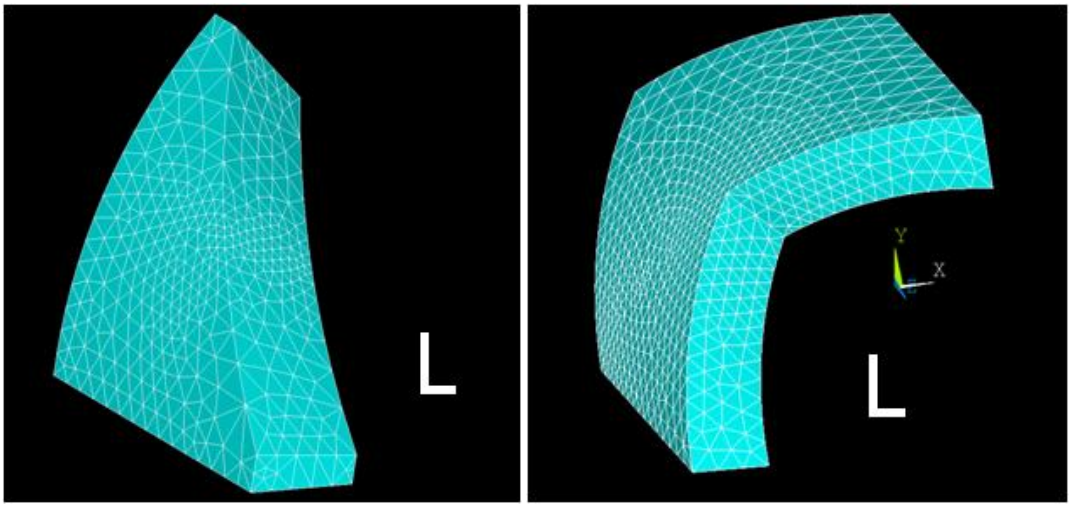

Figure 6.2: Arterial tissue mesh of diamond (left) and w (right) shape. The mesh has been made denser at areas of high stress. The 'L' illustrates the location of the luminal side.

Mesh convergence analyses were completed for all four cases to determine the sufficient mesh density. For mesh convergence, maximum displacement and maximum midline perimeter stress were monitored as the mesh was made finer. Maximum midline stress was chosen as a stable measure of stress and was measured around the perimeter of the shape as seen in Figure 6.3. Once a mesh density was selected, a 20% PVA cryogel layer was added on the luminal side of the artery that was either 100 μm or 200 μm thick. Neither the size nor the shape of the arterial tissue was altered,

only an extra layer was added to the luminal side as shown in Figure 6.3. Contact between the two materials was modeled by having nodes on the area where the two materials met shared by elements on either side of the boundary such that their displacements were matched. The maximum and average stress of a plane at the midline of the artery (surface contained within the perimeter shown in Figure 6.3) as well as maximum prolapse (radial displacement) of arterial lumen nodes are reported as a means of comparing the different cases.

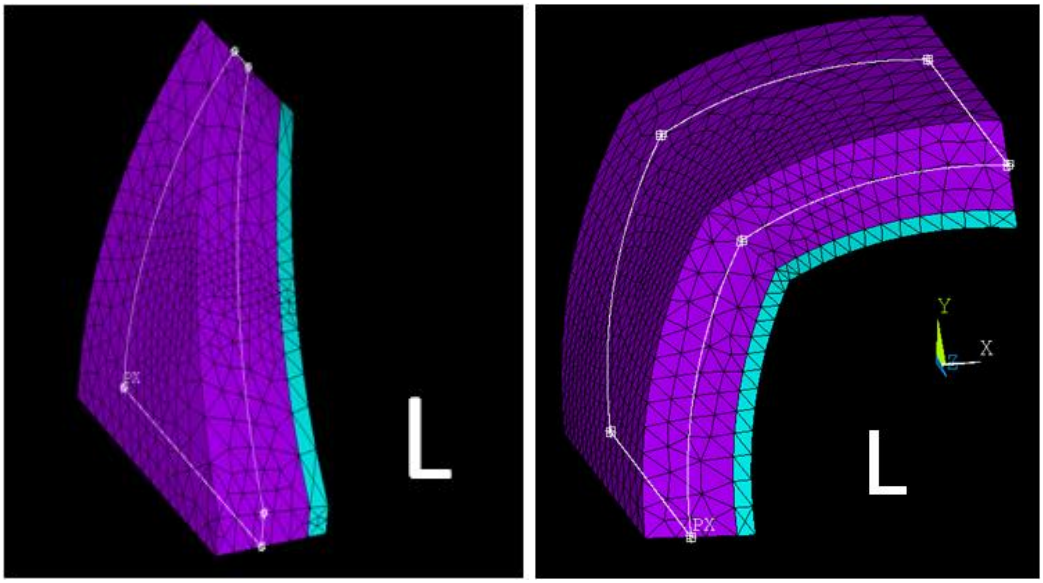

Figure 6.3: Diagram showing different material models for elements which represent artery (purple) and 20% PVA cryogel (green) for diamond (left) and w (right) shape. The white line marks the path along which the midline perimeter stress was taken for mesh convergence. The 'L' illustrates the location of the luminal side.

6.3 Results

Mesh convergence results for the small and large diameter diamond-shapes can be seen in Figures 6.4 and 6.5. The chosen mesh density had less than 5% difference in maximum displacement and maximum midline perimeter stress between itself and the finest mesh.

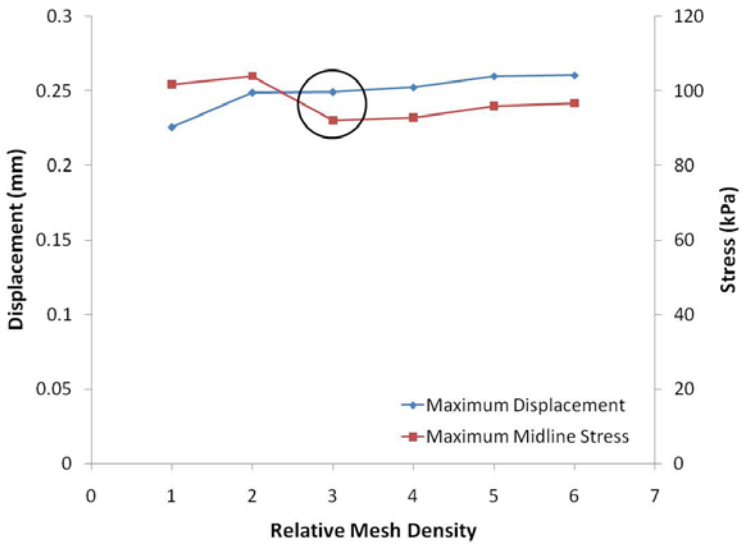

Figure 6.4: Mesh convergence for small diameter diamond-shape. Mesh density increases to the right. Circle is chosen mesh density.

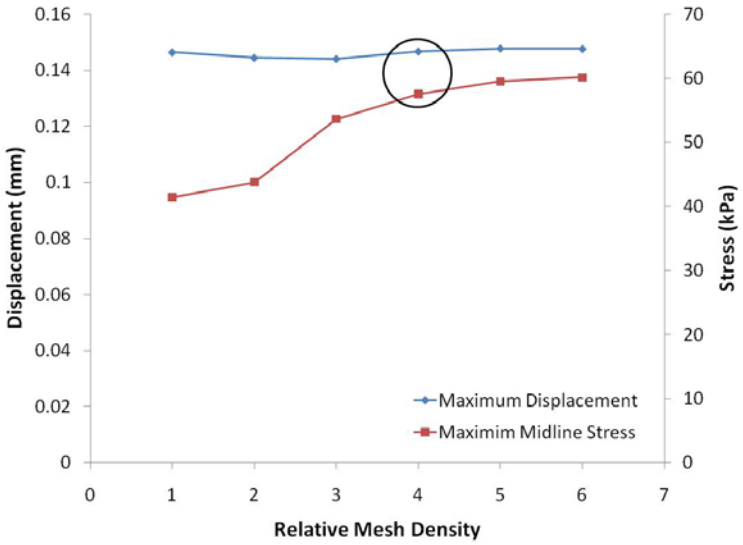

Figure 6.5: Mesh convergence for large diameter diamond-shape. Mesh density increases to the right. Circle is chosen mesh density.

Mesh convergence results for the small and large diameter w-shapes can be seen in Figures 6.6 and 6.7. For the small diameter w-shape, there was less than a 5% difference between the finest mesh and the chosen mesh density for maximum displacement and maximum midline perimeter stress. For the large diameter w-shape, there was less than a 5% difference between the finest mesh and the chosen mesh density for maximum displacement and less than a 10% difference for maximum midline perimeter stress.

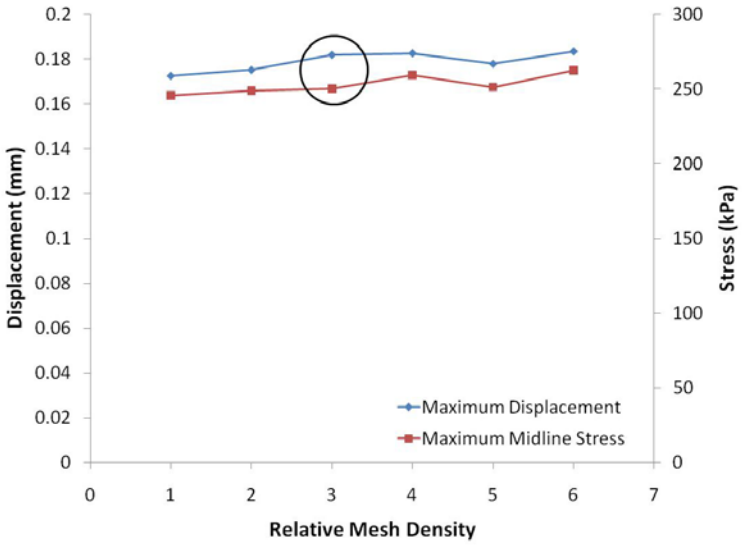

Figure 6.6: Mesh convergence for small diameter w-shape. Mesh density increases to the right. Circle is chosen mesh density.

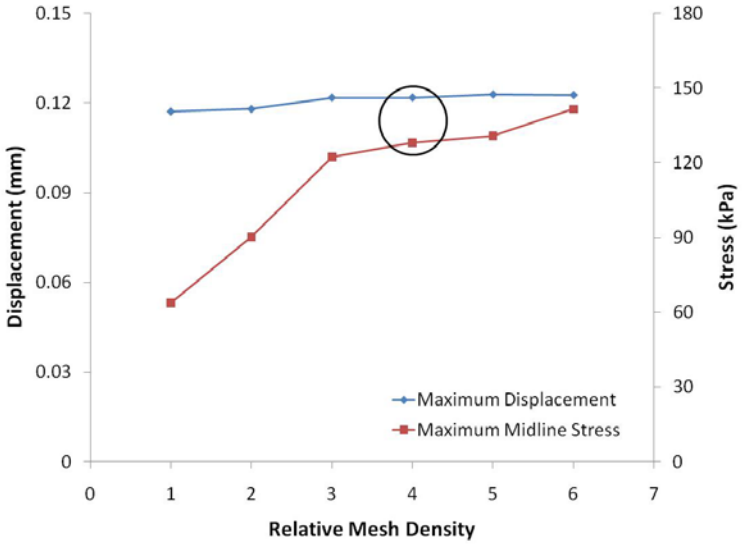

Figure 6.7: Mesh convergence for large diameter w-shape. Mesh density increases to the right. Circle is chosen mesh density.

Maximum midline stress, average midline stress, and maximum prolapse for each of the four cases are reported in Tables 6.2 to 6.5 and can be seen in Figures 6.8 to 6.19. Maximum prolapse, δ, is the radial displacement of the nodes on the luminal arterial surface and was calculated by

$$\delta = \sqrt{U_x^2 + U_y^2} \tag{6.4}$$

where U_x and U_y are the displacements in the x- and y-direction, respectively. Prolapse was greater in the smaller diameter vessels for both shapes. The diamond-shape elicited more prolapse than the w-shape at both vessel diameters. Overall, the stent covering caused a reduction in prolapse. The reductions in prolapse were greater for the smaller diameter vessels than for the larger diameter vessels. The small diameter diamond-shape had the largest percent reduction in prolapse of 13% with the addition of a 200 μm thick PVA cryogel layer. Reductions in prolapse caused by the addition of a PVA cryogel layer strongly correlated with prolapse in the uncovered state for both the 100 μm ($r=0.964$, $p=0.036$) and the 200 μm ($r=0.981$, $p=0.019$) thick PVA cryogel layer.

Maximum and average midline stresses were higher in the smaller diameter vessel for both shapes. When comparing stent shapes, maximum midline stress was higher for the w-shape while the average midline stress was higher for the diamond-shape. The stent covering reduced the stress values in the midline of the artery wall. Furthermore, the thicker the covering, the more the stress was reduced. Overall, stresses were reduced by a larger percent than prolapse. The small diameter diamond-shape had the largest percent reduction in stress with a 29% reduction of the maximum midline stress and a 23% reduction in average midline stress when a 200 μm thick PVA cryogel layer

was added. Reductions in maximum midline stress caused by the 100 μm thick PVA cryogel layer strongly correlated with the maximum midline stress caused by the uncovered stent ($r=0.968$, $p=0.032$). Reductions in average midline stress caused by the 200 μm thick PVA cryogel layer strongly correlated with the average midline stress caused by the uncovered stent ($r=0.960$, $p=0.040$).

Table 6.2: Prolapse and midline stress for small diameter diamond-shape.

PVA Cryogel Thickness (μm)	0	100	200
Maximum Prolapse (mm)	0.241	0.228	0.210
Maximum Midline Stress (kPa)	153.86	133.73	108.61
Average Midline Stress (kPa)	82.51	73.81	63.89

Table 6.3: Prolapse and midline stress for large diameter diamond-shape.

PVA Cryogel Thickness (μm)	0	100	200
Maximum Prolapse (mm)	0.138	0.138	0.138
Maximum Midline Stress (kPa)	57.50	55.58	53.08
Average Midline Stress (kPa)	34.27	32.98	31.09

Table 6.4: Prolapse and midline stress for small diameter w-shape.

PVA Cryogel Thickness (μm)	0	100	200
Maximum Prolapse (mm)	0.182	0.178	0.171
Maximum Midline Stress (kPa)	250.52	225.41	218.07
Average Midline Stress (kPa)	77.43	73.37	65.53

Table 6.5: Prolapse and midline stress for large diameter w-shape.

PVA Cryogel Thickness (μm)	0	100	200
Maximum Prolapse (mm)	0.117	0.117	0.116
Maximum Midline Stress (kPa)	127.98	119.84	116.97
Average Midline Stress (kPa)	32.15	31.36	29.97

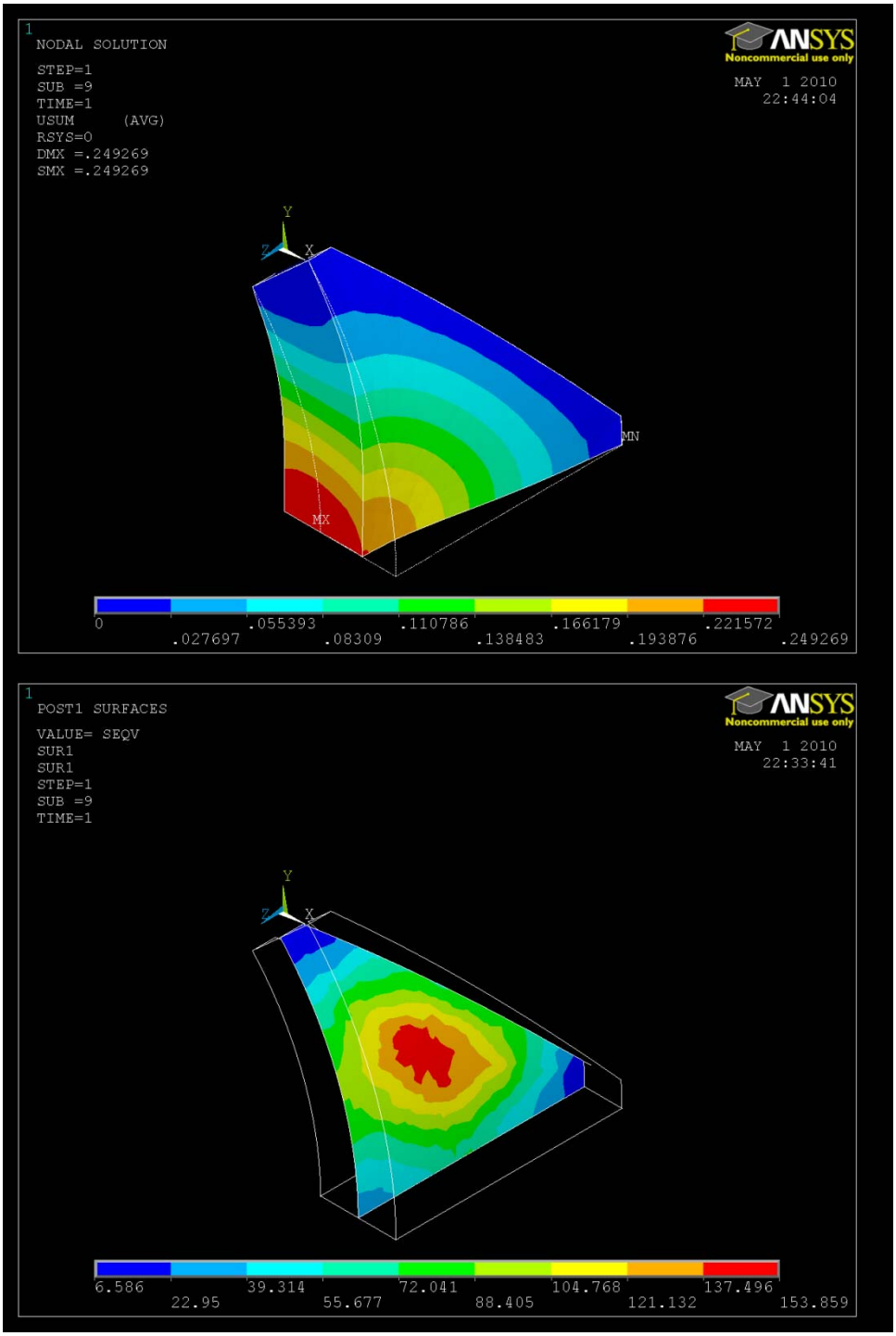

Figure 6.8: Displacement with undeformed edge (top) and midline stress (bottom) for small diameter diamond-shape with no PVA cryogel layer.

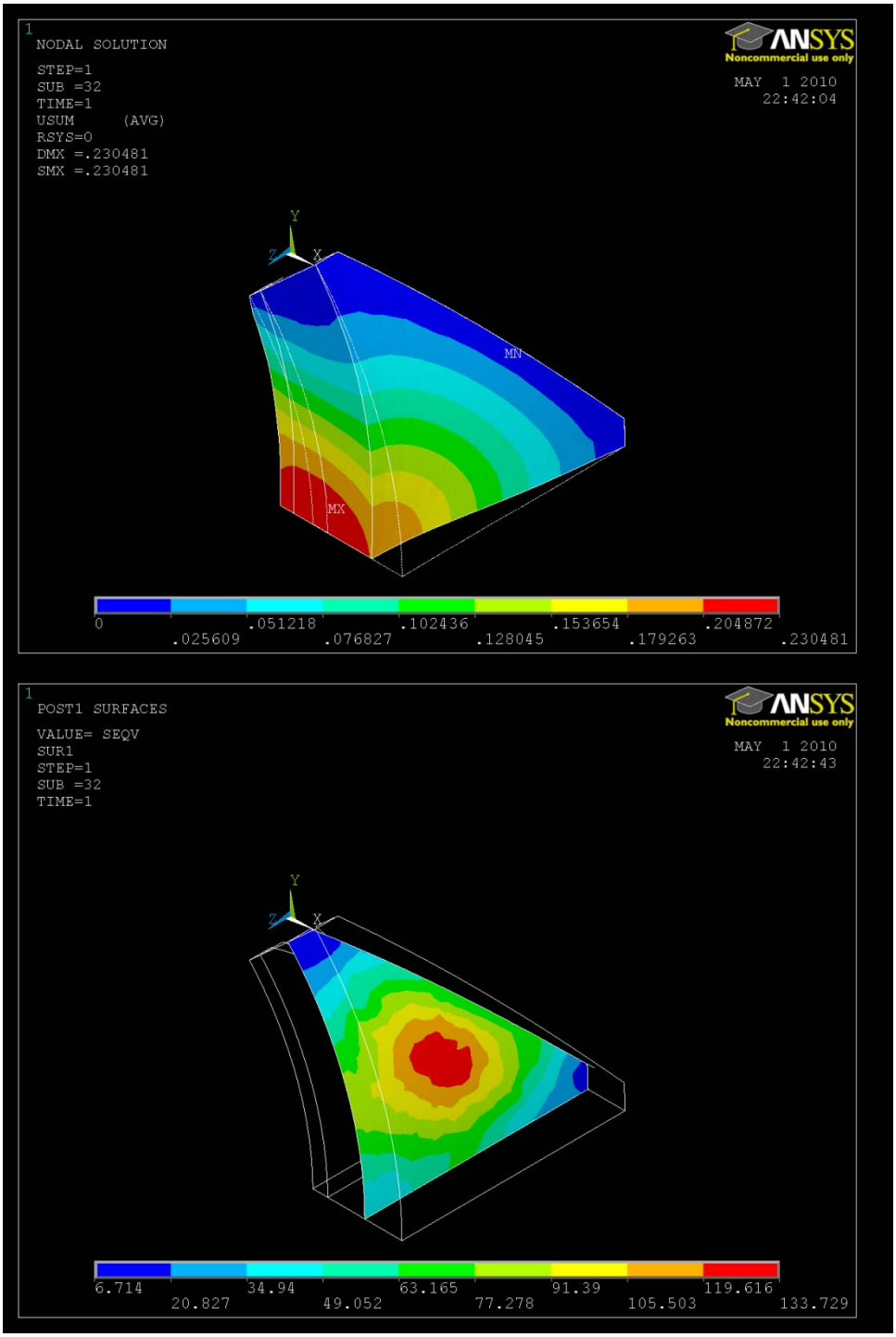

Figure 6.9: Displacement with undeformed edge (top) and midline stress (bottom) for small diameter diamond-shape with 100 μm thick PVA cryogel layer.

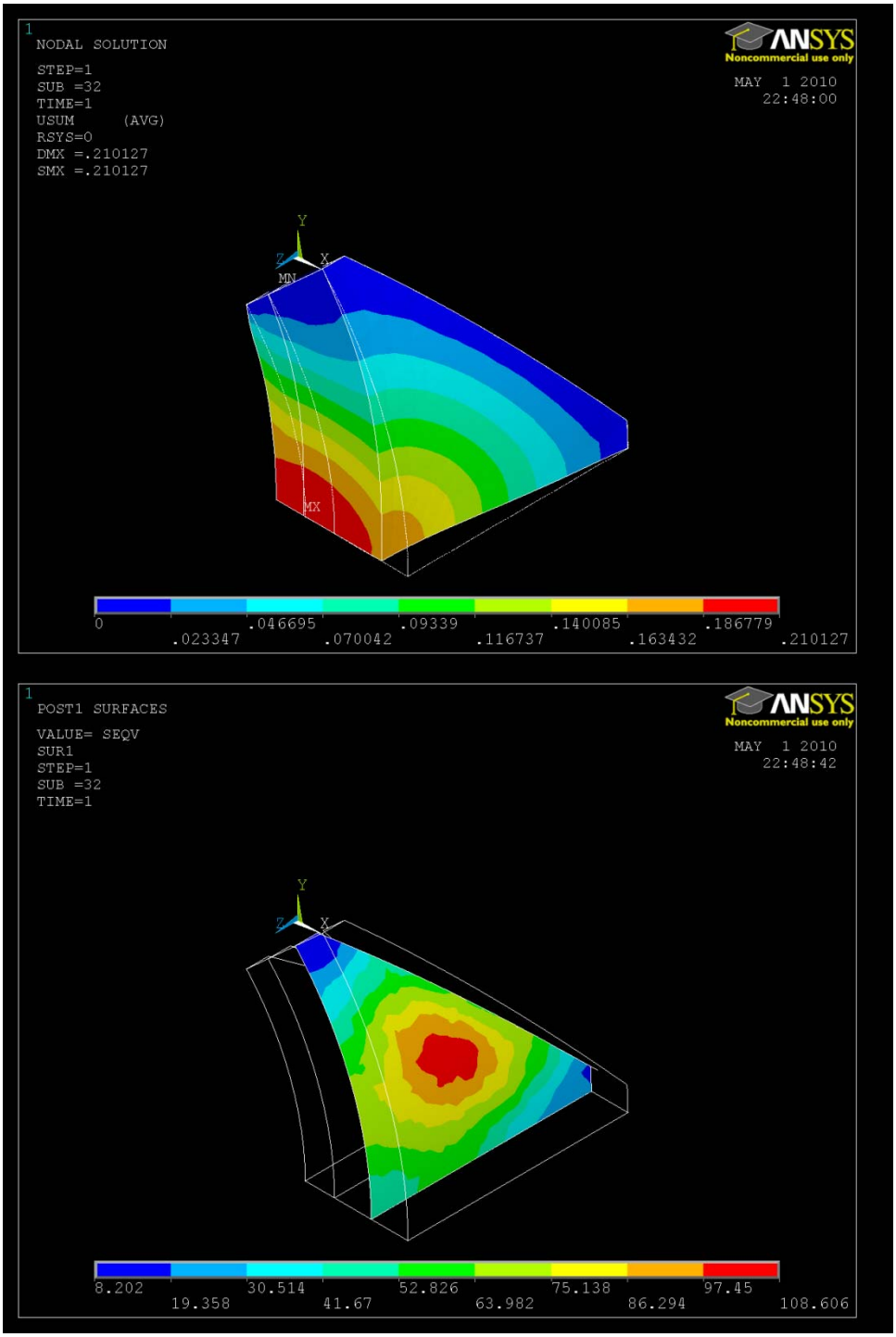

Figure 6.10: Displacement with undeformed edge (top) and midline stress (bottom) for small diameter diamond-shape with 200 μm thick PVA cryogel layer.

Figure 6.11: Displacement with undeformed edge (top) and midline stress (bottom) for large diameter diamond-shape with no PVA cryogel layer.

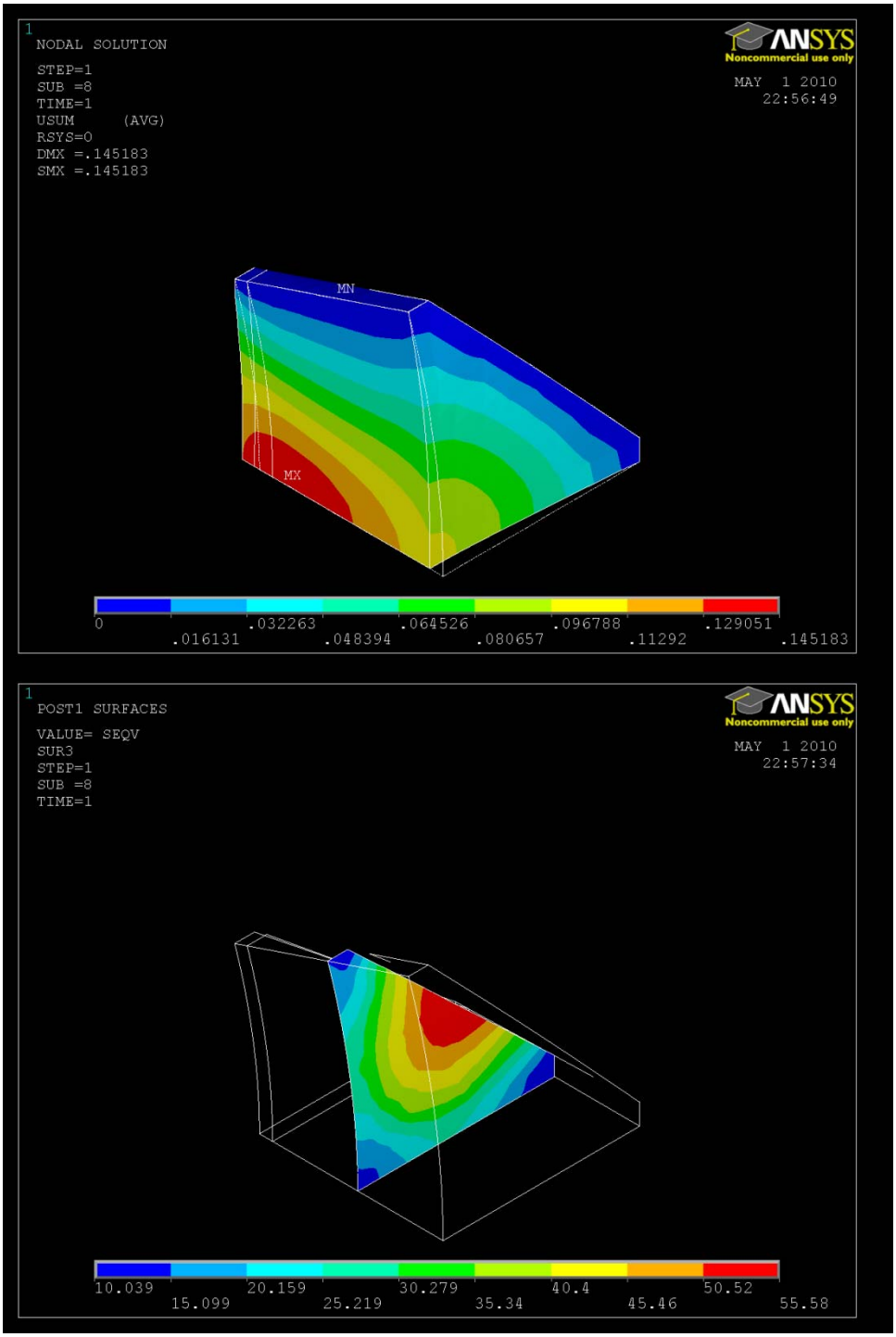

Figure 6.12: Displacement with undeformed edge (top) and midline stress (bottom) for large diameter diamond-shape with 100 μm thick PVA cryogel layer.

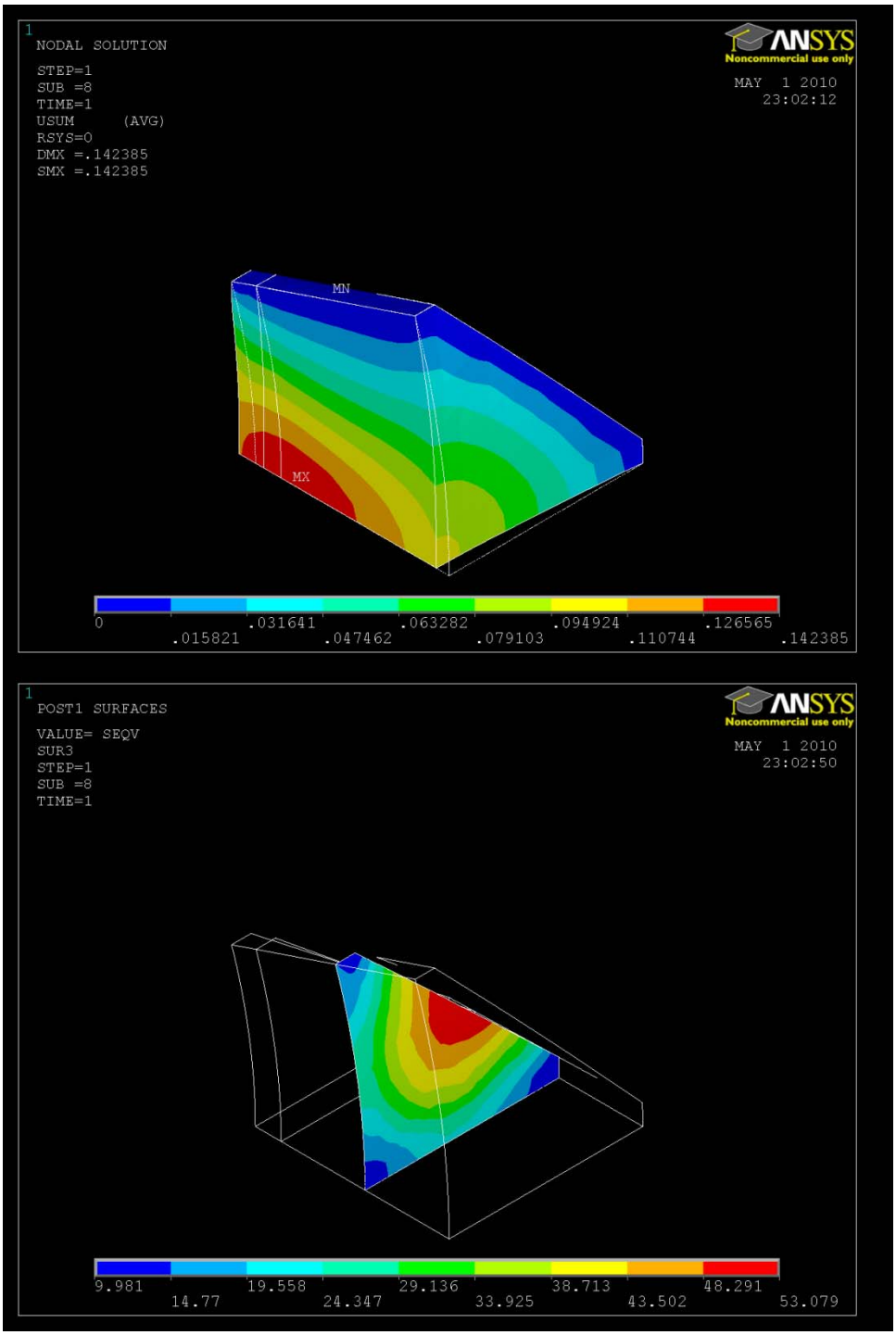

Figure 6.13: Displacement with undeformed edge (top) and midline stress (bottom) for large diameter diamond-shape with 200 μm thick PVA cryogel layer.

Figure 6.14: Displacement with undeformed edge (top) and midline stress (bottom) for small diameter w-shape with no PVA cryogel layer.

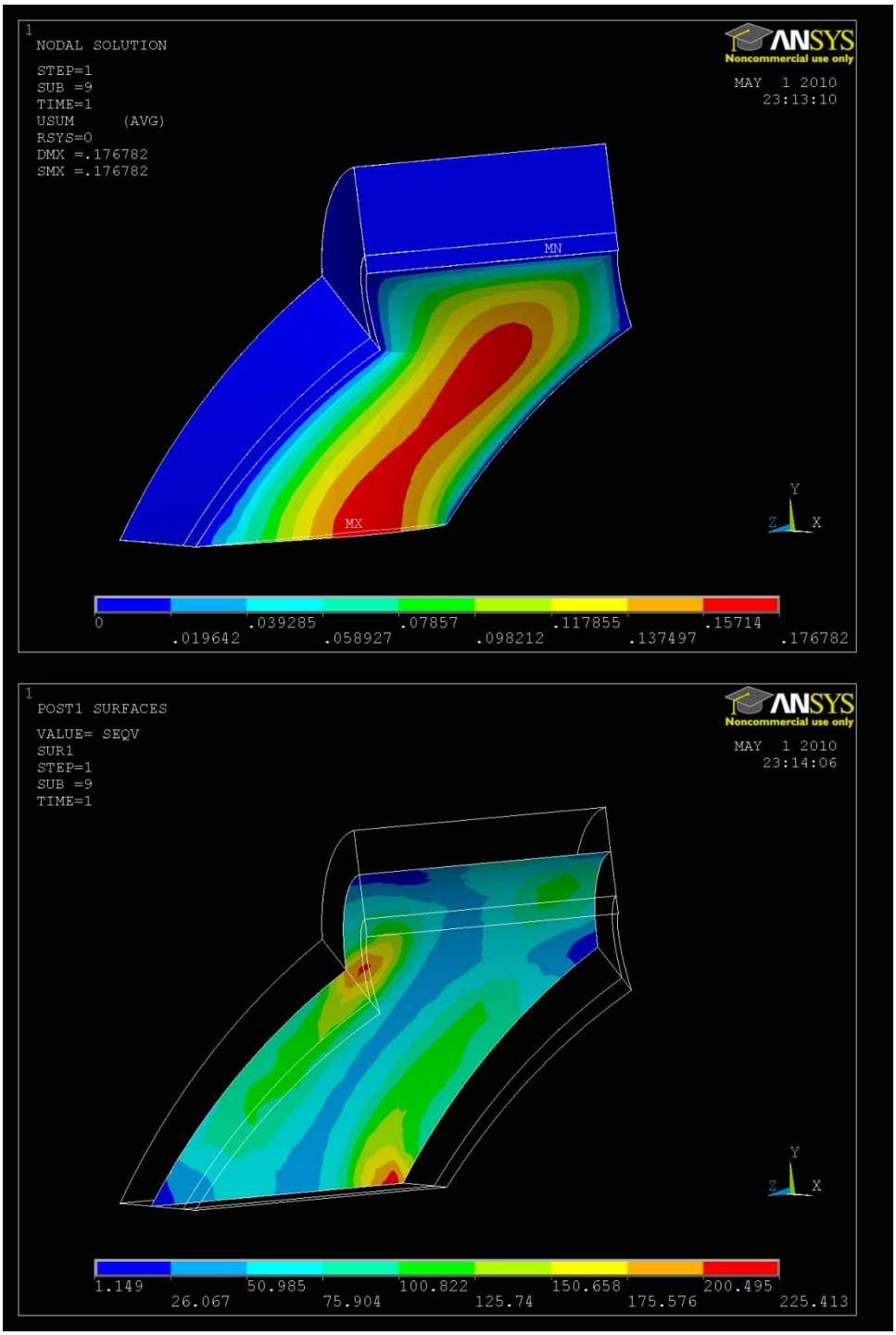

Figure 6.15: Displacement with undeformed edge (top) and midline stress (bottom) for small diameter w-shape with 100 μm thick PVA cryogel layer.

Figure 6.16: Displacement with undeformed edge (top) and midline stress (bottom) for small diameter w-shape with 200 μm thick PVA cryogel layer.

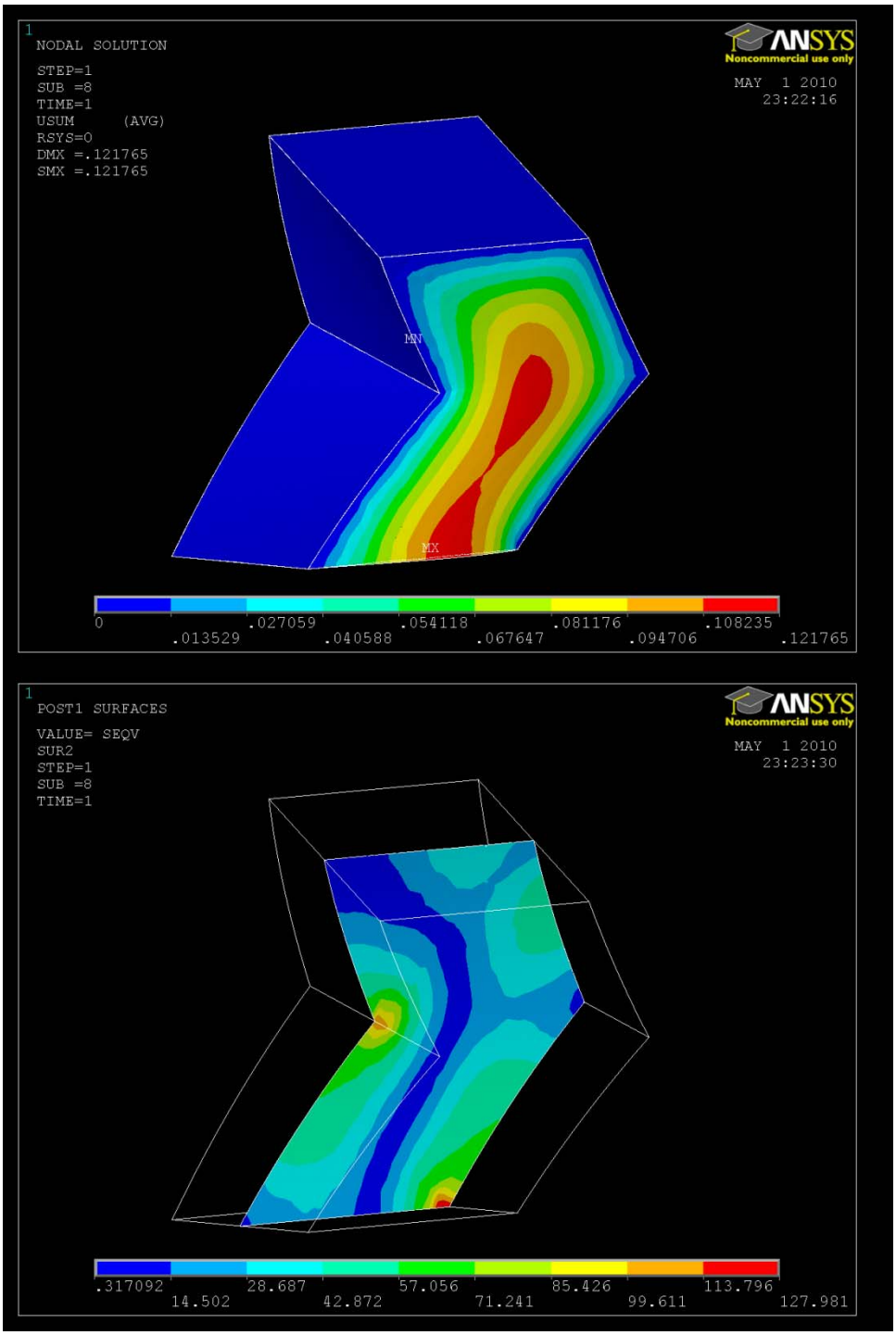

Figure 6.17: Displacement with undeformed edge (top) and midline stress (bottom) for large diameter w-shape with no PVA cryogel layer.

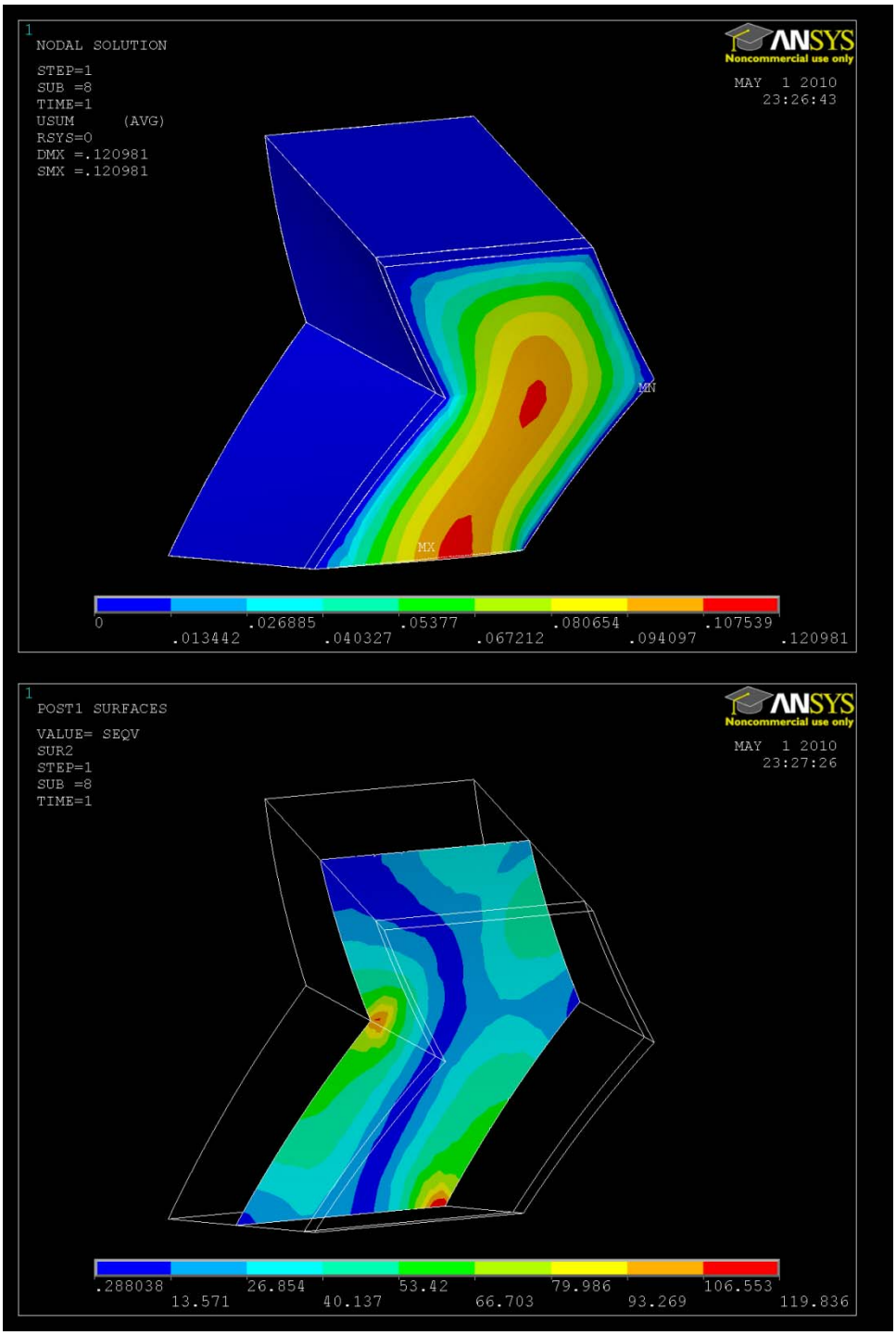

Figure 6.18: Displacement with undeformed edge (top) and midline stress (bottom) for large diameter w-shape with 100 μm thick PVA cryogel layer.

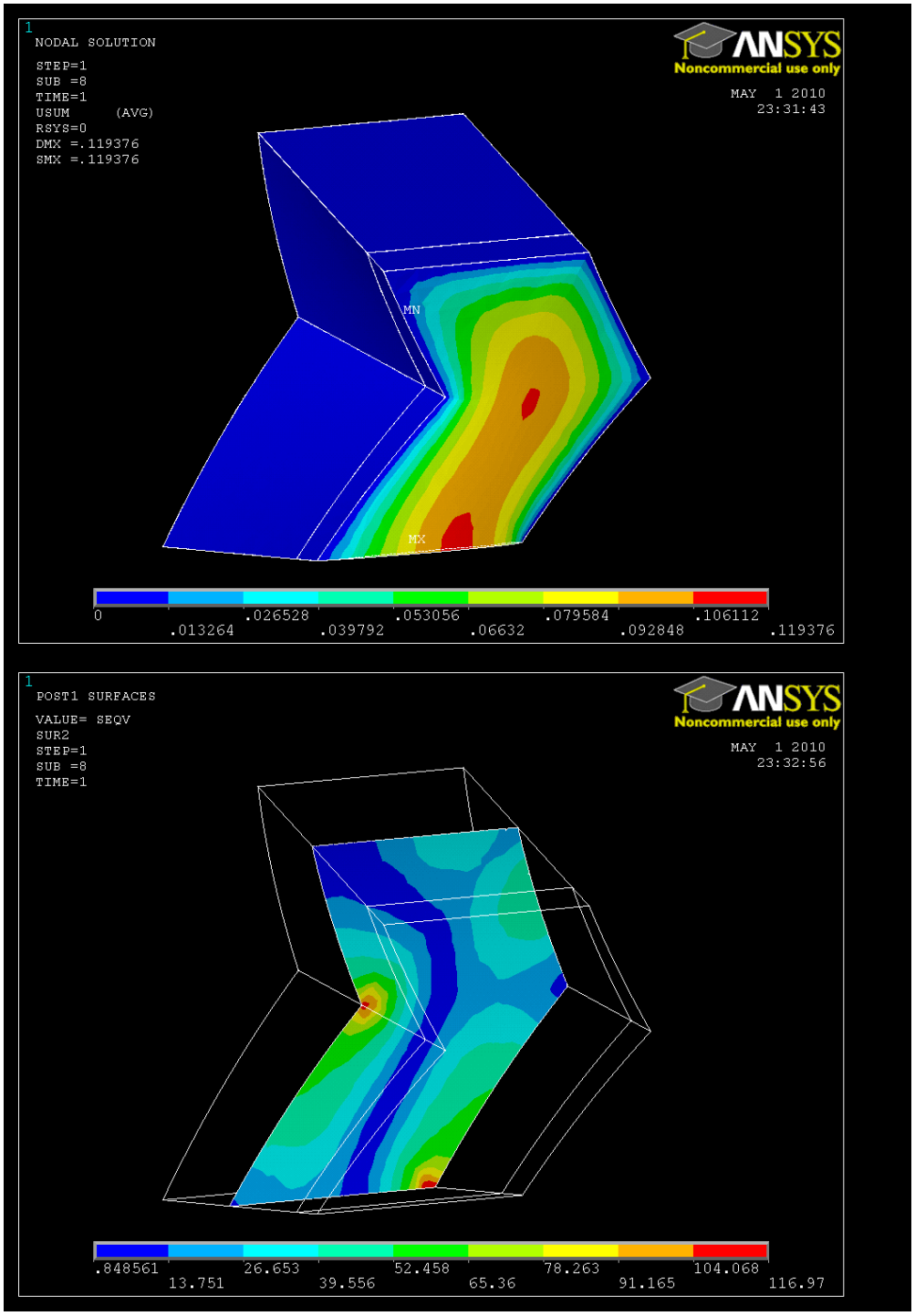

Figure 6.19: Displacement with undeformed edge (top) and midline stress (bottom) for large diameter w-shape with 200 μm thick PVA cryogel layer.

6.4 Discussion

FEA was used to analyze the effects of stent cell geometry, vessel diameter, and covered stent membrane thickness on tissue prolapse and arterial wall stress. Generally speaking, the addition of a PVA cryogel layer does reduce both prolapse and arterial wall stress, although the amount the stress or prolapse was reduced varied greatly among the four cases investigated. The covered stent membrane reduced tissue prolapse by a maximum of 13%, maximum midline artery stress by a maximum of 29%, and average midline artery stress by a maximum of 23%. The greater the initial stress or prolapse, the greater was the reduction by adding the PVA cryogel layer. Whether or not these reductions in prolapse and artery wall stress would cause a clinically measurable change in restenosis rate would need to be validated by a clinical trial.

Of note is that the artery wall stress was higher in both smaller diameter vessels when compared to the larger diameter vessels. As previously mentioned, one FEA study of two stents demonstrated higher artery wall stress in a stent which had a higher clinical restenosis rate[1]. The results here confirm that idea by showing higher artery wall stress in smaller vessels which have been shown to restenose at a higher rate when the same stent design is deployed in different size vessels [15]. Previous studies of prolapse in uncovered stents have found radial deflections between 0.11 mm and 0.48 mm [10, 11]. The results here are within that range, although slightly different techniques were used. Artery wall stress results were also found to be similar in magnitude to other previous investigations of uncovered stent expansion [7, 11].

This study is limited in that it does not model the expansion of the stent and its contact with the vessel wall; the stent was assumed to be already expanded and in contact with

the artery. The stent was assumed to be rigid and did not deflect under the applied extraluminal pressure, although it is possible that an elastic stent might deflect under these conditions [11]. Additionally, the vessel wall was assumed to be isotropic and homogenous when it is in fact composed of an intima, media, and adventitia [13]. This simplifying assumption, however, is made often in FEA analyses of stented arteries and is expected to be reasonable because the load is carried mostly by the media [7, 11].

In conclusion, the PVA cryogel layer was found to reduce both prolapse and artery wall stress, although the actual reduction varied depending on the artery shape and diameter. Reducing artery wall stress is of interest because it could reduce the clinical restenosis rate, although it is not known if the reductions caused by the PVA cryogel layer shown here are large enough to cause such a change.

6.5 References

1. Lally, C., F. Dolan, and P.J. Prendergast, *Cardiovascular stent design and vessel stresses: a finite element analysis.* J Biomech, 2005. **38**(8): p. 1574-81.

2. Medtronic DISTANCE trial: whitepaper reporting on the direct stenting with angiographic and clinical evaluation of the S7 (DISTANCE) trial: medtronic AVE, UC200203607EE 6M 5/02.

3. Rutsch, W., et al., *Clinical and angiographic results with the NIR stent: First International NIR Endovascular Stent Study (FINESS-II).* Int J Cardiovasc Intervent, 2000. **3**(3): p. 143-151.

4. Etave, F., et al., *Mechanical properties of coronary stents determined by using finite element analysis.* J Biomech, 2001. **34**(8): p. 1065-75.

5. Migliavacca, F., et al., *Mechanical behavior of coronary stents investigated through the finite element method.* J Biomech, 2002. **35**(6): p. 803-11.

6. Auricchio, F., M. Di Loreto, and E. Sacco, *Finite-element Analysis of a Stenotic Artery Revascularization through a Stent Insertion.* Computer Methods in Biomechanics and Biomedical Engineering, 2001. **4**(3): p. 249-263.

7. Timmins, L.H., et al., *Stented artery biomechanics and device design optimization.* Med Biol Eng Comput, 2007. **45**(5): p. 505-13.

8. Hong, M.K., et al., *Long-term outcomes of minor plaque prolapsed within stents documented with intravascular ultrasound.* Catheterization and Cardiovascular Interventions, 2000. **51**(1): p. 22-26.

9. Kim, S.W., et al., *Frequency and severity of plaque prolapse within Cypher and Taxus stents as determined by sequential intravascular ultrasound analysis.* American Journal of Cardiology, 2006. **98**(9): p. 1206-1211.

10. Capelli, C., et al., *Assessment of tissue prolapse after balloon-expandable stenting: influence of stent cell geometry.* Med Eng Phys, 2009. **31**(4): p. 441-7.

11. Prendergast, P.J., et al., *Analysis of prolapse in cardiovascular stents: a constitutive equation for vascular tissue and finite-element modelling.* J Biomech Eng, 2003. **125**(5): p. 692-9.

12. Gu, L.X., et al., *Finite element analysis of covered microstents.* Journal of Biomechanics, 2005. **38**(6): p. 1221-1227.

13. Schulze-Bauer, C.A., C. Morth, and G.A. Holzapfel, *Passive biaxial mechanical response of aged human iliac arteries.* J Biomech Eng, 2003. **125**(3): p. 395-406.

14. Rachev, A., T. ElShazly, and D.N. Ku. *Constitutive Formulation of the Mechanical Properties of Synthetic Hydrogels*. in *ASME International Mechanical Engineering Congress*. 2004. Anaheim, CA USA.

15. Henry, M., et al., *Palmaz stent placement in iliac and femoropopliteal arteries: primary and secondary patency in 310 patients with 2-4-year follow-up.* Radiology, 1995. **197**(1): p. 167-74.

CHAPTER 7:

Prevention of Smooth Muscle Cell Migration With Polyvinyl Alcohol Cryogels

7.1 Background

7.1.1 Restenosis Biology

Angiographic restenosis has been defined clinically as an obstruction of 50% or greater by diameter stenosis [1]. While this definition of restenosis is binary and does not give information on the severity of the stenosis, it is important because coronary flow reserve becomes reduced for diameter stenoses greater than 50% [2, 3]. Stents today have restenosis rates of 20% to 45% which depend on risk factors such as diabetes, number of stents implanted, and stent length among others [4-9]. Restenosis can be separated into three unique processes: elastic recoil, negative remodeling, and intimal hyperplasia [2, 10]. Elastic recoil and negative remodeling are generally associated with balloon angioplasty whereas neointimal hyperplasia is generally associated with in-stent restenosis [2]. However, all three processes can contribute to restenosis after balloon angioplasty [10].

Elastic recoil is an immediate mechanical response after balloon angioplasty. Within a few minutes of balloon deflation, the artery recoils similar to a rubber band after being stretched; this can lead to a loss in cross sectional area of up to 50% [11]. Negative remodeling is a change in arterial size after vascular injury [12]. This process is initiated by the conversion of adventitial fibroblasts to myofibroblasts (by inflammatory cells) which then secrete extracellular matrix, causing vessel constriction and the formation of

a fibrotic scar at the injury site [13]. This process can be observed approximately 1 to 6 months after an angioplasty procedure [10]. Neointimal hyperplasia is the process by which the intimal layer of the artery thickens. Medial vascular smooth muscle cells (SMC) migrate to the intima and begin to proliferate and secrete large amounts of extracellular material – reducing the luminal diameter [14, 15].

7.1.2 Stents & Neointimal Hyperplasia

Bare metal stents (BMS) are metal scaffolds that are delivered to the lesion site via catheter where they are expanded either by balloon- or self-expansion. While BMS have been able to eliminate the deleterious effects of elastic recoil and negative remodeling, they increase the level of neointimal hyperplasia when compared to angioplasty alone. However, the initial gain in lumen diameter is so much greater with stents that it outweighs the late lumen loss of neointimal hyperplasia and gives lower overall restenosis rates [2, 10, 16].

Injury from balloon angioplasty can cause dissection through the tunica media and exposure of the external elastic lamina [17, 18]. The endothelial denudation causes the loss of normally present anti-thrombotic factors such as nitric oxide, prostaglandin, and tissue plasminogen activator promoting platelet adhesion and aggregation [10]. Platelets bound to fibrin release cytokines such as platelet-derived growth factor (PDGF), thromboxane A2, and adenosine diphosphate which signal further platelet aggregation and thrombus formation. PDGF and epidermal growth factor released by the platelets serve as mitogens and chemotaxis agents for vascular SMC and macrophages. The vascular SMC, which normally lay in a quiescent phase in the media, then migrate to the site of injury in the intima and begin to proliferate and produce

extracellular material [10, 18, 19]. The composition of intimal hyperplasia regions is quite different from that of atherosclerotic plaques. While an atheroma tends to be mostly acellular and contain cholesterol, necrotic regions, macrophages, and possibly calcium deposits, the thickened intima contains mostly vascular SMC which produce large amounts of extracellular matrix [20].

BMS provide no barrier to vascular SMC migration and cells pass directly through the area between stent struts forming a thick neointima that can completely envelop stent struts [21]. Drug-eluting stents (DES) are BMS coated with a polymer which allows the passive diffusion of an anti-neoplastic drug, e.g. paclitaxel or sirolimus, across the stent surface [2, 10, 22] to prevent cellular proliferation and eliminate neointimal hyperplasia. DES have had particular success in the coronary arteries, reducing restenosis rates by a relative 50% to 80% [2], although concerns over late stent thrombosis (beyond the first year of implantation) are growing as more long term data on DES become available. One recent meta-analysis of 14 contemporary clinical trials of coronary stenting noted that DES carry a four to five fold increased risk of late stent thrombosis over BMS [23]. As an alternative to the prevention of neointimal hyperplasia by DES, vascular SMC migration could be blocked by the physical barrier of a covered stent membrane.

7.1.3 Types of Migration Assays

Two common *in vitro* methods for measuring cellular migration include the wound assay and the modified Boyden chamber assay [24]. In the wound assay, cells are grown to confluence in a dish and then a wound is created by scratching the surface with a cell scraper or similar device. The cell migration across the surface can then be monitored by taking microscopic images at regular intervals until the cells have filled the wound [24,

25]. Modified Boyden chambers consist of an upper and a lower chamber which are separated by a thin, porous filter as shown in Figure 7.1. Cells suspended in media are loaded in the upper chamber while the lower chamber contains media and a chemoattractant. The cells are allowed to migrate towards the chemoattractant for a fixed incubation period. Afterwards, the filters are fixed and stained and the cells that migrated to the bottom of the filter are counted under magnification [24, 26, 27]. Since the cellular migration in intimal hyperplasia is perpendicular to a surface (through stent struts) and not across a surface, the modified Boyden chamber assay is selected as an analogous model.

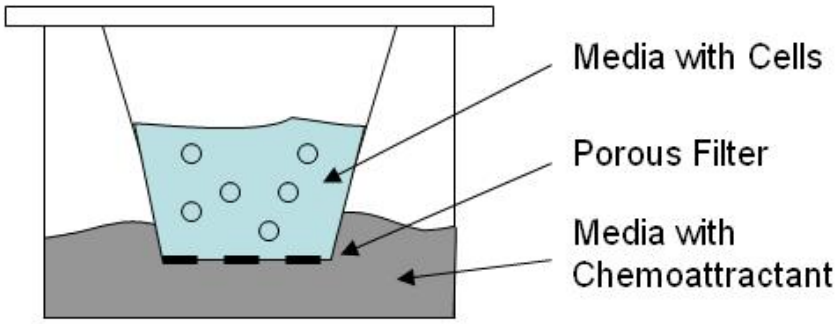

Figure 7.1: Modified Boyden chamber layout. Upper chamber contains media and cells in suspension. Lower chamber contains a chemoattractant and is separated from the upper chamber by a porous filter.

7.2 Methods

7.2.1 Cell Isolation & Culture

Porcine aortic SMC were isolated from tissue donated by a local abattoir following a protocol similar to Butcher et al. [28]. Aortas were removed from farm pigs shortly after sacrifice. The aortas were then rinsed in Hank's Buffered Saline Solution and incubated in a 5X antibiotic/antimycotic solution for one hour. Endothelial cells were removed by using a collagenase digestion combined with a gentle scraping method. To isolate SMC, the aortic tissue was cut into small pieces with sterile scissors. The pieces were then shaken in T75 flasks with 300 U/mL collagenase type 2 in Dulbecco's Modified Eagle Medium (DMEM) for four hours. The cell and tissue liquid was subsequently filtered and spun down in a centrifuge. The cells were then counted and plated at a density of 3,500 cells/cm^2.

Growth media was prepared with 500 mL DMEM (Cellgro); 50 mL fetal bovine serum (FBS) (Cellgro); 5 mL L-glutamine (Cellgro); 5 mL penicillin-streptomycin solution (Cellgro); and 2.9789 g HEPES buffer (Cellgro). HEPES buffer (unsterile) was added to the DMEM to give a concentration of 25 mM and passed through a 0.22 μm sterile filter; the FBS, L-glutamine, and penicillin-streptomycin were then added. Cells were cultured in T75 culture flasks (Corning) with growth media that was replaced every third day until they reached approximately 80% confluency in a cell culture incubator at 37°C and 5% CO_2. To passage cells, the growth media was aspirated and the cells were rinsed with Dulbecco's phosphate buffered saline (DPBS) (Cellgro). Once the DPBS was aspirated, 3 mL of 0.05% trypsin (Invitrogen) was added and the cells were incubated for

approximately five minutes until the detached cells could be seen in the flask. Six milliliters of growth media was then added to inactivate the trypsin.

To count the cells, 50 µL of the cell suspension was added to 20 mL DPBS and counted with a Multisizer II (Beckman Coulter). Size limits for SMC were set between 8 µm and 30 µm and each sample was run twice in order to take an average reading. The number of cells in a suspension was determined by

$$Cell(\#) = \frac{\text{Coulter Result Sum}}{2} \cdot 9mL \cdot 802 \tag{7.1}$$

where *Coulter Result Sum* is the sum of both readings and 802 is a dilution factor based on the volume of the cell suspension and DPBS. The cell suspension was then spun down in a centrifuge, the trypsin/media aspirated, and an appropriate amount of media was added to obtain the desired cell concentration.

7.2.2 Modified Boyden Chamber Preparation

The modified Boyden chambers (BD), inserts, used in this study had 8 µm pores and were either covered or uncovered with a polyvinyl alcohol (PVA) cryogel. The pore size was chosen based on previous studies of SMC migration in modified Boyden chambers [27, 29]. To make the covered inserts, two formulations of PVA were prepared at 10% and 20% by weight by adding PVA powder to deionized water per Equation 2.1. These formulations were chosen to represent a low and high percent weight PVA that might be used in covered stents. The PVA-water mixture was heated in an autoclave at 120°C in order to dissolve the PVA and sterilize the resulting solution. After sterilization, the

mixture was moved to the biosafety hood and mixed manually to ensure an even consistency. At the same time, individual inserts were placed right side up and PVA solution was poured into the upper chamber so as to completely coat the porous membrane. The inserts were then inverted and excess PVA solution was removed. The covered inserts were placed into sterile containers and put into an incubator for three freeze-thaw cycles. After thermal cycling, the covered inserts were placed into sterile containers with deionized water until testing. Uncovered inserts also underwent thermal cycling to ensure that it was not a source of differences between the groups.

Since thickness of the porous membrane was not available from the manufacturer, precise measurements of the PVA cryogel covering thickness were not taken. However, to give an approximation, the PVA cryogel covering from one 20% PVA cryogel insert was removed after testing. A section of the covering was cut and imaged next to a reference object of known size. The number of pixels was then measured and compared with the reference object in order to give a thickness measurement using GNU Image Manipulation Program (GNU Project).

It is expected that a covered stent membrane would become covered with fibronectin or other proteins after implantation [30]. Therefore, some inserts were coated with human fibronectin (BD) in order to more closely match the *in vivo* situation. Fibronectin solutions were prepared at 5, 10, or 20 μg/mL by resuspending fibronectin in sterile deionized water and then making further dilutions with DPBS per manufacturer recommendations. This concentration range was chosen based on previous investigations of cellular migration with fibronectin coated inserts [27, 31]. Inserts were coated by placing 700 μL of the fibronectin solution into the lower chamber and 200 μL

into the upper chamber. Inserts were left overnight at 20°C and then rinsed with DPBS before beginning a migration experiment.

7.2.3 Migration Assay Protocol

All SMC used in migration assays were between passage number 7 and 10. After counting the cells and spinning them down, they were resuspended in DMEM with 1% bovine serum albumin (BSA) to give a concentration of 50,000 cells per 300 µL. This media was prepared by taking 100 mL of DMEM (with HEPES), dissolving 1 g BSA (Fisher Scientific), and then passing it through another 0.22 µm filter. One milliliter L-glutamine and 1 mL penicillin-streptomycin were added, but no FBS.

The lower chamber was filled with 800 µL growth media (DMEM + 10% FBS) while the upper chamber contained the cells resuspended in DMEM + 1% BSA so that the cells would be attracted to the higher level of serum and migrate towards the lower chamber. Three hundred microliters of media with resuspended cells (50,000) were placed in the upper chamber and the chambers were incubated for 24 h. Three sets of migration experiments were completed.

a) Uncovered inserts vs. PVA cryogel covered inserts without fibronectin coating
b) Fibronectin pilot study of uncovered inserts
c) Uncovered inserts vs. PVA cryogel covered inserts with fibronectin coating

In experiment (a), three groups were evaluated: uncovered inserts, 10% PVA cryogel covered inserts, and 20% PVA cryogel covered inserts. Six inserts were used in each group for a total of 18. In experiment (b), three fibronectin concentrations were

evaluated: 5, 10, and 20 μg/mL in uncovered inserts. As this was a pilot study, only one insert in each group (total of three) were used. Experiment (c) was identical to experiment (a) except that the inserts were coated with 10 μg/mL fibronectin (concentration determined from pilot study (b)). Four inserts were used in each group for a total of 12.

7.2.4 Histology & Migrated Cell Counting

After 24 h migration, inserts were removed from the well plate and the upper surface was wiped with a cotton swab to remove any adherent cells that had not migrated to the lower surface. Removing cells from the upper surface is necessary in order to avoid accidentally counting them as migrated cells. A HemaColor Stain Set (EMD Chemicals) was used to fix and stain the inserts by progressively placing each insert into methanol fixative, eosin stain, methylene blue stain, and three rinses of deionized water for two minutes each. After drying, inserts were visualized with an Eclipse TE2000-U inverted microscope (Nikon) with a 20X objective. Three digital images were taken at different locations on each insert. Cells were counted manually using ImageJ software (National Institutes of Health) and are reported as the average number of migrated cells per high power field.

7.3 Results

7.3.1 Experiment (a): Uncovered Inserts vs. PVA Cryogel Covered Inserts Without Fibronectin Coating

The thickness of one PVA cryogel membrane was determined to be 170 μm – approximately the size of a stent strut. PVA cryogel covered inserts (10% and 20% formulations) had a significantly reduced amount of migrated cells per high power field when compared to uncovered inserts, $p<0.05$. Migration in the positive control was modest with an average of 5.6 cells per high power field, see Figure 7.2. Sample pictures of migrated cells are shown in Figure 7.3. The 10% PVA formulation had zero migrated cells and the 20% formulation had an average of 0.2 cells per high power field. There was no statistically significant difference in migrated cells between the two PVA cryogel formulations.

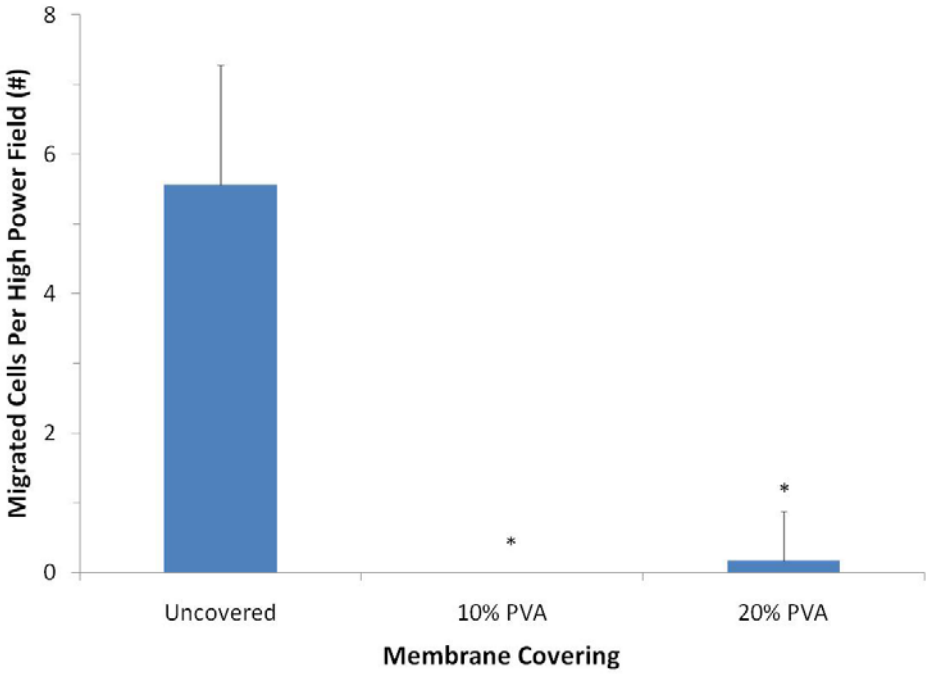

Figure 7.2: Average migrated cells per high power field without fibronectin coating. Error bars represent one standard deviation. Each group represents 6 inserts and 3 pictures were taken of each insert. * is statistically significant from uncovered inserts, $p<0.05$.

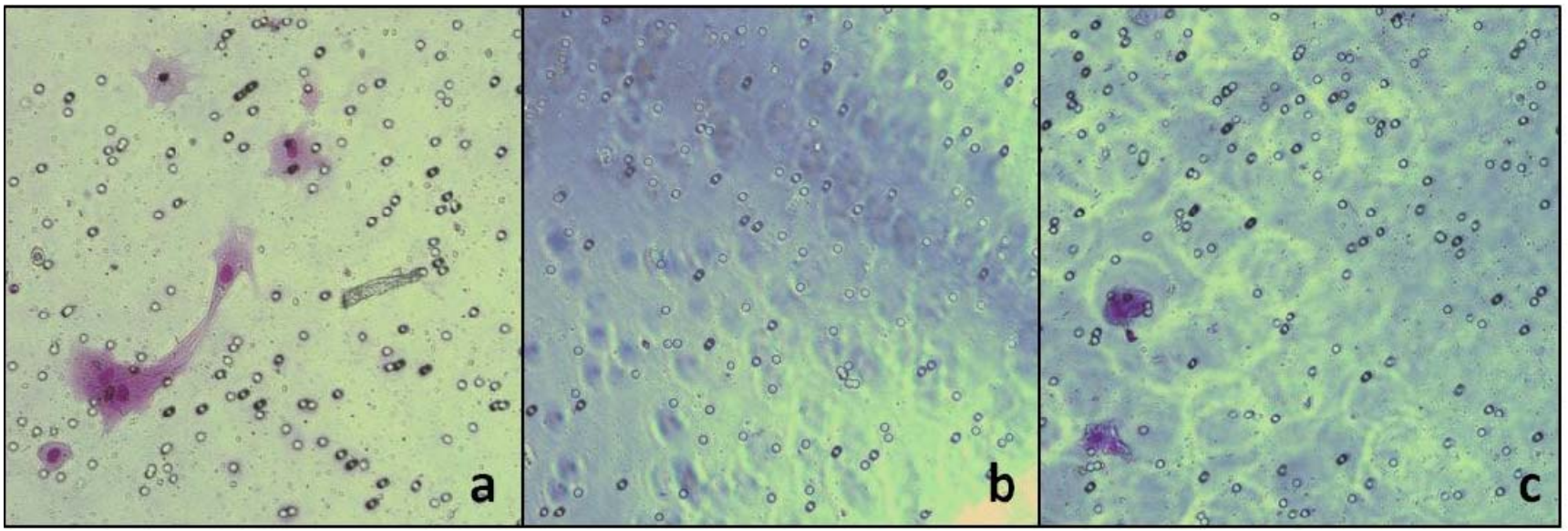

Figure 7.3: Sample pictures of migrated cells without fibronectin coating on (a) uncovered membrane, (b) 10% PVA cryogel covered membrane, and (c) 20% PVA cryogel covered membrane. The membrane shown in (c) is of the only cells that could be found in the 20% PVA cryogel group. The small black circles are 8 μm pores.

7.3.2 Experiment (b): Fibronectin Pilot Study of Uncovered Inserts

Fibronectin coating increased SMC migration at all concentrations. The 10 µg/mL concentration had the highest amount of migrated cells, see Figure 7.4, and was thus chosen for Experiment (c) so as to provide the most migration possible. Sample pictures of migrated cells are shown in Figure 7.5. There was no statistically significant difference between the groups.

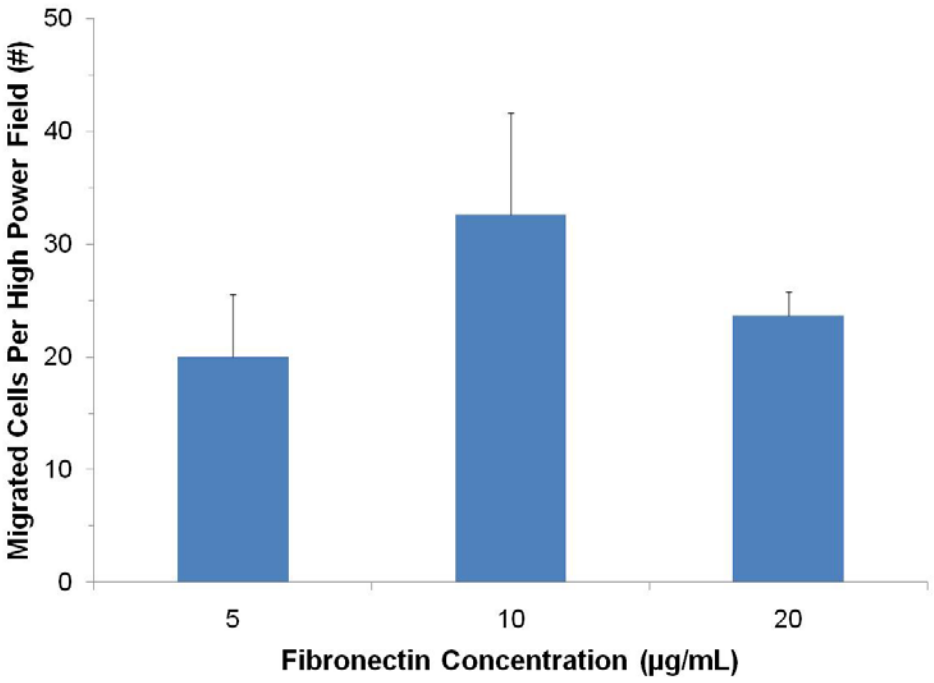

Figure 7.4: Average migrated cells per high power field on uncovered inserts with varying fibronectin concentration. Error bars represent one standard deviation.

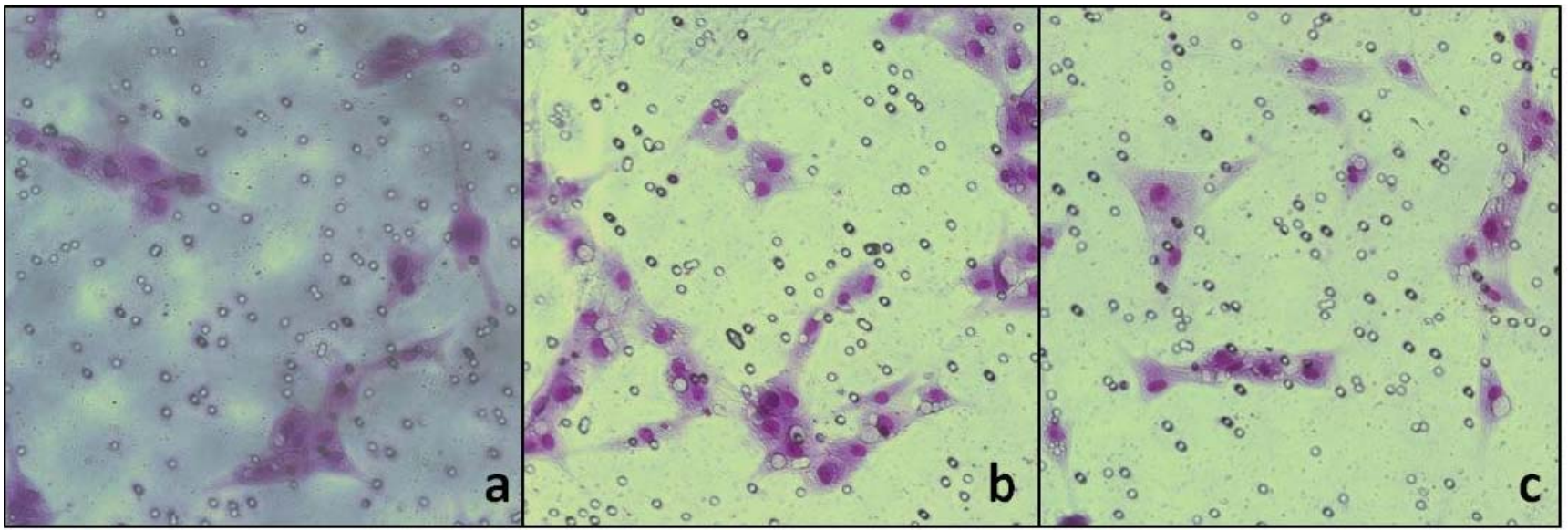

Figure 7.5: Sample pictures of migrated cells on uncovered inserts with fibronectin concentrations of (a) 5 µg/mL, (b) 10 µg/mL, and (c) 20 µg/mL. The small black circles are 8 µm pores.

7.3.3 Experiment (c): Uncovered Inserts vs. PVA Cryogel Covered Inserts With Fibronectin Coating

Fibronectin coated uncovered inserts had a larger number of migrated cells than uncoated uncovered inserts from Experiment (a), see Figure 7.6. Sample pictures of migrated cells are shown in Figure 7.7. Migration through PVA cryogel covered inserts was unchanged with fibronectin coating; the 10% formulation had zero migrated cells and the 20% formulation had 0.42 migrated cells per high power field. The difference between uncovered and PVA cryogel covered inserts was significant ($p<0.05$), although there was no statistically significant difference between the two PVA formulations.

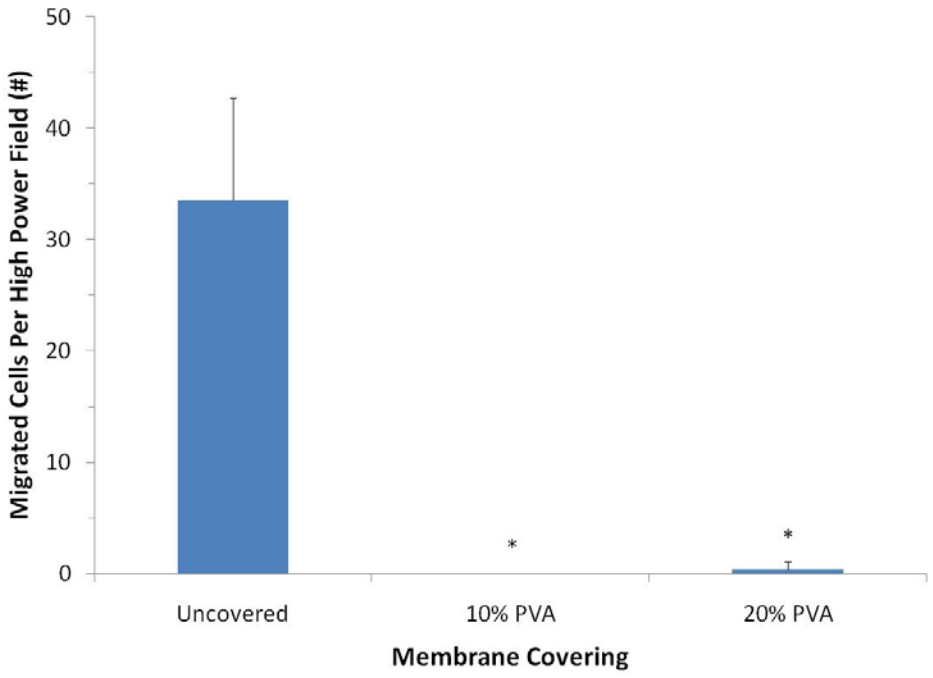

Figure 7.6: Average migrated cells per high power field with 10 µg/mL fibronectin coating. Error bars represent one standard deviation. Each group represents 4 inserts and 3 pictures were taken of each insert. * is statistically significant from uncovered inserts, $p<0.05$.

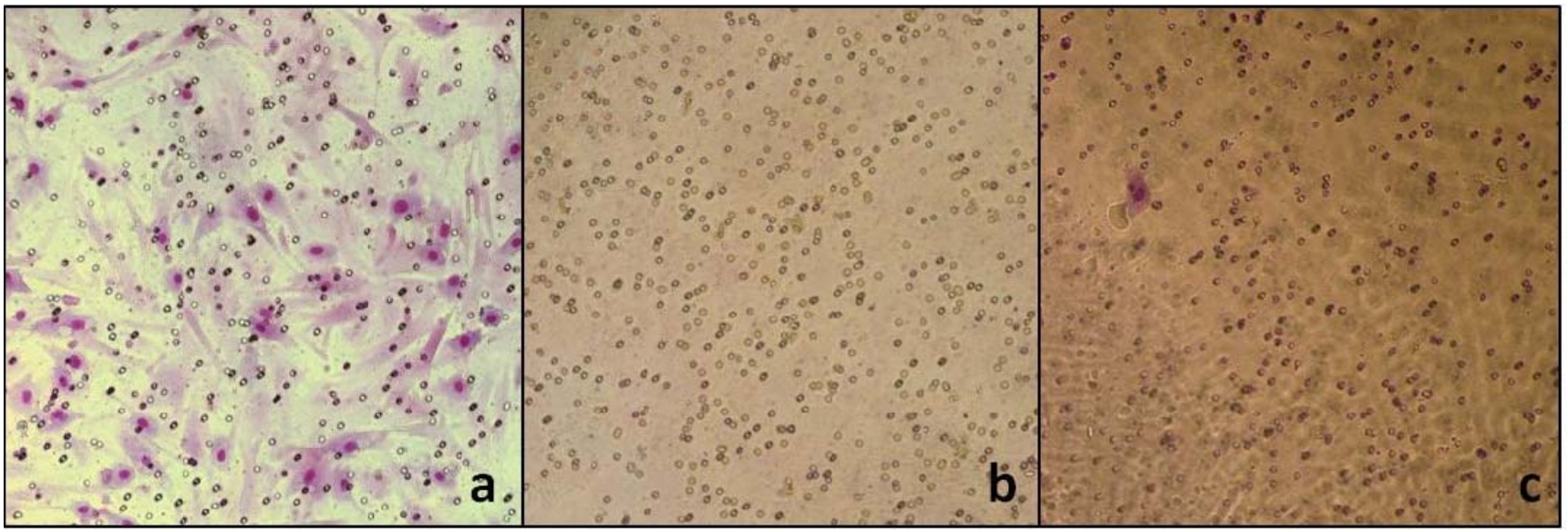

Figure 7.7: Sample pictures of migrated cells witn 10 µg/mL fibronectin coating on (a) uncovered membrane, (b) 10% PVA cryogel covered membrane, and (c) 20% PVA cryogel covered membrane. The small black circles are 8 µm pores.

7.4 Discussion

PVA cryogel coverings were shown to eliminate virtually all SMC migration in the absence and presence of fibronectin. There was no statistical difference in number of migrated cells between the two PVA cryogel formulations in any experiment. The 10% formulation completely stopped migration while there was a small number of migrated cells seen with the 20% formulation. This result is contrary to expectations as thickness was anticipated to be higher and porosity lower in the higher percent weight cryogel [32]. One possible explanation for this behavior lies in the fact that the 20% PVA solution is more viscous than the 10% once the PVA is dissolved into the water. Tiny air bubbles, trapped within a more viscous solution, would be less likely to flow out of the insert and may become stuck. If those bubbles were to later pop, e.g. during thermal cycling, they would leave the original surface exposed and cells would be able to migrate through the 8 μm pores uninhibited.

The thickness of one PVA cryogel covering was determined to be 170 μm – approximately the size of a stent strut [33]. While this measurement was only taken of one insert, all inserts had similar thicknesses based on visual inspection. Although the PVA cryogel covered stents made in Chapter 4 had thinner membranes, SMC migration is not expected to be different with covered stents because the pore size of PVA cryogels is less than 1 μm [32] – much smaller than SMC (8 μm to 30 μm). Further experiments including *in vivo* studies, e.g. pig or rabbit, of in-stent restenosis are recommended to validate the present results.

One limitation of the current study is that in-stent restenosis occurs on a time scale of months and these experiments were all completed in 24 hours. In-stent restenosis is

typically studied in animal models and few *in vitro* models for studying restenosis exist [34]. However, the cellular migration in modified Boyden chambers is analogous to the SMC migration seen during neointimal hyperplasia. Furthermore, a strong correlation has been shown between a tumor cell's invasive potential *in vivo* and its ability to invade *in vitro* in the modified Boyden chamber [35]. Because of this, the modified Boyden chamber is expected to be a reasonable *in vitro* model of the cellular migration seen during neointimal hyperplasia. However, in several studies of in-stent restenosis in covered stents, neointimal hyperplasia has been seen to grow inward from the edges [36, 37]. This type of cellular ingrowth, termed the candy wrapper effect because of its angiographic appearance, may be related to procedural differences during implantation [38]. Since this type of migration is not simulated well by the modified Boyden chamber assay, it should be evaluated *in vivo*.

In conclusion, both the low and high percent weight PVA cryogel formulations were shown to significantly reduce SMC migration in an *in vitro* model of cellular migration. This result demonstrates that PVA cryogels have the potential to reduce in-stent restenosis by preventing SMC migration. Future work should include animal testing of PVA cryogel covered stents to determine if they are able to prevent in-stent restenosis *in vivo*.

7.5 References

1. Roubin, G.S., S.B. King, 3rd, and J.S. Douglas, Jr., *Restenosis after percutaneous transluminal coronary angioplasty: the Emory University Hospital experience.* Am J Cardiol, 1987. **60**(3): p. 39B-43B.

2. Topol, E.J., *Textbook of Interventional Cardiology*. 5th ed. 2008, Philadelphia: Saunders/Elsevier. xxi, 1286 p.

3. Gould, K.L., K. Lipscomb, and G.W. Hamilton, *Physiologic basis for assessing critical coronary stenosis. Instantaneous flow response and regional distribution during coronary hyperemia as measures of coronary flow reserve.* Am J Cardiol, 1974. **33**(1): p. 87-94.

4. Colombo, A., et al., *Randomized study to assess the effectiveness of slow- and moderate-release polymer-based paclitaxel-eluting stents for coronary artery lesions.* Circulation, 2003. **108**(7): p. 788-94.

5. Fajadet, J., et al., *Maintenance of long-term clinical benefit with sirolimus-eluting coronary stents: three-year results of the RAVEL trial.* Circulation, 2005. **111**(8): p. 1040-4.

6. Kasaoka, S., et al., *Angiographic and intravascular ultrasound predictors of in-stent restenosis.* J Am Coll Cardiol, 1998. **32**(6): p. 1630-5.

7. Kastrati, A., et al., *Predictive factors of restenosis after coronary stent placement.* J Am Coll Cardiol, 1997. **30**(6): p. 1428-36.

8. Schampaert, E., et al., *The Canadian study of the sirolimus-eluting stent in the treatment of patients with long de novo lesions in small native coronary arteries (C-SIRIUS).* J Am Coll Cardiol, 2004. **43**(6): p. 1110-5.

9. Schofer, J., et al., *Sirolimus-eluting stents for treatment of patients with long atherosclerotic lesions in small coronary arteries: double-blind, randomised controlled trial (E-SIRIUS).* Lancet, 2003. **362**(9390): p. 1093-9.

10. Slavin, L., A. Chhabra, and J.M. Tobis, *Drug-eluting stents: preventing restenosis.* Cardiol Rev, 2007. **15**(1): p. 1-12.

11. Rensing, B.J., et al., *Quantitative angiographic assessment of elastic recoil after percutaneous transluminal coronary angioplasty.* Am J Cardiol, 1990. **66**(15): p. 1039-44.

12. Edelman, E.R. and C. Rogers, *Pathobiologic responses to stenting.* Am J Cardiol, 1998. **81**(7A): p. 4E-6E.

13. Wilcox, J.N., et al., *The role of the adventitia in the arterial response to angioplasty: the effect of intravascular radiation.* Int J Radiat Oncol Biol Phys, 1996. **36**(4): p. 789-96.

14. Bauters, C., et al., *Mechanisms and prevention of restenosis: from experimental models to clinical practice.* Cardiovasc Res, 1996. **31**(6): p. 835-46.

15. Schwartz, S.M., D. deBlois, and E.R. O'Brien, *The intima. Soil for atherosclerosis and restenosis.* Circ Res, 1995. **77**(3): p. 445-65.

16. Kuntz, R.E., et al., *Generalized model of restenosis after conventional balloon angioplasty, stenting and directional atherectomy.* J Am Coll Cardiol, 1993. **21**(1): p. 15-25.

17. Schneider, J.E., et al., *Probucol decreases neointimal formation in a swine model of coronary artery balloon injury. A possible role for antioxidants in restenosis.* Circulation, 1993. **88**(2): p. 628-37.

18. Scott, N.A., et al., *Identification of a potential role for the adventitia in vascular lesion formation after balloon overstretch injury of porcine coronary arteries.* Circulation, 1996. **93**(12): p. 2178-87.

19. Schwartz, R.S. and T.D. Henry, *Pathophysiology of coronary artery restenosis.* Rev Cardiovasc Med, 2002. **3 Suppl 5**: p. S4-9.

20. Sommer, B.G., Henry, M.L., *Vascular Access for Hemodialysis -- II*. 1991: W.L. Gore & Associates, Inc., and Precept Press, Inc.

21. Lowe, H.C., S.N. Oesterle, and L.M. Khachigian, *Coronary in-stent restenosis: current status and future strategies.* J Am Coll Cardiol, 2002. **39**(2): p. 183-93.

22. Burt, H.M. and W.L. Hunter, *Drug-eluting stents: a multidisciplinary success story.* Adv Drug Deliv Rev, 2006. **58**(3): p. 350-7.

23. Bavry, A.A., et al., *Late thrombosis of drug-eluting stents: a meta-analysis of randomized clinical trials.* Am J Med, 2006. **119**(12): p. 1056-61.

24. Gerthoffer, W.T., *Mechanisms of vascular smooth muscle cell migration.* Circ Res, 2007. **100**(5): p. 607-21.

25. Hsu, P.P., et al., *Effects of flow patterns on endothelial cell migration into a zone of mechanical denudation.* Biochem Biophys Res Commun, 2001. **285**(3): p. 751-9.

26. Ma, G., D.P. Mason, and D.B. Young, *Inhibition of vascular smooth muscle cell migration by elevation of extracellular potassium concentration.* Hypertension, 2000. **35**(4): p. 948-51.

27. Pauly, R.R., et al., *Migration of cultured vascular smooth muscle cells through a basement membrane barrier requires type IV collagenase activity and is inhibited by cellular differentiation.* Circ Res, 1994. **75**(1): p. 41-54.

28. Butcher, J.T. and R.M. Nerem, *Porcine aortic valve interstitial cells in three-dimensional culture: comparison of phenotype with aortic smooth muscle cells.* J Heart Valve Dis, 2004. **13**(3): p. 478-85; discussion 485-6.

29. Onoue, N., et al., *Increased static pressure promotes migration of vascular smooth muscle cells: involvement of the Rho-kinase pathway.* J Cardiovasc Pharmacol, 2008. **51**(1): p. 55-61.

30. Courtney, J.M., et al., *Biomaterials for blood-contacting applications.* Biomaterials, 1994. **15**(10): p. 737-44.

31. Huang, Q., H.M. Shen, and C.N. Ong, *Emodin inhibits tumor cell migration through suppression of the phosphatidylinositol 3-kinase-Cdc42/Rac1 pathway.* Cell Mol Life Sci, 2005. **62**(10): p. 1167-75.

32. Depp, M.M., *PVA cryogel optimization and diffusion studies*. 1998, School of Chemical Engineering, Georgia Institute of Technology, 1999. Directed by David N. Ku. p. x, 232 leaves.

33. Hara, H., et al., *Role of stent design and coatings on restenosis and thrombosis.* Adv Drug Deliv Rev, 2006. **58**(3): p. 377-86.

34. Voisard, R., et al., *A human arterial organ culture model of postangioplasty restenosis: results up to 56 days after ballooning.* Atherosclerosis, 1999. **144**(1): p. 123-34.

35. Shaw, L.M., *Tumor cell invasion assays.* Methods Mol Biol, 2005. **294**: p. 97-105.

36. Deutschmann, H.A., et al., *Placement of Hemobahn stent-grafts in femoropopliteal arteries: early experience and midterm results in 18 patients.* J Vasc Interv Radiol, 2001. **12**(8): p. 943-50.

37. Jahnke, T., et al., *Hemobahn stent-grafts for treatment of femoropopliteal arterial obstructions: midterm results of a prospective trial.* J Vasc Interv Radiol, 2003. **14**(1): p. 41-51.

38. Saxon, R.R., et al., *Long-term results of ePTFE stent-graft versus angioplasty in the femoropopliteal artery: single center experience from a prospective, randomized trial.* J Vasc Interv Radiol, 2003. **14**(3): p. 303-11.

CHAPTER 8:

Part 2: Conclusions, Significance, and Future Directions

Finite element analysis (FEA) was employed to investigate tissue prolapse and artery wall stress for two different stent cell geometries (diamond- and w-shape) and two different vessel diameters (3.5 mm coronary and 7.4 mm iliac) with uncovered and PVA cryogel covered stents. The addition of a PVA cryogel layer was found to reduce tissue prolapse by up to 13% and maximum midline artery stress by up to 29%. The amount that the prolapse or artery wall stress was reduced depended on the vessel diameter and stent cell geometry. Furthermore, the greater the prolapse or artery wall stress caused by the uncovered stent, the greater was the reduction in prolapse or artery wall stress caused by the PVA cryogel covering. Also of note was that higher stresses were found in smaller vessels with the same stent cell geometry. These higher stresses may be indicative of a higher likelihood for restenosis as at least one other study has shown a link between high artery wall stresses and restenosis. Generally, reducing tissue prolapse and artery wall stress may help reduce clinical restenosis rates, but it is unknown at this point if the reductions seen in this study will lead to clinically measureable improvements.

Future FEA work might seek to increase model sophistication by incorporating interactions between the artery, plaque, stent, and PVA cryogel in order to more precisely determine the biomechanical benefits of PVA cryogel covered stents – especially if more flexible self-expanding stents are to be used. Additionally, it may be interesting to model the expansion of a PVA cryogel covered stent versus an equivalent uncovered stent without any artery interactions to see if there are major differences in

balloon inflation pressure, elastic recoil, and longitudinal shortening between the two stent types. Together, these two types of simulations could guide PVA cryogel covered stent design in order to create a reliable device capable of reducing both tissue prolapse and artery wall stress.

Migration through a modified Boyden chamber was used as a model for the cellular migration between stent struts seen during the process of in-stent restenosis. The results of this study indicate that PVA cryogel membranes (approximately 170 μm thick) are capable of stopping smooth muscle cell migration *in vitro* in both the absence and presence of fibronectin – suggesting that the same effect would be seen *in vivo*. Future work should include animal or human trials of restenosis that compare uncovered and PVA cryogel covered stents to determine if PVA cryogel covered stents are able to reduce in-stent restenosis *in vivo*.

Altogether, the FEA and migration assay results point to the conclusion that PVA cryogel covered stents may be able to prevent in-stent restenosis – both by blocking smooth muscle cell migration and by reducing artery wall stress and prolapse. Future FEA work might focus on increasing model sophistication and investigating covered stent design parameters in order to enhance device performance and potentially reduce artery wall stress and prolapse further. Most importantly, these *in vitro* results which suggest that PVA cryogels prevent restenosis need to be verified with *in vivo* studies in animals or humans that directly compare restenosis between uncovered and PVA cryogel covered stents.

PART 3:

Thrombogenicity Testing of Polyvinyl Alcohol Cryogels

CHAPTER 9:

In Vitro Biomaterial Thrombogenicity Testing

9.1 Background

9.1.1 In-Stent Thrombosis & Blood Contacting Biomaterials

In-stent thrombosis is the process of clot formation within the stented region of a vessel. Angioplasty and stenting damage the vessel wall and expose the thrombotic components (von Willebrand factor, collagen, fibronectin, and tissue factor) below the endothelial layer [1-4]. Platelets then adhere and aggregate to form a thrombus which can completely occlude the vessel. Fortunately, the combined practices of high balloon inflation pressure to ensure proper stent apposition and dual anti-platelet therapy, i.e. aspirin and ticlopidine, have reduced the risk of bare metal stent (BMS) thrombosis to less than 1% to 2% at one month [5]. Recently however, late stent thrombosis has become a concern for drug-eluting stents (DES) [6]. One recent 9-month study of paclitaxel- and sirolimus-eluting stents found that there was a 45% mortality rate associated with stent thrombosis [7]. After stenting, a re-endothelialization process occurs and patients must take anti-platelet medication until this process is complete in order to minimize thrombotic complications [8, 9]. For BMS, this process can take 6 – 7 months, but for DES may take in excess of 40 months [10]. Premature discontinuation of antiplatelet therapy is a strong predictor of stent thrombosis and was associated with a 30 fold greater risk in one study [11]. The ideal duration of antiplatelet therapy remains unknown, although it may be longer than one year [9, 12]. Not surprisingly, the controversy over DES in the past five years has led to a 20% decline in their use [13].

Synthetic vascular grafts are another research area where thrombosis and biomaterial thrombogenicity are paramount. Large diameter (greater than 7 mm) synthetic vascular grafts made of poly[ethylene terephthalate] (polyester or trade name Dacron™) and poly[tetrafluoroethylene] (PTFE) have been successful, with patency rates approaching 90% after five years in the abdominal aortic bifurcation [14]. Smaller diameter synthetic vascular grafts, however, have had lower patency rates, e.g. in the femoropopliteal artery [15]. While patency is lowered in part by neointimal hyperplasia, both of these hydrophobic biomaterials engender thrombus formation on the graft lumen [16]. In larger vessels, a certain amount of thrombus can be tolerated, but in smaller vessels, like the coronary or femoropopliteal arteries, this thrombus can lead to flow cessation. Consequently, the development of a synthetic vascular graft for smaller diameter vessels remains a challenge [16, 17].

Many studies have demonstrated that certain biomaterials or surface coatings are more thrombogenic than others [18-20]. Poly[ethylene oxide] (PEO) is a polymer that can be adsorbed onto surfaces and it has been shown *in vitro* that surfaces coated with PEO have reduced protein and cellular adsorption [21]. PEO containing block copolymers are a promising biomaterial, but have limited blood compatibility due to the non-PEO phase. PEO networks or hydrogels, by themselves, do not possess the mechanical properties required in many applications [22]. Polyurethanes, whose problems with *in vivo* degradation are being overcome by modifications to make them carbonate-based, are now being used for hemodialysis access with a one year patency rate of 66.7% [16, 23]. Albumin coated surfaces have been produced with encouraging *in vitro* results, but clinical studies failed to show improved performance over non-coated vascular prostheses [24]. Heparin, given its strong anticoagulative properties, has been examined as a potential surface coating. However, heparin-coated Dacron grafts did not

show improved patency over uncoated expanded PTFE (ePTFE) at 5 years in one clinical trial [15]. Elastins have been investigated as a surface covering in order to passivate blood-contacting surfaces after the observation that, as part of the vascular wall, elastin elicits minimal platelet adhesion and aggregation [25]. Thus far, elastin coated PTFE grafts have demonstrated low thrombogenicity in a primate *ex vivo* shunt model [17], although no large scale clinical trial has been done. Poly[vinyl alcohol] (PVA) hydrogels exhibit hydrophilic properties. One study has shown that because of the hydrophilicity of PVA cryogels, cell adhesions proteins did not adsorb to PVA hydrogels and cells were therefore unable to attach [26]. The inability of cells to attach to PVA hydrogels could be useful in vascular applications where platelet adhesion is undesirable. One *in vitro* study of a PVA cryogel prosthetic venous valve with whole porcine blood showed that Dacron™ coated valves were more thrombogenic than uncoated PVA cryogel valves [27]. No other published data regarding the thrombogenicity of this biomaterial is currently available.

9.1.2 Biomaterial Thrombogenicity Tests

Virchow's triad describes the three controlling factors for coagulation *in vivo* as endothelial injury, stasis, and hypercoagulability of the blood [1]. While arterial thrombosis can be influenced by these factors, it occurs through different mechanisms and under very different flow conditions that include high shear [1, 28]. Currently, there is no standard thrombogenicity test for new materials [29]. As a result, many different kinds of thrombogenicity and hemocompatibility tests with different methods, endpoints, and results have been published; a brief summary of some of these methods is presented here. Perhaps the simplest test is an incubation or binding study wherein the biomaterial is incubated with blood or plasma for a specified time [19, 29]. While these

tests can provide useful information about cell adhesion and protein adsorption, they fail to take into account shear, which is known to influence thrombus growth [28, 30]. The Modified Chandler loop has been used to compare platelet adhesion and activation among stent coatings [20, 31]. In this test, stents (or any tubular material section) are deployed inside tubes which are connected at both ends to form an annulus. The tube is then filled with blood and the entire loop is made to rotate for a fixed amount of time – causing passive flow of the blood over the stent without the use of a pump that could damage red blood cells or activate platelets [32]. A common system for investigations into platelet adhesion is the parallel plate flow chamber. These systems can be used to perfuse blood at varying shear rates and allow for visualization of flow throughout the experiment [29, 33]. While useful for certain types of investigations, few of the published reports of current *in vitro* flow loops are run to the clinically relevant endpoint of complete occlusion [34, 35]. Animal models are another method of evaluating biomaterials although they tend to be more expensive and time consuming than *in vitro* tests. Several common models used in the evaluation of blood contacting devices include sheep, pigs, and dogs [36-38]. In lieu of surgical implantation, e*x vivo* shunts can be used to evaluate different biomaterials. Baboons and dogs are typical animal models for *ex vivo* shunt experiments [35, 39, 40].

9.2 Methods

9.2.1 Blood Collection

Porcine blood is chosen for these experiments because it is readily available in the necessary quantities and because thrombus has been shown to form with both human and porcine blood when run at similar flow conditions [30]. Porcine blood was obtained

from a local abattoir (Holifield Farms of Covington, GA) using the method described by Ku et al. [28]. Briefly, one liter jars were prepared with 3500 USP heparin sodium (APP Pharmaceuticals). Immediately after sacrifice, blood was collected during exsanguination and 1 L was transferred into the jar with heparin after removing any particulate matter from the top. Blood was brought to the laboratory in a thermally insulated case in order to minimize temperature variations. The jars were then placed onto an orbital mixer table in order to reduce separation of the blood while the flow loop was prepared. Immediately before testing, blood was gently mixed by rotating the jar of blood several times to ensure uniformity.

9.2.2 *In Vitro* Flow Loop

Blood was made to flow through the gravity fed system shown in Figure 9.1 at room temperature. Three independent flow loops were run simultaneously with the following 4 cm long test sections at the outlet which flowed into the bottom reservoir: polyester (negative control), no test section (positive control), and 20% PVA cryogel. All tubing in which blood flowed downward was made of silicone (except test sections) and 4 mm in inner diameter, except for a connector piece between the top reservoir spout and the downward flowing silicone tube. The height of the upper reservoir, 63 cm, was chosen in order to give initial flow rates that are similar to those found in the human left main coronary artery [41]. Polyester test sections of 4 mm inner diameter were cut from a large piece of commercially available polyester and hand sewn with surgical grade polyester sutures. Consistent polyester test sections diameters were achieved by tightly sewing the polyester material onto a 4 mm metal rod which was subsequently removed. PVA cryogel tubes were prepared using metal and nylon molds with a 4 mm inner diameter as described in Section 2.2.1 of this dissertation. Roller pumps (Cole Parmer)

were used to return blood to the top reservoir in 6 mm diameter silicone tubing. The roller pump for each flow loop was controlled independently and the flow rate was adjusted manually in order to maintain each reservoir at an appropriate and constant level. Flow rate was read off the roller pump controller display every 10 minutes to an accuracy of ± 10 mL/min.

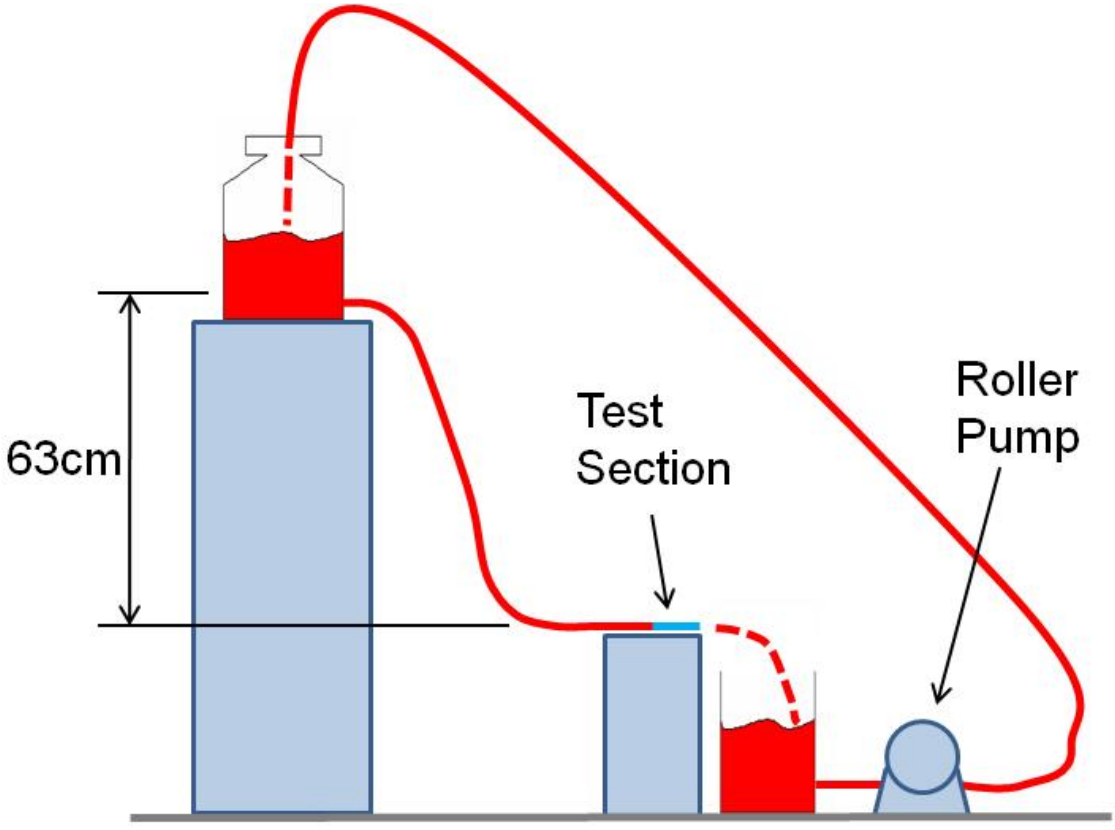

Figure 9.1: *In vitro* flow loop for thrombogenicity testing.

All three flow loops were run simultaneously (to minimize any potential blood variability with time) with a staggered start in order to allow time for measurement taking and flow rate adjustments of each flow loop. Tests were run until there was complete flow cessation in the polyester test section or until such a point when complete flow cessation seemed unlikely. The location of the occlusion was verified to be in the test section by removing the polyester piece and verifying that flow would reinitiate without that section present. The other two flow loops (no test section and 20% PVA cryogel) were then run to match the time of the occlusion of the polyester test section and a final flow rate was noted. The test was run seven times with blood from seven different porcine donors.

Assuming Poiseuille Flow in the test section, the shear rate, *G*, can be calculated by

$$G = \frac{4Q}{\pi \cdot r_0^3} \tag{9.1}$$

where *Q* is flow rate and r_0 is the radius of the test section. Additionally, the Reynold's Number can be calculated by

$$\mathrm{Re} = \frac{\rho v D}{\mu} = \frac{4\rho Q}{\pi \mu D} \tag{9.2}$$

where ρ is blood density (1025 kg/m3), μ is blood viscosity (0.0038 kg/ms), and *D* is the test section diameter. This experimental apparatus controls for shear by using identical setups in each loop and controls for blood hypercoagulability by using blood from the same donor and running experiments simultaneously. Differences in material

thrombogenicity can therefore be elucidated because the flow loops are otherwise identical.

9.2.3 Blood Counts

Within 30 minutes of test completion, the blood from each individual flow loop was allowed to collect into either the top or bottom reservoir. This blood was then mixed gently to ensure uniformity and a sample of approximately 1.8 mL was collected and placed into a sterile container. A 1.8 mL sample was also collected from blood which had not gone through the flow loop and instead had remained on the orbital mixer table during the experiment. All four samples were then taken to the Stamps Health Services for testing on an Excell 22 Auto Hematology Analyzer (Drew Scientific). Each sample was processed twice and the average values are reported.

9.2.4 Histology

Immediately after test completion, polyester and PVA cryogel test sections were rinsed gently in phosphate buffered saline to remove any non-adherent material. Test sections were then placed into containers of 10% formalin for fixation for a period of no less than 24 h in order to ensure that the entire sample was completely fixed. After fixation, samples were prepared for histological processing in one of two orientations – longitudinal or axial. Axial samples were cut into three sections: proximal, medial, and distal. Samples were processed in a series of alcohol and xylene baths in an Excelsior ES Tissue Processor (Thermo Scientific). When processing was complete, samples were placed in paraffin wax in a heated vacuum chamber overnight in order to allow the

paraffin to fully infiltrate the samples and facilitate slide preparation. Samples were then embedded in paraffin wax and brought to room temperature.

Samples were cut on a Microm 355H microtome in 5 μm sections and placed onto glass slides. Once dry, slides were deparaffinized with an Autostainer XL (Leica Microsystems). Slides were then stained using Carstair's method [42] as outlined below:

1. Rinse with distilled water
2. Mordant sections in 5% ferric alum for 10 minutes and rinse in tap water
3. Stain with Harris' hematoxylin for 5 minutes and rinse in tap water
4. Stain in picric acid-orange G solution for 30 minutes (up to one hour)
5. Rinse once with distilled water
6. Stain in ponceau fuchsin for 5 minutes
7. Rinse once in distilled water
8. Differentiate with 1% phosphotungstic acid for 2 minutes and rinse well in distilled water
9. Stain with aniline blue solution for 10 minutes (up to one hour)
10. Rinse several times in distilled water

With Carstair's method, fibrin appears red, platelets appear blue-gray to navy, red blood cells appear clear yellow, muscle appears red, and collagen appears bright blue. After staining, samples were protected with a standard coverslip and photographed on a Nikon E600 and Q-Imaging System.

9.3 Results

9.3.1 *In Vitro* Flow Loop & Flow Rates

Of the seven tests run, five of the polyester samples occluded completely with an average time to occlusion of 71 ± 40 minutes. In the two tests that had no occlusion in the polyester test section, the flow rate was significantly reduced. The flow rates versus time for the tests in which the negative control did completely occlude are shown in Figure 9.2. Due to the high variability between samples, the time axis was normalized by dividing by the final time and the flow rate was normalized by dividing by the initial flow rate. Final normalized flow rates for all tests are given in Table 9.1. Statistically significant differences were seen between the negative control and the positive control and between the negative control and the 20% PVA cryogel, $p<0.05$. No statistically significant differences were seen between the positive control and the 20% PVA cryogel. After testing and once the blood was removed from the tubes, small amounts of white thrombus could be seen on the 4 mm silicone tubing at the junction between the upper reservoir and the downward flowing tube or at the junction of the 4 mm silicone tube with the test section. This thrombus tended to form equivalently in all flow loops.

Table 9.1: Final normalized flow rates.

	Polyester (neg. control)	**No Test Section (pos. control)**	**20% PVA Cryogel**
Tests to Occlusion (n=5)	0.00 ± 0.00	0.72 ± 0.14*	0.61 ± 0.19*
All Tests (n=7)	0.08 ± 0.14	0.76 ± 0.14*	0.64 ± 0.17*

Mean ± standard deviation. * is statistically different from polyester, $p<0.05$

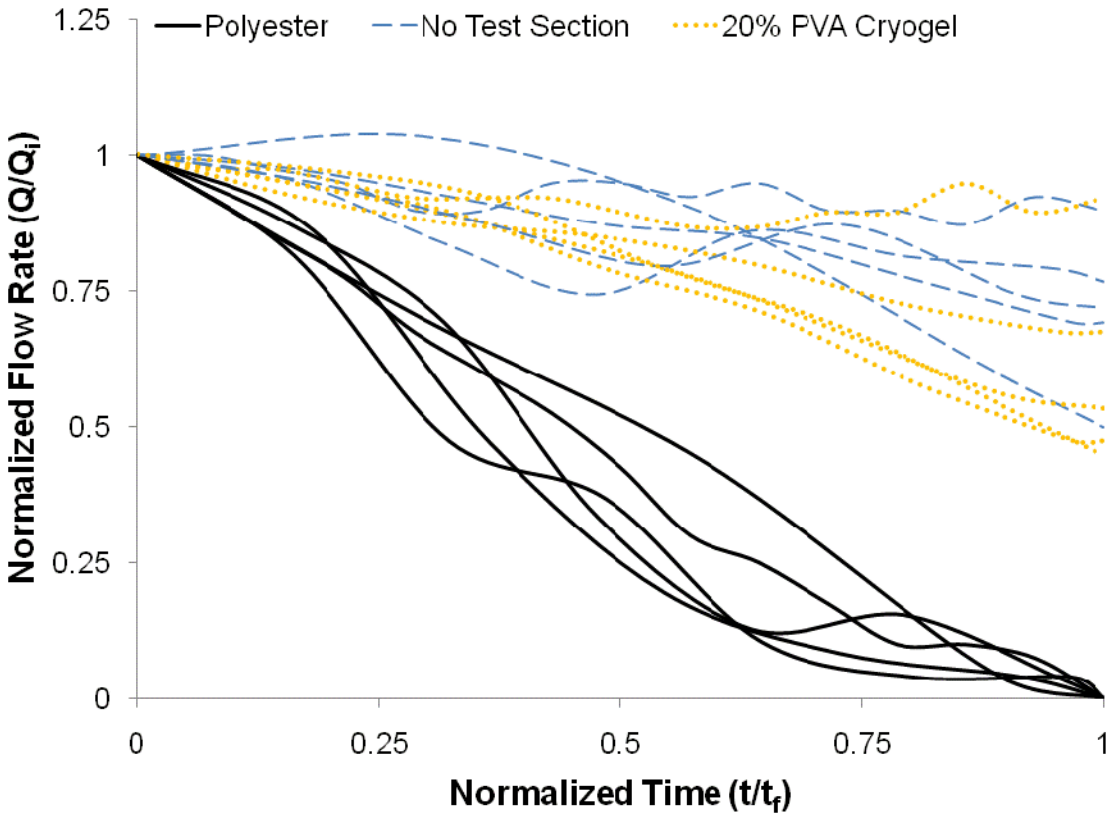

Figure 9.2: Normalized flow rate (current flow rate over initial flow rate) versus normalized time (current time over final time) for all materials from tests in which the negative control completely occluded.

Initial flow rates for all samples varied between 300 and 400 mL/min. Using Equation 9.1, the initial shear rate in the test section varied between 800 s^{-1} and 1000 s^{-1}. Using Equation 9.2, initial Reynold's Number varied between 430 and 570, which is similar to the maximum flow conditions in the human left main coronary artery [41] and justifies the assumption of Poiseuille Flow.

9.3.2 Blood Counts

Blood counts were obtained for all tests in which the negative control completely occluded, except for one sample due to a logistical problem (n=4). Hematocrit, platelet concentration, and mean platelet volume are shown for each flow loop and for blood that was not put into the test apparatus in Table 9.2. Two hematocrit readings and one mean platelet volume reading were not available as the hematology analyzer could not provide readings for these samples. There were no statistically significant differences between the groups in the reported measures.

Table 9.2: Blood count results.

	Without Testing	**Polyester**	**No Test Section**	**20% PVA Cryogel**
Platelet Concentration (1000/μL)	111 ± 21	102 ± 56	130 ± 35	115 ± 23
Mean Platelet Volume (fL)	9.15 ± 0.69	9.50 ± 0.71	9.64 ± 0.53	9.98 ± 0.51
Hematocrit (%)	45.4 ± 1.6	46.6 ± 1.6	46.1 ± 1.7	45.3 ± 1.7

Mean ± standard deviation.

9.3.3 Histology

Polyester and 20% PVA cryogel test sections from the experiments when the polyester sample completely occluded were processed for histology. Test sections from three experiments were prepared in an axial orientation and the remaining two were prepared

in a longitudinal orientation. Microscopic images of all these samples are shown in Figure 9.3 to 9.10. Generally, thrombus was persistent throughout the polyester test sections with completely occlusive thrombi forming at different locations in each experiment. Thrombus that consisted mostly of platelets, red blood cells, and collagen can be seen attached to the polyester fibers, which appear as white triangles with rounded edges in cross section. Small amounts of thrombus were present on PVA cryogel test sections as well although PVA cryogel test sections generally had much less thrombus than polyester test sections. Due to the differences in stiffness of the polyester and thrombus materials, images of the thrombus show gaps where the material fragmented during the sectioning process. Since PVA cryogels are similar in stiffness to soft tissue, sample fragmenting was not a problem during sectioning of those test sections.

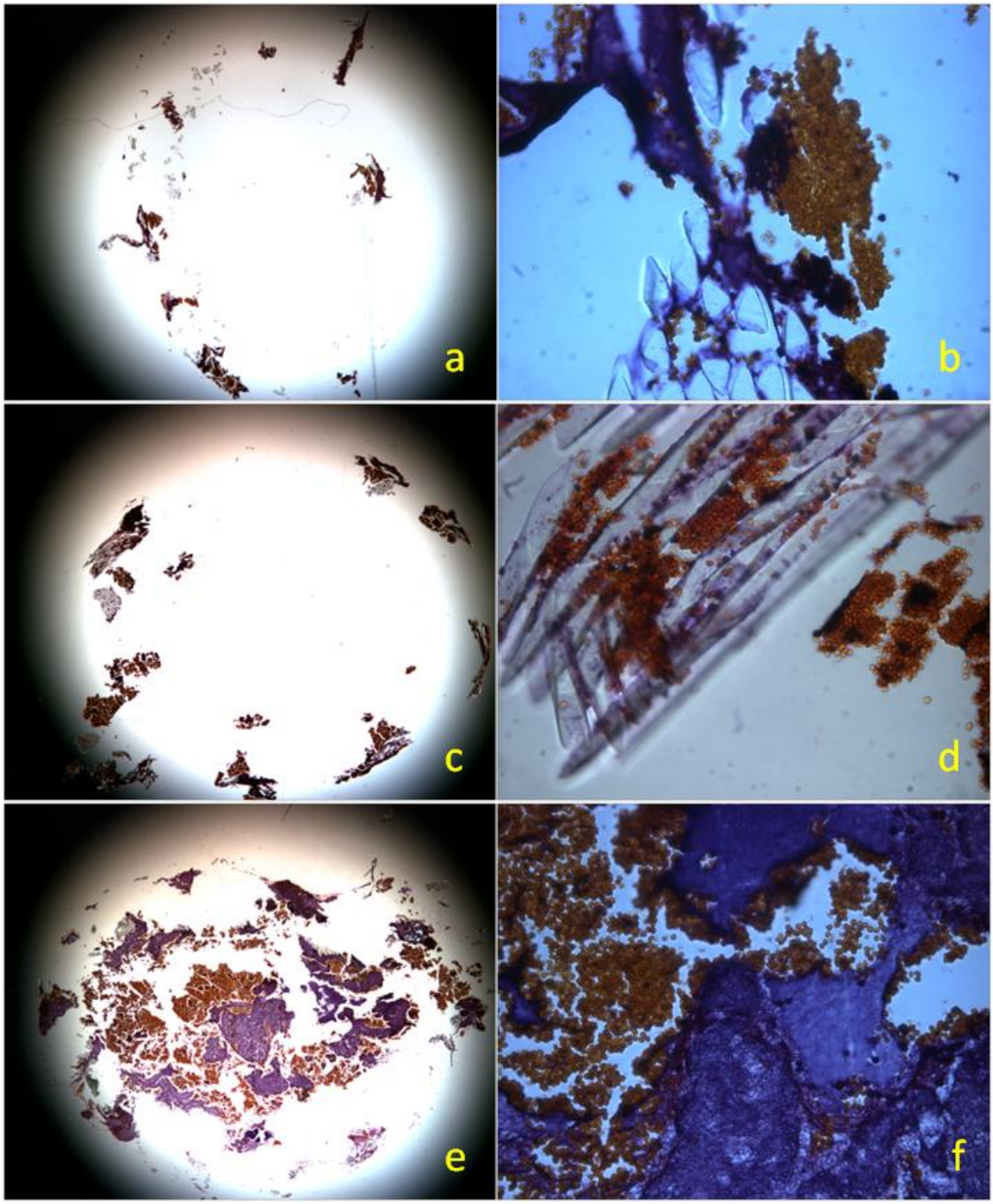

Figure 9.3: Polyester test section from experiment on Feb. 1, 2010 in axial orientation. Images (a) and (b) are from the proximal region, (c) and (d) from the medial region, and (e) and (f) from the distal region. Images (a), (c), and (e) were taken with a 2X objective while images (b), (d), and (f) were taken with a 40X objective. An occlusive thrombus consisting of platelets, red blood cells, and collagen can be seen in (e) and (f).

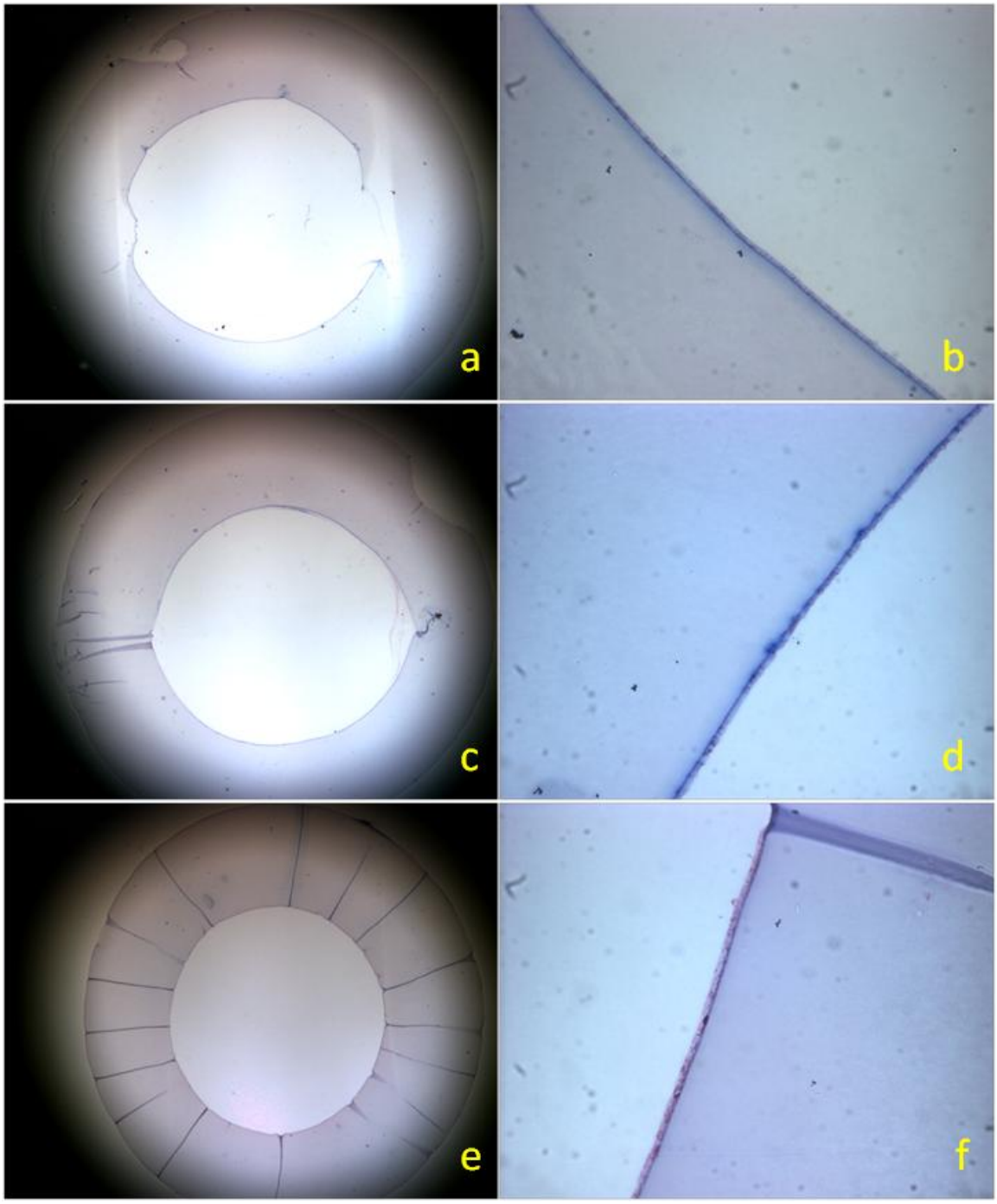

Figure 9.4: PVA cryogel test section from experiment on Feb. 1, 2010 in axial orientation. Images (a) and (b) are from the proximal region, (c) and (d) from the medial region, and (e) and (f) from the distal region. Images (a), (c), and (e) were taken with a 2X objective while images (b), (d), and (f) were taken with a 40X objective. No thrombus can be seen in any view.

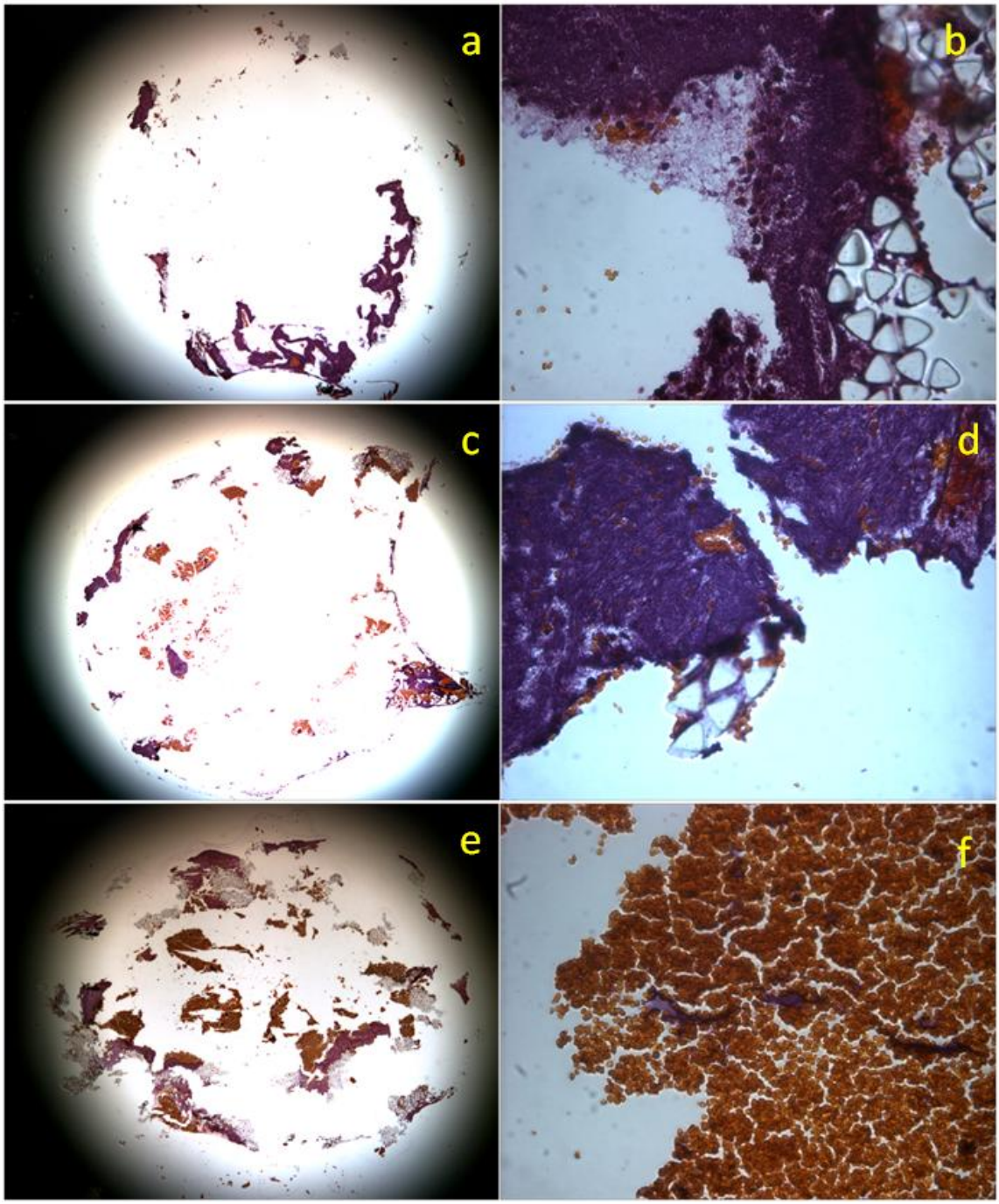

Figure 9.5: Polyester test section from experiment on Feb. 8, 2010 in axial orientation. Images (a) and (b) are from the proximal region, (c) and (d) from the medial region, and (e) and (f) from the distal region. Images (a), (c), and (e) were taken with a 2X objective while images (b), (d), and (f) were taken with a 40X objective. A slightly fragmented occlusive thrombus consisting of platelets, red blood cells, and collagen can be seen in (e) and (f).

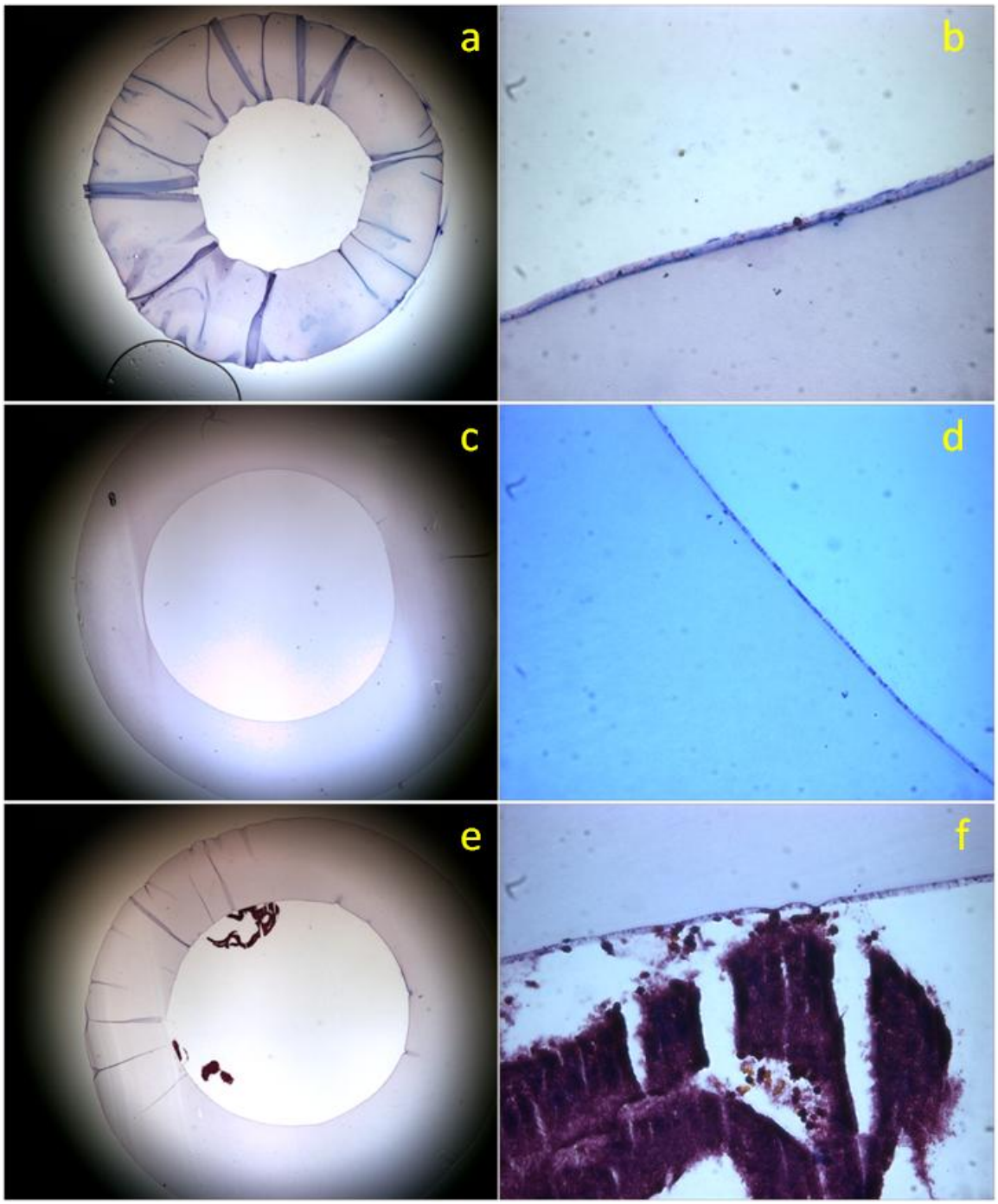

Figure 9.6: PVA cryogel test section from experiment on Feb. 8, 2010 in axial orientation. Images (a) and (b) are from the proximal region, (c) and (d) from the medial region, and (e) and (f) from the distal region. Images (a), (c), and (e) were taken with a 2X objective while images (b), (d), and (f) were taken with a 40X objective. A small amount of adherent thrombus consisting of platelets, red blood cells, and collagen can be seen in (e) and (f).

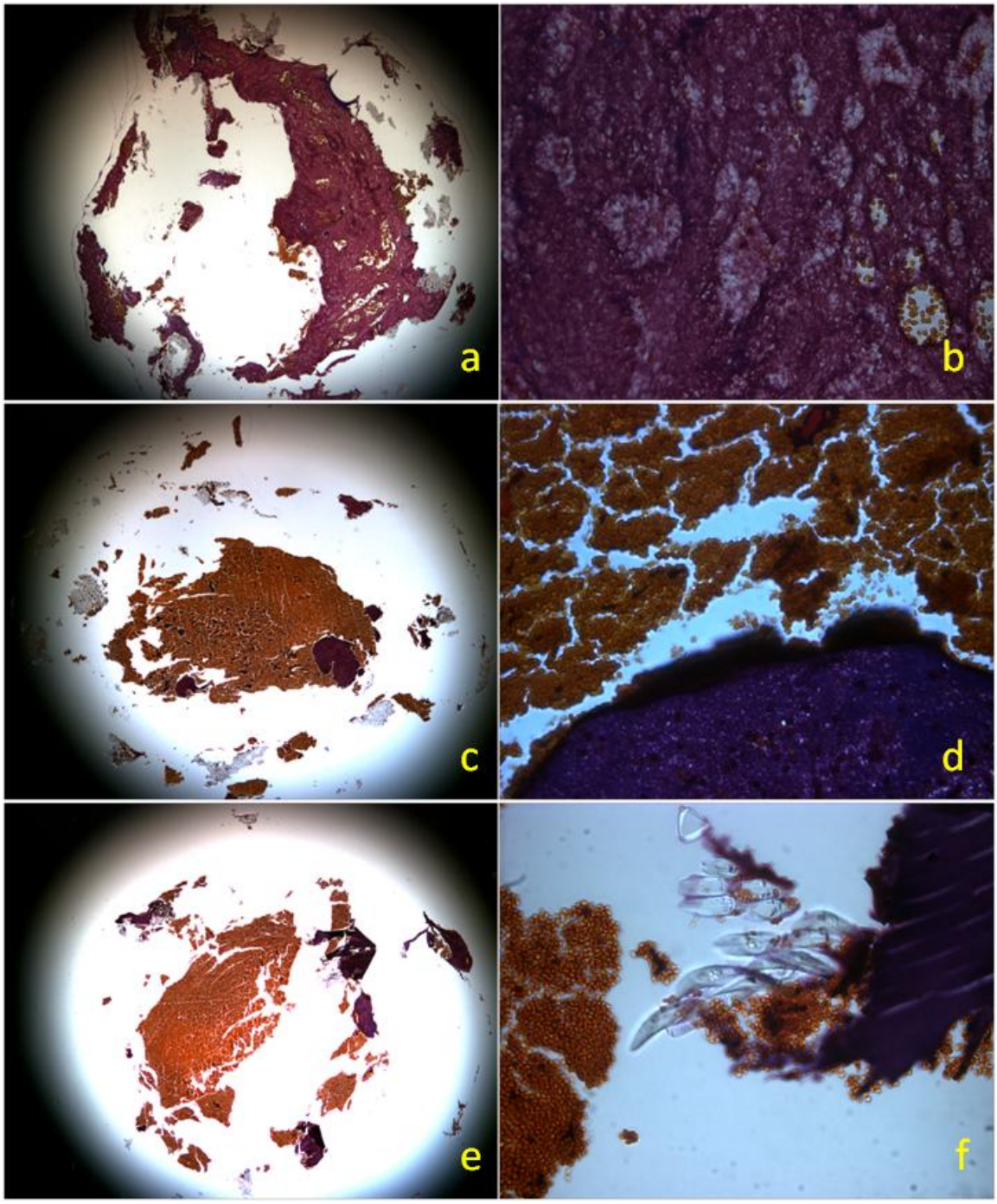

Figure 9.7: Polyester test section from experiment on Feb. 24, 2010 in axial orientation. Images (a) and (b) are from the proximal region, (c) and (d) from the medial region, and (e) and (f) from the distal region. Images (a), (c), and (e) were taken with a 2X objective while images (b), (d), and (f) were taken with a 40X objective. An occlusive thrombus consisting of platelets, red blood cells, and collagen can be seen in (c), (d), (e), and (f).

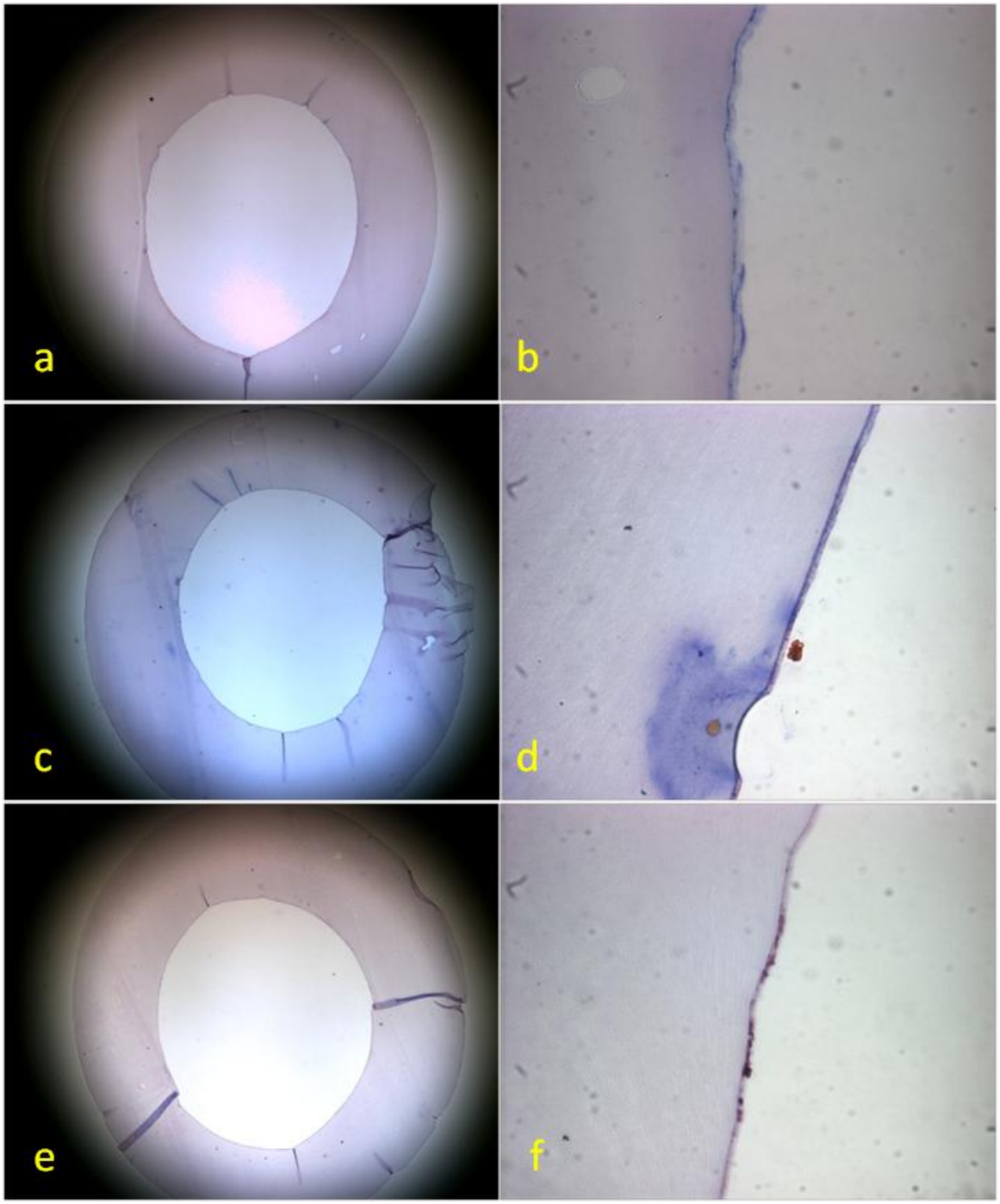

Figure 9.8: PVA cryogel test section from experiment on Feb. 24, 2010 in axial orientation. Images (a) and (b) are from the proximal region, (c) and (d) from the medial region, and (e) and (f) from the distal region. Images (a), (c), and (e) were taken with a 2X objective while images (b), (d), and (f) were taken with a 40X objective. No thrombus can be seen in any view.

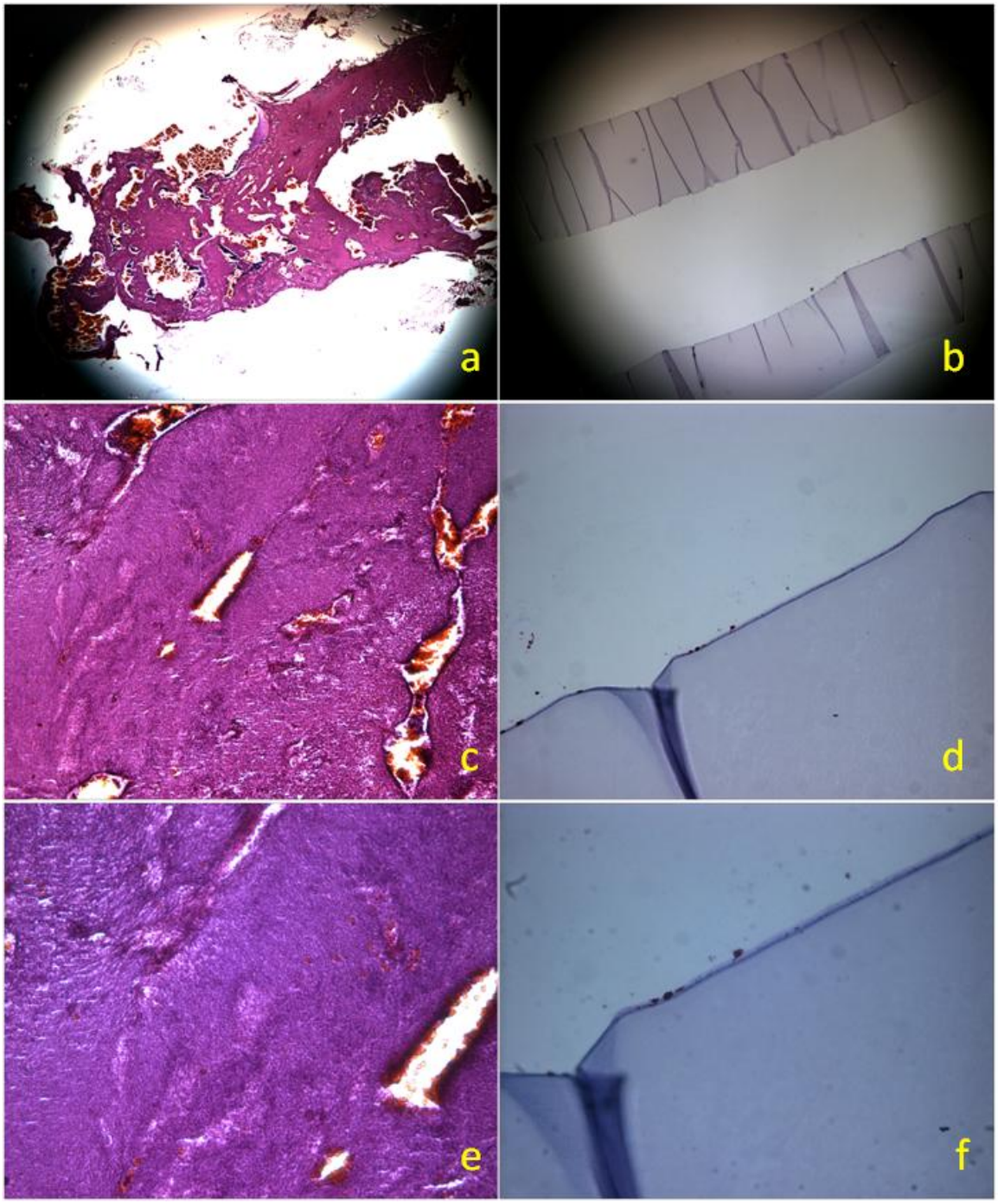

Figure 9.9: Polyester [(a), (c), and (e)] and PVA cryogel [(b), (d), and (f)] test sections from experiment on March 1, 2010 in longitudinal orientation. Flow is from right to left. Images (a) and (b) were taken with a 2X objective, (c) and (d) with a 20X objective, and (e) and (f) with a 40X objective. An occlusive thrombus can be seen in the polyester test section. A small amount of thrombus can be seen on the PVA cryogel test section.

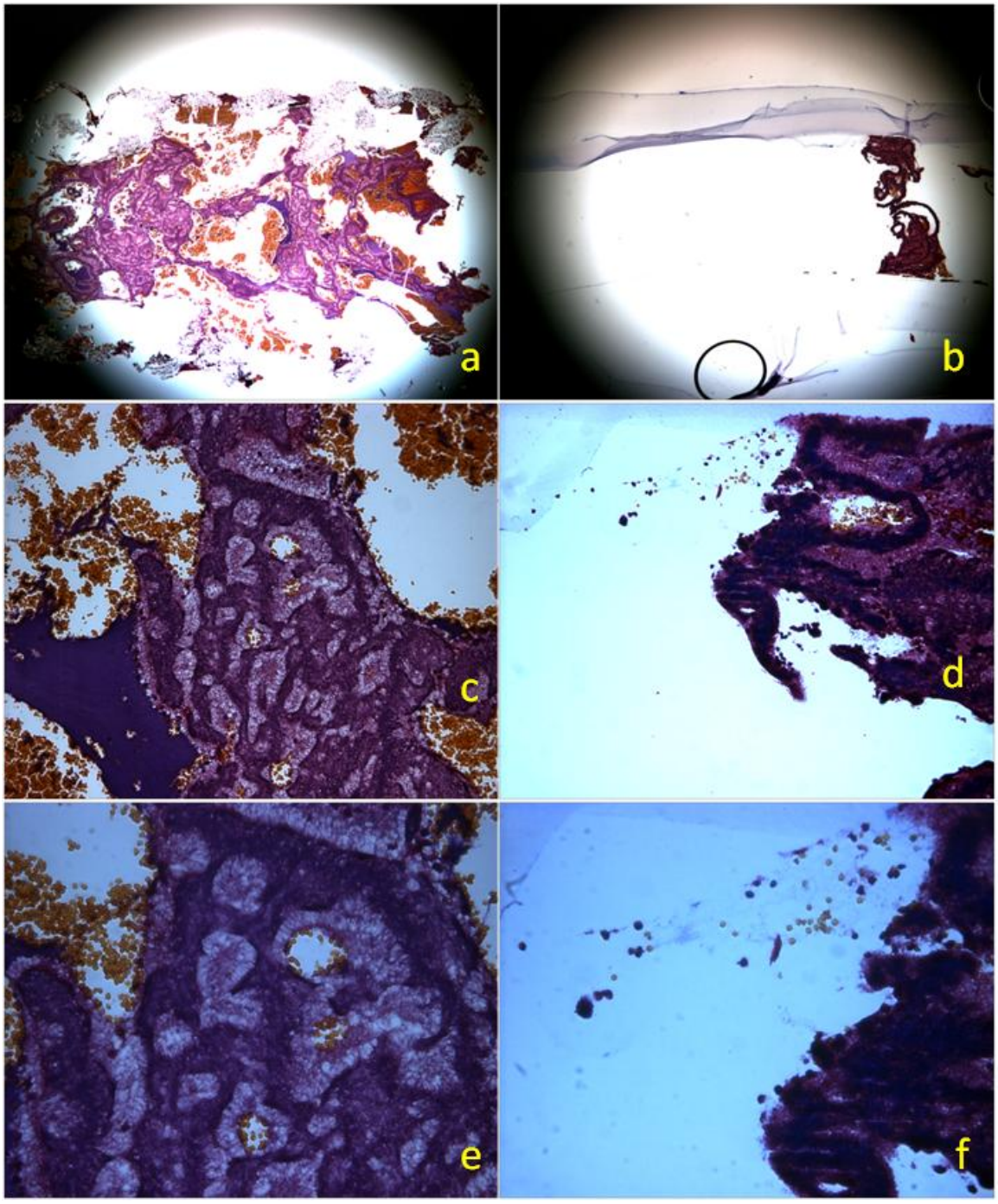

Figure 9.10: Polyester [(a), (c), and (e)] and PVA cryogel [(b), (d), and (f)] test sections from experiment on March 8, 2010 in longitudinal orientation. Flow is from right to left. Images (a) and (b) were taken with a 2X objective, (c) and (d) with a 20X objective, and (e) and (f) with a 40X objective. An occlusive thrombus can be seen in the polyester test section. A small, non-occlusive thrombus can be seen on the PVA cryogel test section.

9.4 Discussion

Using this gravity-fed flow loop system, PVA cryogels outperformed flow-matched polyester controls by having a higher final relative flow rate. While most of the polyester test sections occluded (five of seven), the flow rates in the loop with no test section and in the PVA cryogel loop dropped by only 30%. This 30% reduction in flow rate was due to thrombus forming on the silicone tubing (not test sections) near junctions and occurred evenly in all flow loops. As such, it was deemed irrelevant to the final conclusions of the experiment. Furthermore, PVA cryogel test sections were not statistically different from the flow loop with no test section in terms of final flow rate – suggesting that the PVA cryogel had no effect on thrombus formation. This experimental setup, which matched physiological flow conditions of the human left main coronary artery and showed complete occlusion of polyester test sections, mirrored the clinical experience of thrombotic occlusion in small diameter synthetic vascular grafts [21]. This test provides a benchtop verification method for comparison of biomaterial thrombogenicity that uses the clinically relevant endpoint of complete occlusion and takes into account flow, a factor which is known to influence thrombus growth [28]. Histology confirmed flow rate observations that large amounts of thrombus formed in the polyester test sections while the PVA cryogel test sections remained mostly clear of thrombus. In the future, it would be interesting to compare PVA cryogels directly to PTFE and additionally test covered stents in place of tubes.

Previous studies of PVA-coated tubing have shown an increase in platelet consumption with a canine four day *ex vivo* shunt model [35, 39]. In the present study however, no statistically significant differences in platelet concentration or mean platelet volume were noted for the PVA cryogel tubes. While it is possible that the time frame studied is too

short to obtain measureable differences (large differences in platelet concentration were typically noted beyond day one of the *ex vivo* shunt experiments), the nature of *in vitro* blood experiments limits the maximum experiment duration. Furthermore, the PVA cryogels in the present study were made without the use of a cross-linking agent and may not incite platelet consumption as in previous studies. Future work, including *ex vivo* shunt experiments, with the current PVA cryogels would provide useful information on their thrombogenicity, e.g. platelet consumption, beyond the two hour time period studied here.

Because of the large platelet presence in the occluding thrombus that formed in the polyester test sections, one might expect the platelet concentration of that blood to be significantly lower after testing than the other blood samples. However, by estimating the clot size and composition, it can be shown that the number of platelets in the clot represents less than 5% of the total platelets in the blood. Such a small change in platelet concentration is well within the experimental error of the hematology analyzer (up to 19% for two consecutive readings of the same blood sample) and therefore undetectable by these methods.

One limitation of the current study is that it was conducted with porcine, and not human, blood. While human blood is more directly relevant, porcine blood has a number of similarities with human blood and has been used extensively in thrombosis research [28, 43, 44]. Pigs and humans have similar coagulation and fibrinolytic systems [44]. Furthermore, porcine blood may be considered hypercoagulable when compared to human blood because of higher levels of several coagulation factors (IX, XI, and XII) and lower activity of protein C [43, 44]. Additionally, this study would have been difficult to complete with human blood given the volume of blood used. Future work could include

miniaturizing the experimental setup in order to use a smaller amount of blood that could be more reasonably donated by humans.

In conclusion, this gravity-fed flow loop system represents a new way to test biomaterial thrombogenicity to the clinically relevant endpoint of total occlusion before moving to expensive animal trials. The results presented here show that 20% PVA cryogels are less thrombogenic than polyester – a material which is already used as a synthetic vascular graft. Since the PVA cryogels had similar final flow rates as the flow loop with no test section, they are considered to be relatively non-thrombogenic based on this test. PVA cryogels may represent a new material or coating option for blood-contacting medical devices given their low thrombogenicity. Further study of thrombogenicity in animal models is recommended to understand the long-term effects of blood contact with this material.

9.5 References

1. Kumar, V., et al., *Robbins and Cotran pathologic basis of disease*. 7th ed. 2005, Philadelphia: Elsevier/Saunders. xv, 1525 p.

2. Scott, N.A., et al., *Identification of a potential role for the adventitia in vascular lesion formation after balloon overstretch injury of porcine coronary arteries.* Circulation, 1996. **93**(12): p. 2178-87.

3. Shehab, M., L.K. Michalis, and M.R. Rees, *Balloon angioplasty optimization: should we measure balloon volume as well as pressure?* Cardiovasc Intervent Radiol, 2008. **31**(1): p. 149-57.

4. Ruggeri, Z.M., *Platelets in atherothrombosis.* Nat Med, 2002. **8**(11): p. 1227-34.

5. Topol, E.J. and P.W. Serruys, *Frontiers in interventional cardiology.* Circulation, 1998. **98**(17): p. 1802-20.

6. Bavry, A.A., et al., *Late thrombosis of drug-eluting stents: a meta-analysis of randomized clinical trials.* Am J Med, 2006. **119**(12): p. 1056-61.

7. Iakovou, I., et al., *Incidence, predictors, and outcome of thrombosis after successful implantation of drug-eluting stents.* JAMA, 2005. **293**(17): p. 2126-30.

8. Finn, A.V., et al., *Pathological correlates of late drug-eluting stent thrombosis: strut coverage as a marker of endothelialization.* Circulation, 2007. **115**(18): p. 2435-41.

9. Laskey, W.K., C.W. Yancy, and W.H. Maisel, *Thrombosis in coronary drug-eluting stents: report from the meeting of the Circulatory System Medical Devices Advisory Panel of the Food and Drug Administration Center for Devices and Radiologic Health, December 7-8, 2006.* Circulation, 2007. **115**(17): p. 2352-7.

10. Joner, M., et al., *Pathology of drug-eluting stents in humans: delayed healing and late thrombotic risk.* J Am Coll Cardiol, 2006. **48**(1): p. 193-202.

11. Jeremias, A., et al., *Stent thrombosis after successful sirolimus-eluting stent implantation.* Circulation, 2004. **109**(16): p. 1930-2.

12. Topol, E.J., *Textbook of Interventional Cardiology*. 5th ed. 2008, Philadelphia: Saunders/Elsevier. xxi, 1286 p.

13. Newsome, L.T., M.A. Kutcher, and R.L. Royster, *Coronary artery stents: Part I. Evolution of percutaneous coronary intervention.* Anesth Analg, 2008. **107**(2): p. 552-69.

14. Prager, M., et al., *Collagen versus gelatin-coated Dacron versus stretch polytetrafluoroethylene in abdominal aortic bifurcation graft surgery: results of a seven-year prospective, randomized multicenter trial.* Surgery, 2001. **130**(3): p. 408-14.

15. Devine, C. and C. McCollum, *Heparin-bonded Dacron or polytetrafluorethylene for femoropopliteal bypass: five-year results of a prospective randomized multicenter clinical trial.* J Vasc Surg, 2004. **40**(5): p. 924-31.

16. Kannan, R.Y., et al., *Current status of prosthetic bypass grafts: a review.* J Biomed Mater Res B Appl Biomater, 2005. **74**(1): p. 570-81.

17. Jordan, S.W., et al., *The effect of a recombinant elastin-mimetic coating of an ePTFE prosthesis on acute thrombogenicity in a baboon arteriovenous shunt.* Biomaterials, 2007. **28**(6): p. 1191-7.

18. Ip, W.F. and M.V. Sefton, *Patency of heparin-PVA coated tubes at low flow rates.* Biomaterials, 1989. **10**(5): p. 313-7.

19. Sprague, E.A. and J.C. Palmaz, *A model system to assess key vascular responses to biomaterials.* J Endovasc Ther, 2005. **12**(5): p. 594-604.

20. Tepe, G., et al., *Thrombogenicity of various endovascular stent types: an in vitro evaluation.* J Vasc Interv Radiol, 2002. **13**(10): p. 1029-35.

21. Jordan, S.W. and E.L. Chaikof, *Novel thromboresistant materials.* J Vasc Surg, 2007. **45 Suppl A**: p. A104-15.

22. Lee, J.H., H.B. Lee, and J.D. Andrade, *Blood compatibility of polyethylene oxide surfaces.* Prog Polym Sci, 1995. **20**: p. 1043-79.

23. Wiese, P., et al., *Clinical and Doppler ultrasonography data of a polyurethane vascular access graft for haemodialysis: a prospective study.* Nephrol Dial Transplant, 2003. **18**(7): p. 1397-400.

24. al-Khaffaf, H. and D. Charlesworth, *Albumin-coated vascular prostheses: A five-year follow-up.* J Vasc Surg, 1996. **23**(4): p. 686-90.

25. Baumgartner, H.R., et al., *Platelet adhesion, release and aggregation in flowing blood: effects of surface properties and platelet function.* Thromb Haemost, 1976. **35**(1): p. 124-38.

26. Nuttelman, C.R., et al., *Attachment of fibronectin to poly(vinyl alcohol) hydrogels promotes NIH3T3 cell adhesion, proliferation, and migration.* J Biomed Mater Res, 2001. **57**(2): p. 217-23.

27. Farrell, L.L., *Prosthetic vein valve: delivery and in vitro evaluation*, in *Bioengineering*. 2007, Georgia Institute of Technology.

28. Ku, D.N. and C.J. Flannery, *Development of a flow-through system to create occluding thrombus.* Biorheology, 2007. **44**(4): p. 273-284.

29. Streller, U., et al., *Design and evaluation of novel blood incubation systems for in vitro hemocompatibility assessment of planar solid surfaces.* J Biomed Mater Res B Appl Biomater, 2003. **66**(1): p. 379-90.

30. Para, A.N. and D.N. Ku, *Thrombus growth and occlusion in clinically significant stenoses.* Arteriosclerosis Thrombosis and Vascular Biology, 2008. **28**(6): p. E139-E139.

31. Andersson, J., et al., *Optimal heparin surface concentration and antithrombin binding capacity as evaluated with human non-anticoagulated blood in vitro.* J Biomed Mater Res A, 2003. **67**(2): p. 458-66.

32. Haycox, C.L. and B.D. Ratner, *In vitro platelet interactions in whole human blood exposed to biomaterial surfaces: insights on blood compatibility.* J Biomed Mater Res, 1993. **27**(9): p. 1181-93.

33. Savage, B., E. Saldivar, and Z.M. Ruggeri, *Initiation of platelet adhesion by arrest onto fibrinogen or translocation on von Willebrand factor.* Cell, 1996. **84**(2): p. 289-97.

34. Beythien, C., W. Terres, and C.W. Hamm, *In vitro model to test the thrombogenicity of coronary stents.* Thromb Res, 1994. **75**(6): p. 581-90.

35. Strzinar, I. and M.V. Sefton, *Preparation and thrombogenicity of alkylated polyvinyl alcohol coated tubing.* J Biomed Mater Res, 1992. **26**(5): p. 577-92.

36. Midha, P.A., *Long-term patency of a polymer vein valve*. 2009, Georgia Institute of Technology: Atlanta, Ga. p. 1 v. (various pagings).

37. Rodgers, G.P., et al., *Adjuvant therapy for intracoronary stents. Investigations in atherosclerotic swine.* Circulation, 1990. **82**(2): p. 560-9.

38. Virmani, R., et al., *Histopathologic evaluation of an expanded polytetrafluoroethylene-nitinol stent endoprosthesis in canine iliofemoral arteries.* J Vasc Interv Radiol, 1999. **10**(4): p. 445-56.

39. Ip, W.F. and M.V. Sefton, *Platelet consumption by polyvinyl alcohol coated tubing in canines.* J Biomed Mater Res, 1991. **25**(7): p. 875-87.

40. Hanson, S.R., et al., *Platelet interactions with Dacron vascular grafts. A model of acute thrombosis in baboons.* Arteriosclerosis, 1985. **5**(6): p. 595-603.

41. He, X. and D.N. Ku, *Pulsatile flow in the human left coronary artery bifurcation: average conditions.* J Biomech Eng, 1996. **118**(1): p. 74-82.

42. Sheehan, D.C. and B.B. Hrapchak, *Theory and practice of histotechnology*. 2d ed. 1980, St. Louis: Mosby. xiii, 481 p., [1] leaf of plates.

43. Velik-Salchner, C., *Normal values for thrombelastography (ROTEM (R)) and selected coagulation parameters in porcine blood (vol 117, pg 597, 2006).* Thrombosis Research, 2006. **118**(2): p. 295-295.

44. Olsen, A.K., et al., *The pig as a model in blood coagulation and fibrinolysis research.* Scand. J. Lab. Anim. Sci, 1999. **26**(4).

CHAPTER 10:

PVA Cryogel Covered Stent Implantation as Part of a Prosthetic Vein Valve Study in Sheep

10.1 Background

Chronic venous insufficiency (CVI) and its sequelae are present in nearly 27% of adults [1]. Patients with CVI have reduced blood flow to the heart which causes venous pooling, pain, and reductions in quality of life [2]. One of the main causes of CVI is the failure of native vein valves to prevent retrograde flow [2]. A prosthetic vein valve would represent an alternative treatment option for patients, especially those who are ineligible for other treatments such as valve repair or transplant [3]. Several prosthetic vein valves are in the design and testing phase, although none have arrived to market yet [4]. A major milestone towards the development of a prosthetic vein valve is testing of patency (allowing forward flow) and competency (preventing retrograde flow) in an animal model.

10.2 Methods

10.2.1 Animal Model & Device Description

The sheep external jugular vein is chosen as an animal model because the site is easy to access through open surgery; its size is similar to veins in the human leg; and to facilitate direct comparison with previous studies [4]. The prosthetic vein valve studied here, 10 mm inlet diameter, is made from a polyvinyl alcohol (PVA) cryogel and is described in detail elsewhere [4-7]. Previous animal studies have shown that proper

apposition of a prosthetic valve to the vein wall is highly important for maintaining patency [4]. To that end, a balloon-expandable stent was deployed in the valve inlet as seen in Figure 10.1 and Figure 10.2 after the vein valve was placed. In order to maintain material consistency and avoid exposure of potentially thrombogenic metal to the blood, PVA cryogel covered stents were used. The PVA cryogel covered stents used here were made with the method described in Chapter 4 of this dissertation.

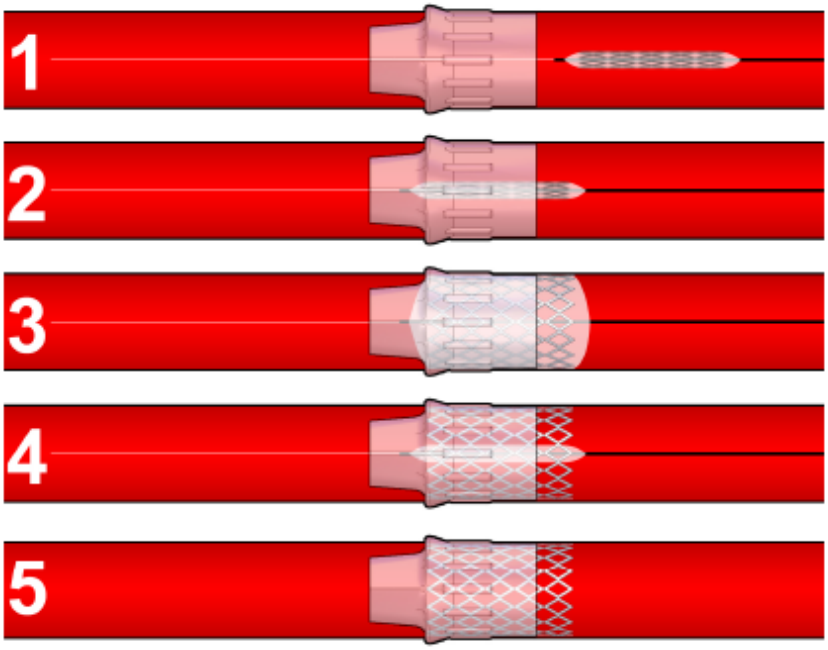

Figure 10.1: Diagram of percutaneous covered stent deployment in prosthetic vein valve inlet. Reprinted with permission from Midha 2009 [4].

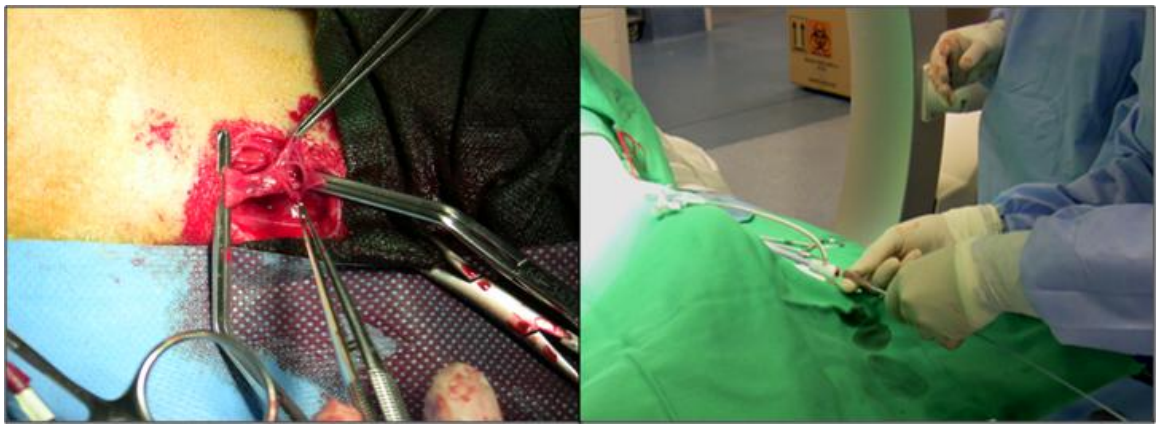

Figure 10.2: View of venotomy (left) and covered stent being introduced into vein along guide wire (right).

10.2.2 Device Implantation

A full description of the vein valve deployment is given by Midha [4]. Briefly, the sheep was anesthetized and a small incision (~2 cm) was made approximately 15 cm upstream of the final covered stent-valve location as shown in Figure 10.3. Once the connective tissue was moved aside and the vein located, a venotomy was made which allowed for insertion of the 18 Fr delivery sheath and dilator device as seen in Figure 10.2. The sheath and dilator were then advanced to the desired location where the sheath was retracted and the vein valve deployed. Once the vein valve delivery system was fully retracted, the PVA cryogel covered stent was deployed as shown in Figure 10.1 and Figure 10.2. The covered stent was hand-crimped onto the balloon catheter and advanced to the vein valve location while being visualized with a fluoroscope. The balloon was inflated with an insufflator until the valve inlet and stent were properly apposed against the vein wall. The balloon was then deflated and withdrawn – leaving

the valve and covered stent in place. In this study, four vein valve-covered stent devices were implanted in three sheep, identified as 482, 827 (left and right side), and 828. All sheep received 325 mg aspirin for one week before surgery and continued to receive the same dosage post-surgery. Sheep were sacrificed after patency was lost.

Figure 10.3: Healed implantation incision (left) and distance from incision site to valve and covered stent (right).

10.2.3 Venogram Follow-Up

Venograms were completed at one week intervals in order to assess device patency. Under anesthesia, radio-opaque contrast media was injected just upstream of the device. The path of the contrast media was followed under a flouroscope to visualize blood flow. If the device was patent, the contrast media would appear as a single stream through the external jugular vein. If the device was no longer patent, contrast media would not flow through the device, but rather around the device and through collateral veins.

10.3 Results

There were no procedural complications during implantation of the valves or covered stents. All four devices were patent at 2 weeks (Figure 10.4) with one remaining patent until 4 weeks. After sacrifice, devices were explanted without difficulty and examined macroscopically. There was no fibrotic encapsulation or inflammatory response by gross pathological examination. Covered stent membranes were intact and had no visible tears, punctures, or separation from the stent metal. One explanted covered stent and vein valve is shown in Figure 10.5.

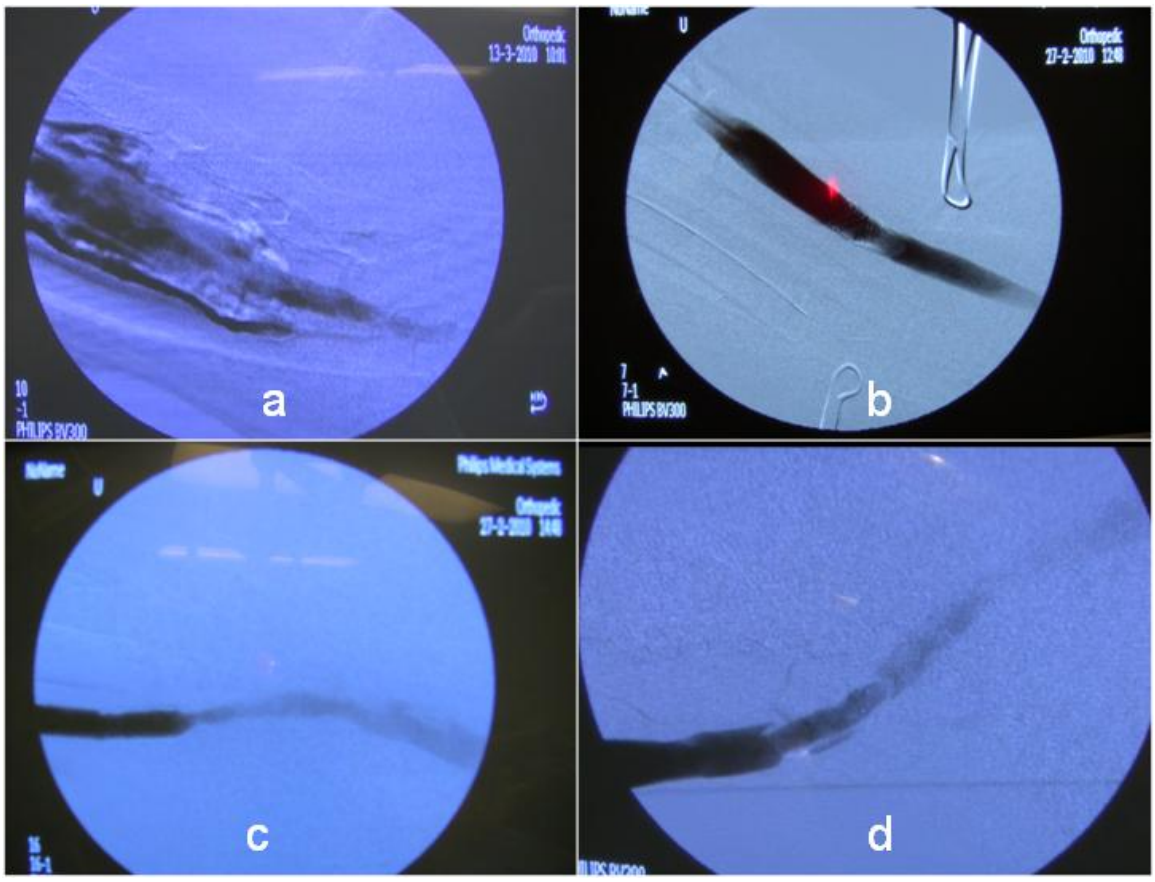

Figure 10.4: Two week patency venograms from (a) sheep 482, (b) sheep 827 left, (c) sheep 827 right, and (d) sheep 828. No collateral flow is seen as the contrast passes straight through the covered stent and vein valve. There was some slight extravasation of contrast in (a), but flow through the device can still be seen.

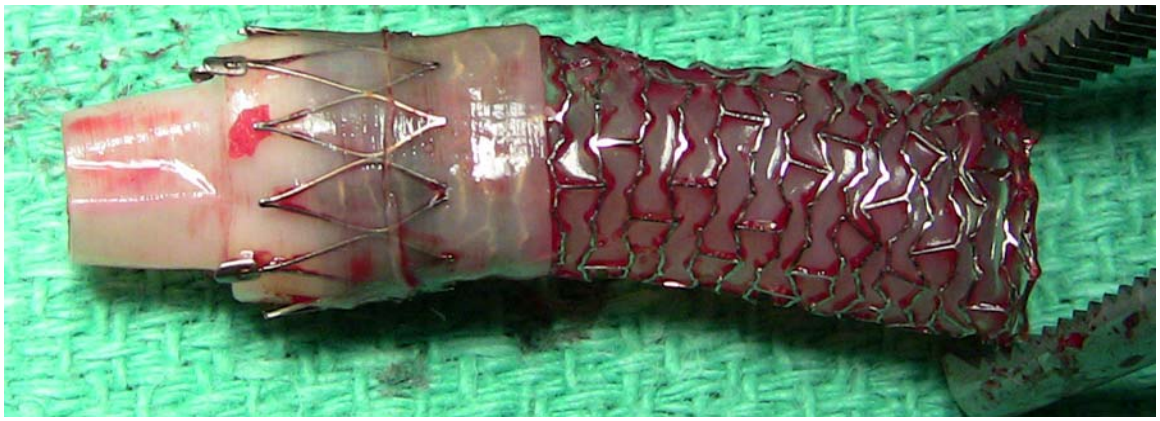

Figure 10.5: Explanted vein valve and covered stent. There are no visible tears in the PVA cryogel membrane or separation of the stent metal from the PVA cryogel.

10.4 Discussion

The work presented here is the first animal implantation of a PVA cryogel covered stent and represents a major step forward in the development of these devices because it demonstrates the ability to make and deploy PVA cryogel covered stents *in vivo*. PVA cryogel covered stents were made by hand, manually crimped onto a balloon catheter by a surgeon, and then deployed at the vein valve inlet site. The delivery catheter used was 18 Fr and is larger than what would be used for a covered stent implantation. While the PVA cryogel covered stent could have been delivered with a smaller delivery sheath, the size and geometry of the prosthetic vein valve necessitated the larger size. After explantation, covered stents were inspected and the membranes were all intact – providing evidence for the mechanical durability of this material in an *in vivo* setting. Also of note is that there was no fibrotic or inflammatory response by gross pathological examination.

One limitation of this study, in terms of the covered stents, was that it was completed in veins and not arteries. While the sheep external jugular vein is an appropriate location for testing vein valve patency, direct analysis of covered stent thrombogenicity is not possible because of the differences between clot formation in arteries and veins [8]. Venous thrombus, commonly referred to as red thrombus, tends to form at areas of stasis and contain more red blood cells than arterial thrombus [8]. Arterial thrombus, commonly referred to as white thrombus, forms at high shear and contains large amounts of platelets and fibrin, but relatively few entrapped red blood cells [9]. To truly evaluate the thrombogenicity of PVA cryogel covered stents for treating atherosclerosis, future animal trials should deploy the covered stents in arteries.

Regarding prosthetic venous valves, an average patency of 2.5 weeks (maximum 4 weeks) in sheep is on par with several completed studies [10, 11] and surpasses at least one other study [12]. Occlusion in the covered stents and vein valves could have been caused by imperfections from the hand-manufacturing of both components. Future work should include the incorporation of good manufacturing practices in order to ensure consistency across the devices and remove this potential issue. As this was the first experience with implantation of PVA cryogel covered stents/vein valves and the delivery system was custom-made for each implantation, there was some variability between the implantations as the operators gained experience in deploying these devices together. Future animal trials should include a larger number of animals and be completed in a more consistent manner in order to elucidate the exact causes and mechanisms of device occlusion and improve next-generation devices.

In conclusion, the present study showed the feasibility of delivering PVA cryogel covered stents via catheter *in vivo*. After device explantation, there was no gross inflammation

or fibrotic response. Covered stent membranes were intact – providing evidence for the mechanical durability of PVA cryogel covered stents. Future studies of PVA cryogel covered stents should include implantation into an arterial model.

10.5 References

1. Brand, F.N., et al., *The epidemiology of varicose veins: the Framingham Study.* Am J Prev Med, 1988. **4**(2): p. 96-101.

2. White, J.V. and C. Ryjewski, *Chronic venous insufficiency.* Perspect Vasc Surg Endovasc Ther, 2005. **17**(4): p. 319-27.

3. Pavcnik, D., et al., *Percutaneous management of chronic deep venous reflux: review of experimental work and early clinical experience with bioprosthetic valve.* Vasc Med, 2008. **13**(1): p. 75-84.

4. Midha, P.A., *Long-term patency of a polymer vein valve*. 2009, Georgia Institute of Technology: Atlanta, Ga. p. 1 v. (various pagings).

5. Farrell, L.L., *Prosthetic vein valve: delivery and in vitro evaluation*, in *Bioengineering*. 2007, Georgia Institute of Technology.

6. Sathe, R.D., *Design and development of a novel implantable prosthetic vein valve*. 2006, Georgia Institute of Technology.

7. Sathe, R.D. and D.N. Ku, *Flexible prosthetic vein valve.* Journal of Medical Devices, Transactions of the ASME, 2007. **1**(2): p. 105-112.

8. Kumar, V., et al., *Robbins and Cotran pathologic basis of disease*. 7th ed. 2005, Philadelphia: Elsevier/Saunders. xv, 1525 p.

9. Ku, D.N. and C.J. Flannery, *Development of a flow-through system to create occluding thrombus.* Biorheology, 2007. **44**(4): p. 273-284.

10. Dalsing, M.C., et al., *An early experience with endovascular venous valve transplantation.* J Vasc Surg, 1996. **24**(5): p. 903-5.

11. Pavcnik, D., et al., *Significance of spatial orientation of percutaneously placed bioprosthetic venous valves in an ovine model.* J Vasc Interv Radiol, 2005. **16**(11): p. 1511-6.

12. Hill, R., et al., *Development of a prosthetic venous valve.* J Biomed Mater Res, 1985. **19**(7): p. 827-32.

CHAPTER 11:

Part 3: Conclusions, Significance, and Future Directions

The gravity-fed flow loop system presented in Chapter 9 represents a new method for testing biomaterial thrombogenicity that includes the clinically relevant endpoint of complete occlusion. Using this test, small diameter polyester test sections failed by complete occlusion – mirroring the clinical experience with small diameter polyester vascular grafts as arterial bypasses. By mimicking flow conditions in the human left main coronary artery, the method gains relevancy for stent and vascular graft materials that are in a similar environment. With this gravity-fed system, measurements of flow rate can be obtained up until complete occlusion. The use of flow rate and complete occlusion as a means of comparison may be more clinically relevant than previous tests which evaluate thrombogenicity by platelet activation assays and scanning electron microscope images of relatively small amounts of thrombus deposition. In the future, the flow system geometry could be modified to investigate thrombogenicity in other regions of the vasculature and other types of blood contacting devices.

Using this test method, 20% PVA cryogel tubes were found to be less thrombogenic (higher final flow rate and less thrombus upon histological examination) than flow-matched polyester test sections. The final flow rates in the PVA cryogel flow loops were not found to be statistically different from a flow loop which had no test section – suggesting that the PVA cryogel tube had no effect on thrombus formation within the system. While platelet consumption has been a concern for PVA hydrogel materials in the past, these results showed no difference in mean platelet volume or platelet

concentration between blood tested with PVA cryogels and blood that was not tested in the flow loop system.

In Chapter 10, PVA cryogel covered stents were deployed into sheep external jugular veins via catheter as part of a study on prosthetic vein valves. The devices were all patent at 2 weeks; this result matched and surpassed several previously published studies of prosthetic vein valves. After sacrifice, gross pathological examination showed no inflammatory or fibrotic response at the deployment site. PVA cryogel membranes were intact after explantation – providing evidence of the *in vivo* durability of PVA cryogel covered stents. Even though covered stents were deployed into veins (and not arteries), this work represents a significant step forward in the development of these devices because the feasibility of making and deploying these devices was demonstrated for the first time.

Overall, the results in Chapters 9 and 10 point to the relatively low thrombogenicity of PVA cryogels as measured *in vitro* and *in vivo*. The outcomes of both of these tests establish the feasibility of using PVA cryogels in blood-contacting medical devices – specifically as covered stent membranes. It is recommended that future work focuses on animal trials, e.g. porcine, that can evaluate PVA cryogels in terms of restenosis and thrombosis.